Development of a New Cell Penetrating Peptide: Design, Synthesis and Applications

Entwicklung eines neuen zell-penetrierenden Peptids: Design, Synthese und Anwendungen

DISSERTATION

der Fakultät für Chemie und Pharmazie

der Eberhard Karls Universität Tübingen

zur Erlangung des Grades eines Doktors

der Naturwissenschaften

2009

vorgelegt von

Deepti Jha

Tag der mündlichen Prüfung: 14.09.09

Dekan: Prof. Dr.Lars Wesemann

1. Berichterstatter   Prof. Dr. Martin E. Maier

2. Berichterstatter   Prof. Dr. Karl-Heinz Wiesmüller

II

Acknowledgements

Abbreviations

A   Adenine

A (Ala)   Alanine

Bhoc   Benzhydryloxycarbonyl

Boc   Butoxycarbonyl

C   Cytosine

C (Cys)   Cysteine

CA   Contrast agent

CF   Carboxyfluorescein

CPP   Cell Penetrating Peptide

CyLoP-1   Cytosol Localizing Peptide-1

D (Asp)   Aspartic acid

D_2O Deuterium oxide

DCM   Dichloromethane

DEE   Diethyl ether

DIC   *N,N'*-diisopropylcarbodiimide

DIPEA   N,N'-diisopropylethylamine

DMF   Dimethylformamide

DMSO   Dimethylsulfoxide

DOTA (tris-t-Bu-ester)   1,4,7,10-tetraazacyclododecane-1,4,7-tris(acetic acid-*tert*-butyl ester)-10-acetic acid

DTPA	Diethylenetriaminepentaacetic acid
ESI-MS	Electrospray Ionization Mass Spectrometry
F(Phe)	Phenylalanine
FITC	Fluorescein isothiocyanate
$GdCl_3.6H_2O$	Gadolinium trichloride hexahydrate
MeOH	Methanol
Fmoc	9-fluorenylmethoxycarbonyl
G	Guanine
HATU	2-(1-H-7-azabenzotriazol-1-yl)-1,1,3,3-tetramethyluronium hexafluorophosphate
HOBt	1-hydroxybenzotriazole
I (Ile)	Isoleucine
K (Lys)	Lysine
M (Met)	Methionine
MR	Magnetic resonance
MRI	Magnetic resonance imaging
MTBE	Methyl *tert*-butyl ether
N (Asn)	Asparagine
P (Pro)	Proline
Pbf	2,2,4,6,7-pentamethyldihydrobenzofuran-5-sulfonyl
PNA	Peptide nucleic acid

Q (Gln)	Glutamine
R (Arg)	Arginine
S (Ser)	Serine
TCP	Tritylchloride polystyrene resin
TCTU	1-H-benzotriazolium-1[bis(dimethylamino)methylene]-5-chloro-tetrafluoroborate(1-),3-oxide
TFA	Trifluoroacetic acid
Trt	Trityl
V (Val)	Valine
W (Trp)	Tryptophan

Table of contents

PART 3. APPLICATION OF CyLoP-1 AS A DELIVERY TOOL

3.1 Efficient intracellular delivery of a MR imaging probe by CyLoP-1

PART 1

INTRODUCTION

1.1 Intracellular delivery- Cell Penetrating Peptides

Many biological techniques make use of a number of proteins and DNA-based strategies to understand cellular functions and mechanisms e.g. antisense mediated gene silencing, gene therapy or, therapeutic antibodies. Such techniques render manipulation of gene expression and regulation to therapeutic applications. In spite of the tremendous potential of these applications they are limited by the inefficiency of the active molecules to pass through plasma membranes. The plasma membrane of a cell serves as a barrier to hydrophilic drugs, peptides and proteins. Thus, in order to achieve any therapeutical effects with these agents, an effective delivery system is mandatory. Only a narrow range of molecules of certain molecular weight, polarity and net charge are capable of diffusing through cell membranes. To overcome the limitation of breaching the membrane barrier for conventional and gene drug delivery, various methods have been developed. Approaches like liposome based delivery (Caplen *et al*., 2001; Martins *et al*., 2002), viral transfection (Hemann *et al*., 2003) electroporation (Siegmund *et al*., 2002) and microinjection (Usui *et al*., 2003) are used. These methods are mainly utilized to deliver hydrophobic molecules. Furthermore, the side effects associated with these methods like cytotoxicity or inefficient delivery, experimental conditions and the fact that their utilization is limited to *in vitro* or *ex vivo* uses have prevented them from becoming an efficient means to deliver compounds to the cell in order to treat diseases and conditions. Thus a more efficient and non-invasive delivery technique for the delivery of hydrophilic drugs and other substances was needed.

In the 1990s the discovery of Cell Penetrating Peptides (CPPs), also called protein transduction domains (PTDs) or membrane translocation sequences (MTS), proved that the translocation of larger molecules through the cell membrane is possible. CPPs are composed of short peptides upto 30 amino acids capable of penetrating the plasma membrane and they are generally net positively charged and amphipathic. These peptides are generally classified into protein derived CPPs, model peptides and designed peptides (Table 1) depending upon the origin of the peptides.

Table 1: Classification of exemplary CPPs

Name	Sequence	Class	Reference
Tat $_{48\text{-}60}$	GRKKRRQRRRPPQ	Protein derived CPP	Vives *et al*, 1997
Penetratin	RQIKIWFQNRRMKWKK	Protein derived CPP	Derossi *et al*, 1994
Transportan	GWTLNSAGYLLGKINLKALAALAKISIL	Designed CPP	Pooga *et al*, 1998
SP-NLS	MGLGLHLLVLAAALQGAWSQPKKKRK	Designed CPP	Chaloin *et al*, 1997
Pep-1	KETWWETWWTEWSQPKKKRKV	Designed CPP	Morris *et al*, 2001
Oligo-arginines	$(R)_7$	Model CPP	Rothbard *et al*, 2002

CPPs originating from protein consist of a minimal effective sequence capable of membrane translocation also known as Protein Transduction Domain (PTD). Prominent examples are Tat (Green and Loewenstein, 1988) and Antennapedia (Joliot *et al*., 1991). Tat is the nuclear transcription activating protein from HIV-1 virus consisting of 86 amino acids with three functional domains: - an acidic N-terminal RNA binding region (Weeks *et al*., 1991), a highly basic domain featuring nuclear and nucleolar localization (Ruben *et al,* 1989) and a cysteine rich DNA binding region important for metal-linked dimerization in vitro (Frankel *et al*., 1988). The basic region of Tat$_{49\text{-}57}$ (RKKRRQRRR) remains in random coil conformation and is continuously applied as Nuclear Localization Sequence (NLS) and a delivery tool. The first non-viral protein transduction domain was Antennapedia derived from Drosophilia homeodomain protein. It is a 60 amino acid DNA binding homeodomain structured in three α-helices and one β-turn (Czajlik *et al,* 2002). The minimal region from the third helix was responsible for translocation of the entire protein. This region of 16 amino acids residues, 43-58, is also referred to as penetratin (Derossi *et al*., 1998; Derossi *et al*., 1994). Designed CPPs are for example chimeric peptides comprised of a hydrophilic and hydrophobic domain from different sources e.g. transportan which is a 27 amino acid long peptide consisting of a peptide sequence from the neuropeptide galanin linked via lysine to the wasp venom peptide, mastoparan. Model peptides are sequences

that in general mimic other CPPs for improvement of the internalization properties e.g. oligoarginines.

Due to their ability of intracellular delivery accompanied with low cytotoxicity, synthesis procedures that offer the possibility easy routine synthesis with the possibility for diverse modifications qualify CPPs as efficient delivery agents for therapeutic and diagnostic applications.

1.2 Mechanism of internalization

It was long questioned which features were necessary for a CPP to exert a translocation function. So far the only aspect found consistently is a high content of basic amino acids resulting in a net positive charge. Although the primary structure of CPPs varies, some common characteristics necessary for uptake can be predicted. Apart from a positive charge, especially originating from arginines (Futaki *et al*., 2001; Wender *et al*., 2000) the presence of hydrophobicity arising from amino acids with bulky side chains (Derossi *et al*., 1998) seems to be beneficial for the uptake. Not only the presence of these motifs but also the location in the peptide chain of these amino acids seemed to be important as it was shown for the tryptophan in penetratin (Dom *et al*., 2003). Generally, an alpha-helical secondary structure seems to be of benefit for CPPs but cannot be taken as a general prerequisite.

However, the high structural diversity that was seen in CPPs implicates an internalization-mechanism being different for distinct CPPs. The mechanism of uptake has been reported to be a multistep process. Cationic CPPs bind electrostatically to the negatively charged head groups of lipids or proteins in the cell membrane (Zorko *et al*., 2005; Gupta *et al*., 2005). Charge is important but not sufficient, as evident from the comparison of the uptake efficiencies of polyarginines and similar length polymers of lysine and histidine. The highly efficient cellular uptake of oligoarginines was attributed to the ability of the guanidine to form bidendate hydrogen bonds with phosphates or sulphates of the membrane (Mitchell *et al*., 2000). Apart from the presence of the guanidinium headgroup their spatial preference is also significant in membrane adherence. An electrostatic interaction and bidendate hydrogen bonds develops between the guanidinium groups and the hydrogen bond acceptors anchored on the surface of the plasma membrane. As the arginine rich peptide reaches the negatively charged surface of the plasma membrane the polar cationic and anionic functionalities converts into lipophilic ion pair.

The bidendate hydrogen bonds with carboxylate, phosphates, and sulphates also contribute to this association (Rothbard *et al.*, 2004) (Figure 1).
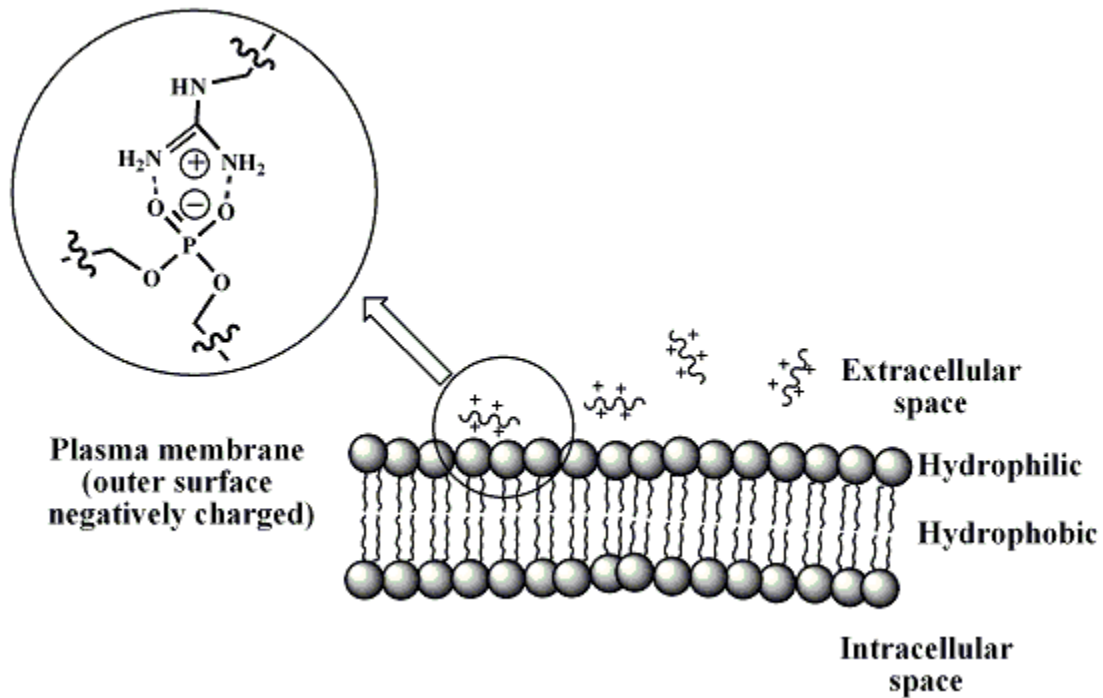
Figure 1: Initial step of CPP and membrane interaction.

Enlarged - Interaction of the positive charged CPP with negative charged phosphates present in the lipid bilayer.

Different uptake mechanisms for CPPs were proposed in the literature. The entry can be supported by an energy-dependent endocytotic mechanism or via an energy-independent passive transport mechanism. Endocytosis is a well regulated process that falls into two broad categories: Phagocytosis (engulfing large particles, performed by specialized cells) and pinocytosis. In the latter case extracellular molecules are encapsulated into lipid vesicles which are then internalized. In pinocytosis can be further divided into four models: macropinocytosis, clathrin-mediated, lipid-raft mediated and clathrin-caveolae independent endocytosis.

These mechanisms differ from each other on the basis of the size of vesicles, mechanism of formation of the vesicles, and the nature of the cargo. Clathrin-mediated endocytosis starts with receptor-binding followed by accumulation of receptors in coated pits on the plasma membrane. Caveolae are a type of lipid rafts, small and flask shaped depressions of the plasma membrane. Macropinocytosis is characterized by protrusion of the plasma membrane formed upon activation

by growth factors or other signals and leads to the formation of macropinosomes. This type of uptake is highly dependent on the actin activity on the cell surface. Another, less defined mechanism is the non-caveolae dependent endocytosis. This pathway is closely linked to the presence of lipid rafts and is distinguished into dynamin dependent and dynamin independent endocytosis. Though less characterized it seems to be functional for the delivery of various molecules. The direct uptake of peptides is possible by disturbing the membrane integrity (Henriques *et al*., 2005).

Since these different uptake mechanisms can operate simultaneously during internalization of extracellular cargo, it will be difficult to predict an exact mechanism of internalization for CPPs. It is therefore not surprising that this is still a matter of debate for most CPPs and is not yet resolved completely. For example, it has been shown that endocytosis plays a dominant role in the import of Antp, Tat and nonaarginines (Duchardt *et al*., 2007). However, it was also reported that the uptake mechanism is strongly cargo specific. A change in uptake mechanism was observed from lipid raft-mediated endocytosis (Fittipaldi *et al*., 2003) to clathrin-dependent endocytosis when CPP was conjugated to a protein instead of a fluorophore (Richard *et al*., 2005).

1.3 Applications

The efficacy and non-invasive nature of CPP-mediated transmembrane passage allows various applications in biomedical research. The delivery of a wide range of biomolecules like antisense oligonucleotides or peptide nucleic acids (PNA) across the plasma membrane had been a major challenge before the advent of the CPPs. Research is now focused on further investigating efficacy of delivery and also toxic effects of the peptides. The peptide concentration, cargo molecules and the coupling strategies can also have a direct effect on these parameters (Andaloussi *et al*., 2007). Especially the delivery efficiency and its mechanism are dependent on the attachment of cargo to the CPP. Studies have been undertaken to investigate the effect of different cargos on the penetration abilities of CPPs (Dietz *et al*., 2004).

Also, different coupling strategies have been employed for CPP cargo conjugation (Meade *et al*., 2008; Crombez *et al*., 2007), e.g. covalent conjugation (Fischer *et al*., 2006) and non covalent linkage (Morris *et al*., 2001). Another promising strategy that was applied linking peptides and

PNA was the use of disulphide linkages (Snyder *et al*., 2004). The advantage of this procedure is an active cleavage of the disulphide bridges in the reducing environment of the cytosol and consequently dissociation of the cargo molecule from the vector after internalization. Fusion schemes can be selected depending on the requirement and the nature of the cargo.

Furthermore, CPPs are already and widely used as delivery vectors in such different areas as cancer immunotherapy, gene delivery and, cellular imaging. Despite of the high delivery efficiency CPPs lack specificity for different cell types. Thus, depending on the requirement of the targeted tissue, a ligand of selective property could optionally be conjugated to the CPP. In this regards, CPPs are already used to carry a wide range of molecules into the cell to fulfill their respective biological actions e.g. DNA, antibodies, contrast agents (CA) (Allen *et al*., 2004), proteins as large as 120 kDa (Schwarze *et al*., 2000; Gupta *et al*., 2005), siRNA (Muratovska and Eccles, 2004), plasmids (Singh *et al*., 1999), peptide nucleic acids (Pooga *et al*., 1998), peptides (Prochiantz *et al*.,1996), and even nanoparticles (Lewin *et al*., 2000).

1.4 Limitations and solutions

Though CPPs are non-invasive carriers of broad range of cargos through the plasma membrane one of the major hurdles in the therapeutic strategies like gene and antisense therapy and vaccine development is the cytoplasmic availability of the biomolecular drugs. The prerequisites for such cargo approaches are that the designed molecules ably penetrate the cell membrane and the interaction with the target, presumably located in the cytosol, will be facilitated. As endocytosis is the exclusive or predominant mechanism of uptake for most of the CPPs, a limiting factor for CPP-based delivery approaches is the confinement in the endosomes (Figure 2) with concomitant degradation in the lysosomes restricting their use as cytosolic/nuclear targeting agents.

Various attempts have been made to achieve endosomal escape, like the application of lysosomotropic agents, fusogenic peptides, and the use of high concentrations of the CPP construct.
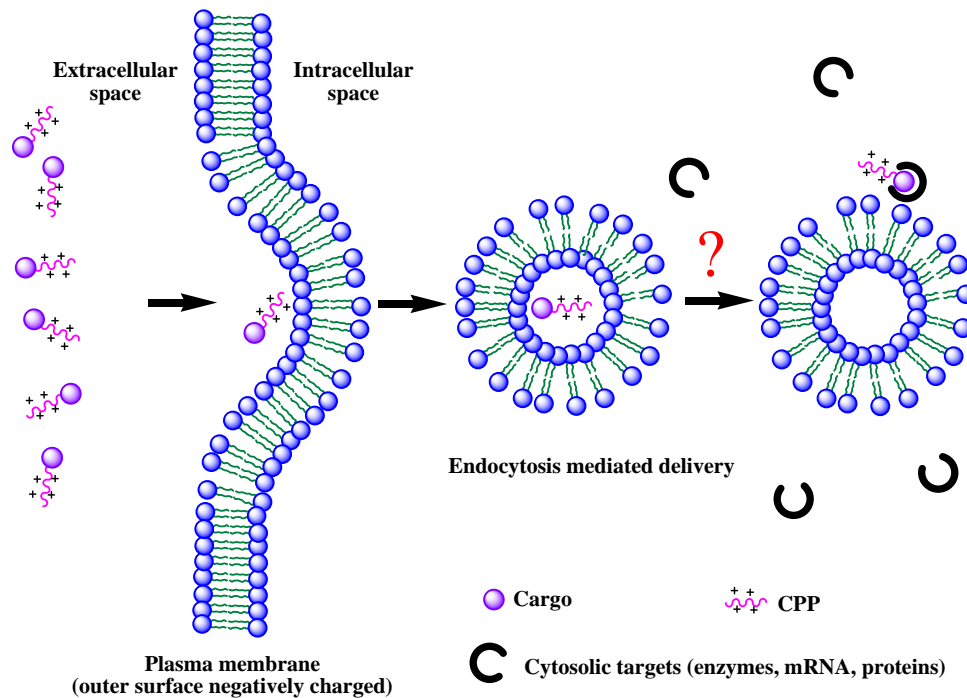
Figure 2: Proposed mechanism of internalization of cargos attached to CPP by endocytosis.

Localization in the nucleus or in the cytosol of these previously investigated peptides was observed together with endosomal trapping, albeit under only a restricted set of conditions (short term incubations, CPP concentration above 10 µM) (Duchardt *et al*., 2007). At such extracellular concentrations, however, elongated incubations (required in the presence of serum) result in a 30-40% increased cell death (unpublished data from our laboratory). These restrictions clearly suggest that the setback of endosomal encapsulation for targeting approaches using CPPs need further investigations.

HA2 fusion peptide, derived from influenza virus has also been used for the endosomal release of various oligonucleotides and proteins (Wadia *et al*., 2004; Turner *et al*., 2005). At physiological pH (7.4) these peptides exist in ionized form and in hydrophilic state whereas in endosomes and especially having lower pHs the peptide becomes protonated. Destabilization of the endosomal membrane facilitates the escape of the peptide conjugates (Planck *et al*., 1994).

Modifications of the CPP have been made to overcome the endosomal entrapment. EB1, a penetratin analogue was designed by replacing certain amino acids by histidine to improve the endosomolytic property. In principle, EB1, upon protonation in endosomes forms an α-helix

leading to endosomolysis. The proof of its application has been shown by down regulation of luciferase expression (Lundberg *et al.*, 2007).

Endosomal release is a real challenge for the therapeutic effects of large hydrophilic molecules. Coupling of the endosome disrupting peptides to a CPP makes the carrier larger than the cargo itself. This not only makes the synthesis more complex but also raises a doubt about the *in vivo* administration and efficiency.

Another attempt for the cytoplasmic release of the potential biotherapeutics was achieved by the use of pH sensitive polymers mimicking the viral peptides. These polymers contain both acidic groups as well as hydrophobic alkyl chains. The polymers showed increased hydrophobicity when protonated at endosomal pHs, followed by membrane disruption. One example reported is a glutathione sensitive, functionalized smart polymer bearing pH dependent membrane disruptive potential. This polymer is shown to be a cytoplasmic delivery vector for biomolecule complexes like with ODNs (Bulmus *et al.*, 2003).

The development of efficient delivery systems capable of endosomal release of biotherapeutics offers numerous applications. An interesting study about the polypeptide, Crotamine (Kerkis *et al.*, 2004) might offer a potential solution to the problem of endosomal entrapment.

1.5 Crotamine

The major neurotoxins present in the venom of the South American rattle snake *Crotalus durissus terrificus* are crotoxin (a presynaptically acting neurotoxin, Faure *et al.*, 1994), convulxin (protein responsible for producing convulsions, De Sousa-e-Silva *et al.*, 2003), gyroxin (a toxin possessing thrombin like activity, De Sousa-e-Silva *et al.*, 2003) and crotamine (Toyama *et al.*, 2000). Crotamine constitutes approximately 10% of dry weight of the venom, and is the most abundant of all the components present in the venom (Yamane *et al.*, 2006). Crotamine is a low molecular-weight polypeptide bearing a single chain of 42 amino acids (YKQCHKKGGHCFPKEKICLPPSSDFGKMDCRWRWKCCKKGSG), enriched in basic amino acids such as arginines, lysines and containing 6 cysteines, the latter are all involved in disulphide-bonds (Kerkis *et al.*, 2004). Crotamine was first isolated by Goncalves and Vieira in 1950.

1.5.1 Structure of Crotamine

In solution NMR studies, Crotamine comprises a small α-helix at the N-terminus (residues 3-7) and a 3-stranded anti-parallel β-sheet, (residues 9-12, 24-25 and 35-38) arranged in $\alpha\beta_1\beta_2\beta_3$ structural topology (Figure 3) (Nicastro *et al*., 2003, Oguiura *et al*., 2005) where both first and second strands run antiparallel to the third one. All six cysteines are reticulated by three disulphide-bonds: Cys4/Cys36 (connects β-sheet to the N-terminal α-helix), Cys11/Cys30, and Cys18/Cys37 which also constitutes the central hydrophobic core (Fadel *et al*., 2005).

Figure 3: Three dimensional structure of Crotamine (adapted from Oguiura *et al*., 2005)

1.5.2 Functions of Crotamine

Crotamine acts as a myotoxin and causes the paralysis of the hind limbs of mice in less than 15 min when injected intraperitoneally (Yamane *et al*., 2006). It alters the performance of voltage-sensitive sodium channels in the sarcolemma of the skeletal muscles. An abnormal influx of sodium ions into the skeletal muscle cells, leads to depolarization and finally muscle contraction. Consequently, the effect result in necrosis of the muscle fibers as characterized by massive vacuolization of the sarcoplasmic reticulum and disruption of actin and myosin filaments (Toyama *et al*., 2000).

Apart from this action Crotamine was also shown to release histamine from mast cells and to have an analgesic activity, 30-fold more effective than morphine (Mancin *et al*., 1998).

1.5.3 Biological Activity of Crotamine

Kerkis *et al*., 2004 have shown the biological effect of Crotamine bearing the ability to transport molecules across the plasma membrane. Apart from this Crotamine also possesses a specific cell targeting capacity for actively proliferating cells (Yamane *et al*., 2006; Kerkis *et al*., 2004). It is similar with other known CPPs with respect to cationic character, high basic amino acid content and low molecular weight. Crotamine is shown to be non-toxic at submicromolar concentrations Crotamine is markedly different from other CPPs because of the 6 cysteines in its sequence. The fold obtained by the 3 disulphides bonds in crotamine yields to conformational restriction and charge distribution with unique properties.

Its size, sequence, charge, and structural conformation indicated its cell-penetrating activity. Kerkis *et al*., 2004 also proposed the penetration ability might not be due to the complete polypeptide but small domains are responsible for transduction (Y**KQCHKKGGHCFPKEKIC**LPPSSDFG**KMDCRWRWKCCKK**GSG). Crot(2-18) and Crot(27-39) were the two most promising NLS (Figure 4). Crot(2-18): KQCHKKGGHCFPKEKIC - 17 amino acid long at the N-terminal part and Crot(27-39): KMDCRWRWKCCKK - 13 amino acid long representing the C-terminus.
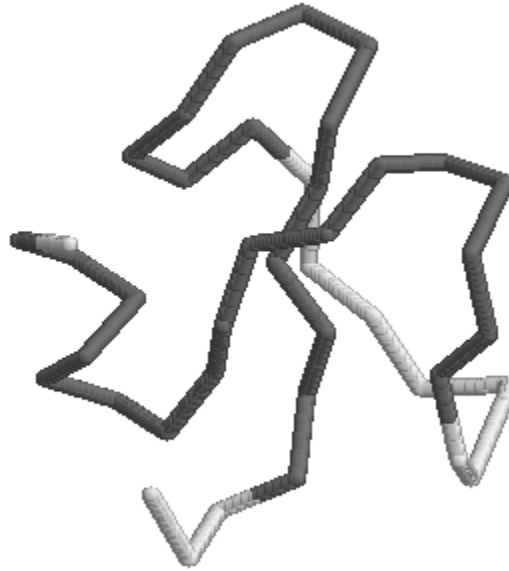
Figure 4: Backbone presentation of crotamine. Crot(2-18) and Crot(27-39) highlighted in grey.

1.6 Aim of the study

The aim of this study was to circumvent the drawback of CPP and cargo confinement in endosomes limiting the practical application of this cell delivery approach. The snake toxin Crotamine from the South American rattle snake *Crotalus durissus terrificus* was used as a promising candidate to achieve this goal and therefore was the guiding motif for this work.

The main goal was the development of a novel CPP which circumvents the drawback of endosomal encapsulation and showing improved intracellular delivery ability. Furthermore, the import efficiency and cellular distribution of the developed CPP has been evaluated with the attachment of various cargos.

(1) To achieve this goal this work should be directed in the first section towards the optimization of Crot(27-39) by structure activity relationship (SAR) studies. Variations should be introduced into the sequence of this NLS either by deletions and/or substitutions of amino acids like cysteine, tryptophan, and methionine. This should also ease the synthesis and reduce the side reactions rendered by these amino acids during the synthesis and work up procedures. Later, all the peptides should be labeled with a fluorophore (FITC) and screened for their internalization

and distribution in NIH/3T3 cells by fluorescence spectroscopy and microscopy. The best peptide (regarding uptake efficiency and cytosolic distribution) obtained as a result of these studies should be further optimized with respect to stereochemistry and position and type of the fluorophore. The potency of internalization of our newly developed CPPs should be compared with existing CPPs Tat, penetratin and octaarginine. The impact of oxidation during cellular import will also be determined by synthesizing the oxidized form of the optimal peptide.

(2) In the second section of this work the capacity of the optimal peptide as a delivery agent should be evaluated. For this purpose it was covalently coupled to cargos of various sizes and nature. The influence of cargo on the internalization and distribution should be investigated.

One main part herein is the application as intracellular contrast agent (CA) for MRI by covalently attaching a MR reporter (Gd-DOTA) to this peptide. The ability to enhance contrast in solution as well as after uptake in cells was evaluated and compared with other intracellular contrast agents synthesized in our laboratory using CPPs like Tat and octaarginine.

Furthermore, two peptides, penetratin and the bioactive SmacN7, should be coupled to investigate the capability of the peptide to be used as a delivery tool. To evaluate its use in antisense targeting, a conjugate with a neutral peptide nucleic acid sequence targeting DsRed gene expression should be studied.

PART 2

IDENTIFICATION AND OPTIMIZATION OF A NEW CYSTEINE RICH

CELL PENETRATING PEPTIDE

2. IDENTIFICATION AND OPTIMIZATION OF A NEW CYSTEINE RICH CELL PENETRATING PEPTIDE

As proposed by Kerkis *et al*., 2004, the ability of crotamine to penetrate the cell membrane may not be due to the complete polypeptide (Y**KQCHKKGGHCFPKEKIC**LPPSSDFG**KMDCRWRWKCCKK**GSG) but two small domains within the sequence might be responsible for nuclear localization. Thus, Crot(2-18) and Crot(27-39) were proposed as the two putative Nuclear Localization Signals (NLS). The C-terminal Crot(27-39) was selected as our starting sequence for Structure Activity Relationship (SAR) studies because of length and high content of lysines and arginines (expected features for the cell penetration). Crot(27-39) (Figure 5) is a tridecapeptide bearing three cysteine residues (marked orange).
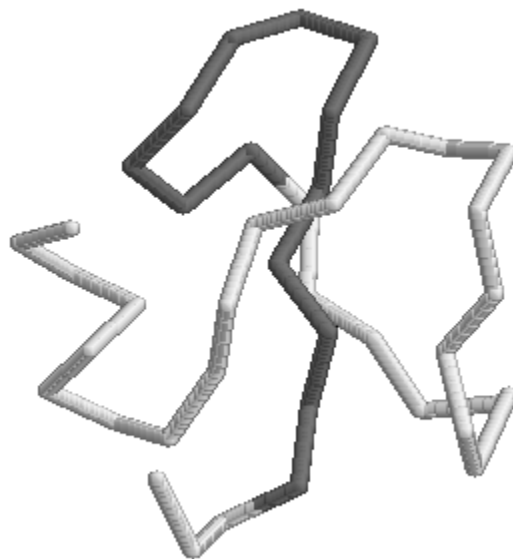
Figure 5: Structure of Crotamine. NLS Crot(27-39) **KMDCRWRWKCCKK,** marked in grey.

High cysteine content in the peptides and proteins are known to influence the biological activity of the peptide by their ability to form intra- and intermolecular bridges and hence promote oligomerization (Andreu *et al*., 1994). However, cysteine, methionine and tryptophan moieties in peptides might also cause side reactions such as racemization, oxidation and alkylation (Siedler *et al*., 1996; Huang *et al*., 1999; Wünsch *et al*., 1977; Giraud *et al*., 1999). Therefore, efforts were carried out to evaluate the functional significance of these residues. The positively charged amino acids were unaltered considering the requirement of cationic residues for membrane

adherence (Futaki *et al*., 2001; Wadia *et al*., 2005). SAR studies were performed to achieve the sequence optimized for efficient cell penetration, as well as for robust production and shelf life time. Variations were introduced in Cro(27-39) including deletions and/or substitutions (Figure 6). Peptides were synthesized on solid phase by Fmoc/tBu chemistry and were then compared for their uptake efficiency and cellular distribution on NIH/3T3 cells by fluorescence spectroscopy and microscopy.

Substitution of cysteine by serine
KMDCRWRWKC**S**KK
KMDCRWRWK**S**CKK
KMD**S**RWRWKCCKK
KMDCRWRWK**SS**KK
KMD**S**RWRWK**SS**KK
KMD**S**RWRWK**S**CKK
KMD**S**RWRWKC**S**KK

Random deletions
KDCRWRWKCCKK
KCRWRWKCCKK
KRWRWKCCKK

Substitution of cysteines and tryptophans
KMDCRWR**P**KCCKK
KMDCR**P**R**P**KCCKK
KMD**X**R**P**R**P**KCCKK
KMD**X**R**P**R**P**K**X**CKK
KMD**X**R**P**R**P**KC**X**KK
KMDCR**P**R**P**K**X**CKK
KMDCR**P**R**P**KC**X**KK

Crot (27-39)
KMDCRWRWKCCKK

Substitution
KMD**X**RWRWKCCKK
KMD**X**RWRWK**X**CKK
KMD**X**RWRWK**XX**KK
KMD**X**RWRWKC**X**KK
KMDCRWRWKC**X**KK

Deletion
KMDCRWRWKCKK
KMDCRWRWKKK
KMDRWRWKKK
MDCRWRWKCCKK
DCRWRWKCCKK
CRWRWKCCKK
RWRWKCCKK

Deletion & substitution
MDCRWRWK**X**CKK
DCRWRWK**X**CKK
DCRWRWKC**X**KK
CRWRWK**X**CKK
CRWRWKC**X**KK
RWRWK**X**CKK
MDCRWRWK**XX**KK
DCRWRWK**XX**KK
CRWRWK**XX**KK
RWRWK**XX**KK

CRWRWKCCKK

Figure 6: Various modifications introduced into Crot(27-39)

2.1 Results

2.1.1 General synthesis

Peptides were synthesized on solid phase by Fmoc/tBu strategy using DIC/HOBt mediated coupling (Figure 7) on a preloaded TCP-resin. Fmoc deprotection was performed by 20% piperidine/DMF and each coupling was performed for 60 min. Deprotection and couplings were monitored by Kaiser Test (Sarin *et al*., 1981) in case of manual synthesis of the peptides. For structure activity studies all peptides were labeled with FITC through a Boc-Lys(Fmoc)-OH as a linker where the ε-group of N-terminal lysine was labeled with FITC. In order to avoid side reactions coupling of fluorophore was performed on resin at the end of the synthesis. Peptide fluorescein conjugates were cleaved off the resin by Reagent K after 2h and precipitated with MTBE two times. Samples were dissolved in water and tert-butanol (1:4) containing 2% acetic acid and freeze-dried. Screening of the peptides was done in the crude form where peptide purity was above 85%. 60 peptides were screened for internalization and cellular distribution and only selected samples showing considerable uptake were purified and tested again.
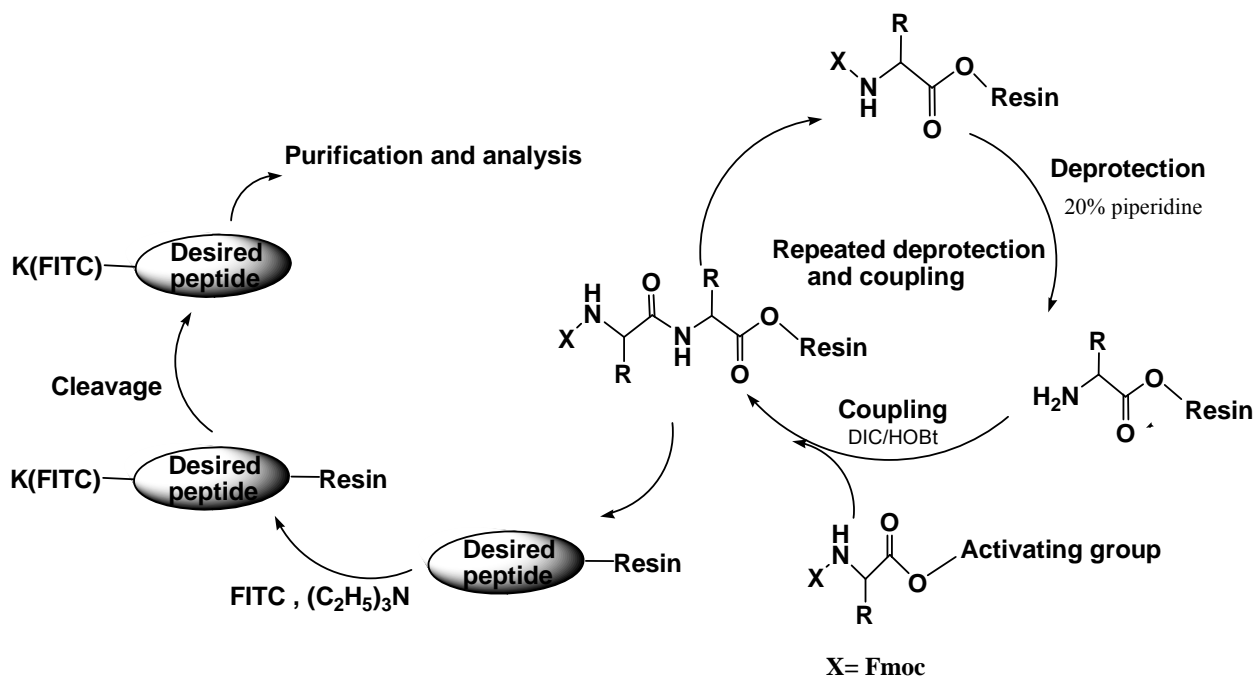
Figure 7: Schematic representation of the peptide synthesis

19

2.1.2 Resin selection (C-terminal functional group)

The effect of minimal structural differences on internalization was addressed for peptides with a free or amidated C-terminus. Amide group at the C-terminus renders stability towards exogenous peptidases and also maintains the native structure of the peptide, if the peptide is derived from natural source. Thus, comparison of protease stable C-terminal amide and protease susceptible free C-terminal end was made. Peptides were synthesized on TCP as well as Rink amide resin offering -COOH or -CONH$_2$ groups, respectively, at the C-terminus. A decrease in the uptake in case of the amide compared to free C- terminus was observed.

2.1.3 Racemization

The application of peptides as drug and other biological targeting agents essentially requires the stereochemical integrity of the peptides. Therefore, measures are taken to maintain stereochemical fidelity of the diverse molecules. Racemization is a serious problem in the peptide synthesis (Siedler *et al*., 1996). Irrespective of the thiol protecting groups used in the synthesis of cysteine rich peptides, propensity of racemization still persists. Also the ester linkage to the resin has an impact on the rate of racemization. Activation protocols incorporating the presence of base, results in measurable level of racemization (Han *et al*., 1997). For example during the coupling reaction performed by TBTU/HOBt in the presence of the base considerable racemization was shown whereas in the absence of the base (via pentafluorophenylester) epimerization was suppressed (Siedler *et al*., 1996). Therefore, a judicious choice of the parameters like resin as well as the coupling reagents used has a direct impact on the epimerization.

Some of the potential steps to minimize racemization-

- ➢ HOBt as a racemization suppressing additive is used as it is known to suppress the chiral purity (Wieland and Bodanszky, 1991)
- ➢ Level of racemization was reduced immensely by avoiding the preactivation step in case of BOP, HATU, HBTU mediated couplings and introducing 5 min preactivation in case of DIC/HOBt couplings (Han *et al*., 1997).

- Application of a weaker base like 2, 4, 6 trimethylpyridine (TMP, collidine) instead of DIPEA, NMM, reduction in the amount of base or optimization of the solvent preference DMF to less polar DCM: DMF (1:1) (Han *et al*., 1997).
- Enantiomerization is observed in activation of Fmoc-Cys(Trt)-OH with base mediated coupling reagents like TBTU (Han *et al*., 1997). Proper choice of the coupling conditions are required to reduce this problem.

In this concern avoiding the base during the coupling steps and uronium type coupling agents advocates the need to optimize the coupling conditions for these syntheses of multiple cysteine containing peptides. Thus, the coupling reagent used in this synthesis was DIC/HOBt as it induces minimal racemization in the course of the synthesis (Han *et al*., 1997). Stereochemical purity of peptide was determined by GC-MS analysis and was found to be >95% (C.A.T. GmbH&Co, Chromatographie und Analysentechnik KG**,** Tübingen, Germany) ensuring the chiral integrity of the peptide backbone.

2.1.4 Optimization of cleavage cocktail

As the peptides in this study are rich in cysteine, the presence of a reductive environment is necessary in order to keep this amino acid in the reduced state. Therefore appropriate choice of scavengers was necessary. Therefore, various cleavage cocktails were prepared and tested in order to achieve an optimal ratio of the required scavengers (Table 2). Peptides were exposed to the cleavage mixture for 1 h and the precipitate was tested by ESI-MS. Amongst five cleavage cocktails tested, Reagent K gave the best results. Thus, Reagent K was further used as a cleavage mixture for the peptides.

Table 2: List of tested cleavage cocktails

S.No.	Composition	Percentage
1	TFA: phenol: water: thioanisole: EDT (Reagent K)	82.5:5:5:5:2.5
2	TFA: thioanisole: EDT: anisole (Reagent R)	90:5:3:2
3	TFA: phenol: water: thioanisole: EDT	95:2:1:1:1
4	TFA: Reagent K: TMSBr	85:14.5:0.5
5	TFA: phenol: water: thioanisole: EDT	85:2.5:5:5:2.5

2.1.5 Ether selection

In order to confirm the contribution of the ether in tert-butylated byproduct DEE and MTBE were used as precipitating agents. Peptide was cleaved by reagent K followed by precipitation with DEE or MTBE. In contrast to the report of De La Torre and Andreu, 2008, the effect of the ether was not significant emphasizing that the precipitating agent plays no role and indicating a direct scavenging of the tert-butyl cation by any of the alkylation prone amino acid residue like Trp or Cys.

2.1.6 Counter ion purity- TFA and acetate content

TFA is a common additive to the solvent system used during reverse-phase HPLC purification of peptides. It is effective in solubilizing hydrophobic peptides because of its high acidity. It is also a purification contaminant as it binds to side chain of exposed arginine, lysine and histidine. Though it is a volatile component, it is known to bind to the proteins as revealed by IR data and induces structural modifications in proteins and peptides (Gaussier *et al*., 2002, Cornish *et al*. 1999). As it is harmful for cells it needs to be eliminated from the samples. Prior to the biological evaluations, efforts have been made to eliminate TFA from the samples by passing through dialysis membranes or multiple freeze drying in the presence of HCl. Concentration of HCl in the range of 2-10 mM was reported to be effective in removing TFA impurities without affecting the peptide (Andrushchenko *et al*., 2007). Therefore, multiple freeze drying with 2 mM HCl was done.

Another attempt to get rid of this counter ion from the samples was freeze drying with tert-butanol and water (4:1) containing 2% acetic acid. The sample was checked for its TFA and acetate content by GC-MS. Measured content of 19.5% TFA and only 0.1% acetate indicates that probably 2% acetic acid was not sufficient for complete exchange of TFA. Thus, the percentage was increased to 5% acetic acid.

Both methods of TFA exchange were comparable, therefore, drying with tert- butanol and 5% acetic acid was carried out for further samples.

2.1.7 Uptake studies

Cell experiments were performed with NIH/3T3 mouse fibroblast cells. Cells were cultured in 96 well microplates for 24 h followed by incubation with fluorescent labeled peptides for additional 18 h. After incubation, cells were counter stained with H33342 for nuclear labeling. External fluorescence was quenched by trypan blue for 3 mins followed by repeated HBSS washings. Cell related FITC fluorescence (CA, green) and nuclear fluorescence (H33342, blue) was evaluated in a multi-plate reader. Subsequently, fluorescence microscopy was performed with the same cells to observe the cellular localization.

2.1.8 Structure Activity Relationship Studies

The initial tridecapeptide Crot(27-39) (peptide 1) was proposed to bear the cell penetrating property (Yamane *et al*., 2006). The presence of lysines and arginines was proposed to support this prediction. Therefore, Crot(27-39) was synthesized and tested on cells for its uptake properties. Apart from being an appropriate candidate as a Cell Penetrating Peptide (CPP) it displayed a unique quality of cytosolic distribution at low concentrations. This additional feature distinguishes it from other CPPs and opens a new avenue for the further optimization. Crot(27-39) includes three cysteine residues, tryptophans, aspartic acid, and methionine along with six basic amino acids (arginine and lysine). Substitution and/or deletion of various amino acids except lysine and arginines (like cysteine, tryptophan, methionine, aspartic acid) in Crot(27-39) were further studied (Table 3).

2.1.8.1 Substitution of cysteine residues

Because of the side reactions associated with cysteine, these residues in Crot(27-39) were substituted by serine and α-amino-n-butyric acid (Abu). Cysteines were replaced one by one and then all together to study the effect of exchange as well as the tolerated number of cysteines being substituted. A set of seven serine substituted peptides with single cysteine exchange [peptide 2-4], dual substituted cysteines [peptide 5-7] and replacement of all 3 cysteines [peptide 8] by serine were synthesized and compared to the initial sequence peptide 1.

Results show a decrease in the cellular uptake along with the number of cysteine substitutions (Figure 8). Complete substitution resulted in complete loss of uptake as well as decrease in the cytosolic gain in the cells.
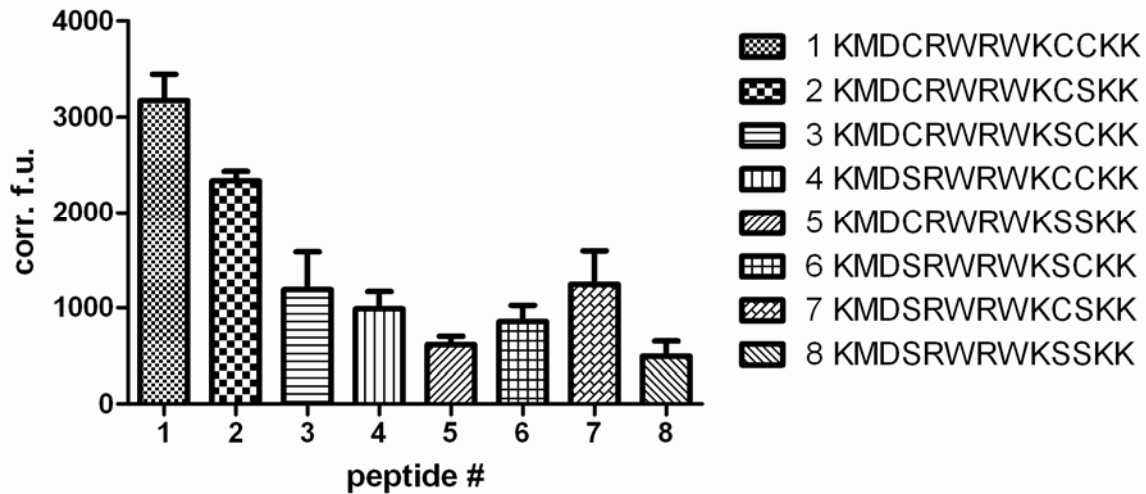
Figure 8: Influence of cysteine substitution by serine on internalization

In order to confirm the reduced uptake and distribution as a function of cysteine replacement by serine, another set of peptides with cysteines substituted by α-amino-*n*-butyric acid (Abu) was studied. Five different mutants with replacement of one, two and three cysteines were synthesized [Peptides 9-13]. Internalization studies showed a decrease in uptake efficiency along with the decrease in the number of cysteines (Figure 9).
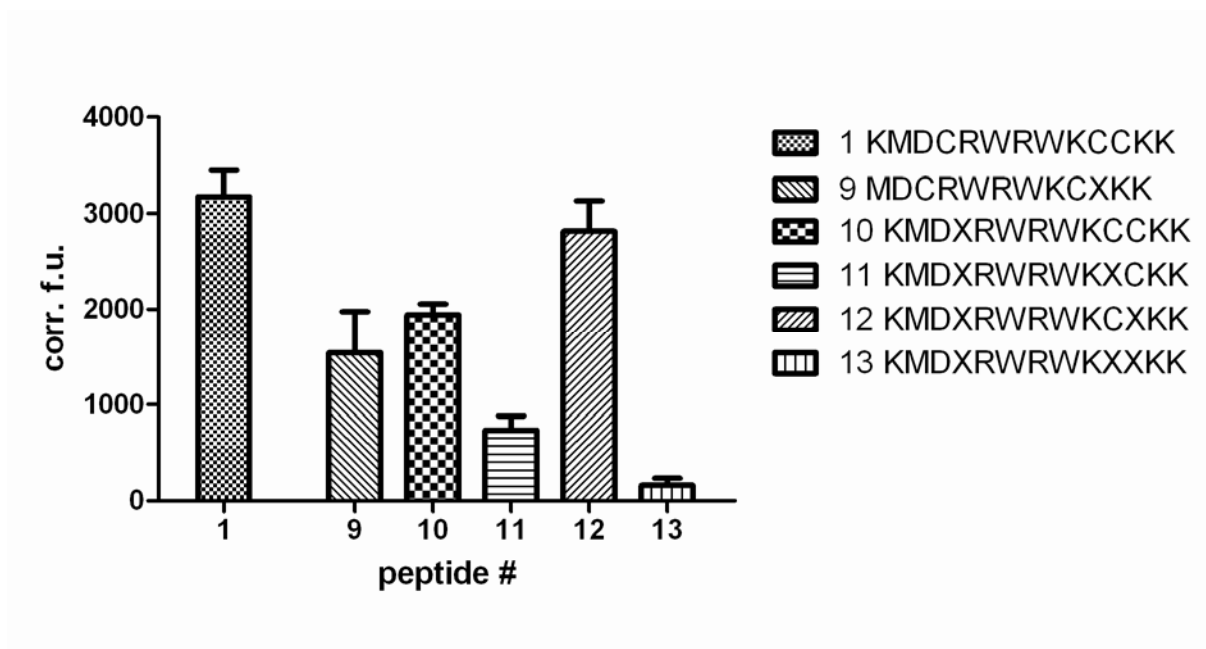
Figure 9: Influence of cysteine substitution on internalization

2.1.8.2 Deletion of cysteine residues

Determining the optimal length of the sequence was also one of the main concerns for SAR studies. Thus, still focusing on the cysteines, peptides were synthesized by the deletion of cysteines one by one [Peptides 14-16]. The results confirmed the observation made with serine/Abu substituted peptides of Crot(27-39). A regular decrease in uptake and cytosolic appearance with the number of deleted cysteines was observed (Figure 10).
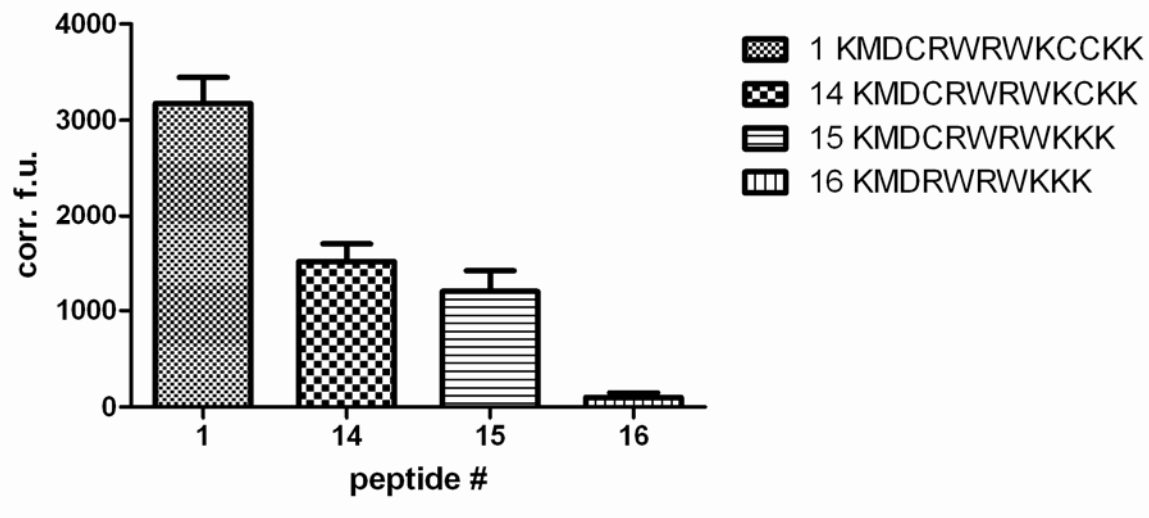
Figure 10: Influence of deletion of cysteines on internalization

2.1.8.3 Substitution of tryptophan by proline residues

Inclusion of a small hydrophobic moiety (biotin) in Tat peptide is shown to increase the cellular uptake (Chen *et al*., 1995). Alterations in the hydrophobic and hydrophilic content of Hel amphipathic peptide, showed an efficient DNA delivery by the region of highest hydrophobic amino acid residues. This could be attributed to the formation of aggregates on delivering the non-covalently bound DNA (Ohmori *et al*., 1998). Effect of modulating the hydrophobicity was also seen in case of penetratin (Dom *et al*., 2003). Lipophilization at the N-terminus by stearoyl, lauroyl, or cholesteryl group is another example where the influence of hydrophobicity on intracellular delivery was studied in case of Tat and polyarginines (Futaki *et al*., 2001). Thus from these observations it was believed that in addition to electrostatic surface interactions hydrophobic interactions also contribute significantly to the process of transmembrane delivery. Therefore, the role played by tryptophan residues was also verified by replacing them one by one with the prolines residues.

The results show a decrease of the uptake efficiency by substitution of tryptophan by prolines (Figure 11). Loss of uptake and cytosolic distribution was observed.

2.1.8.4 Substitution of tryptophan by proline residues and cysteine residues by Abu

In order to study the cumulative effect of both tryptophans and cysteines, a set of peptides with cysteines substituted by Abu concomitant with tryptophan replaced by prolines were synthesized [Peptides 17-23]. A significant decrease in the uptake efficiency and intracellular distribution was observed (Figure 11) supporting the importance of both amino acids in the peptide sequence to maintain the internalization behavior.
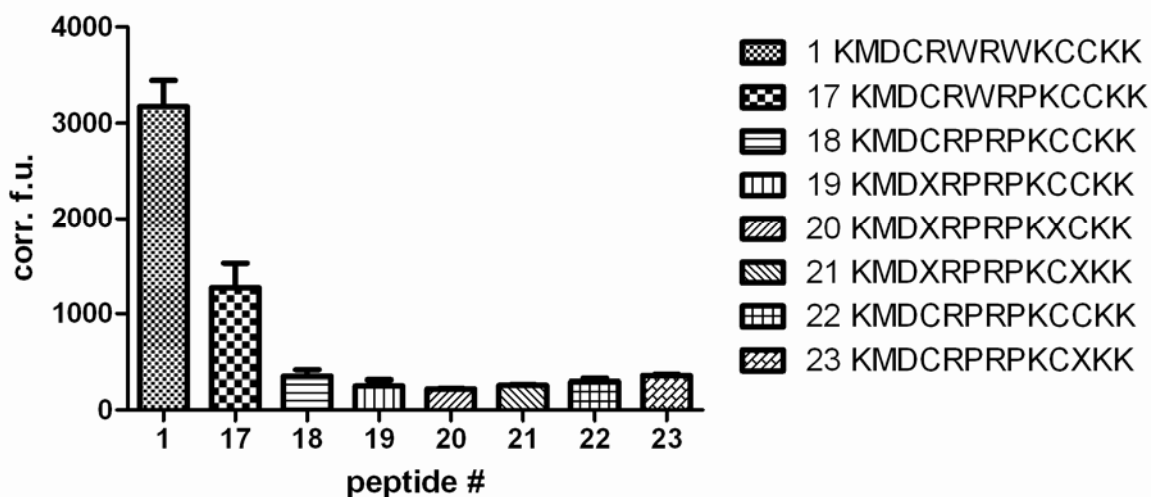
Figure 11: Influence of cysteine and tryptophan substitution on internalization

2.1.8.5 Deletions and substitution of cysteine residues

Deletions as well as substitutions had a great impact on the intracellular localization. Therefore, deletions were further accompanied by substitution of cysteines by Abu in order to study the combined effect of both variations [peptides 24-33]. Various mutants with simultaneous cysteine substitution by Abu and N-terminal deletion of amino acid residues were synthesized. This resulted in a significantly reduced cellular uptake and cytosolic gain (Figure 12). Though there seems to be an influence of length of the peptide chain on the internalization properties but a more pronounced effect was observed for the substitution of cysteine residues.
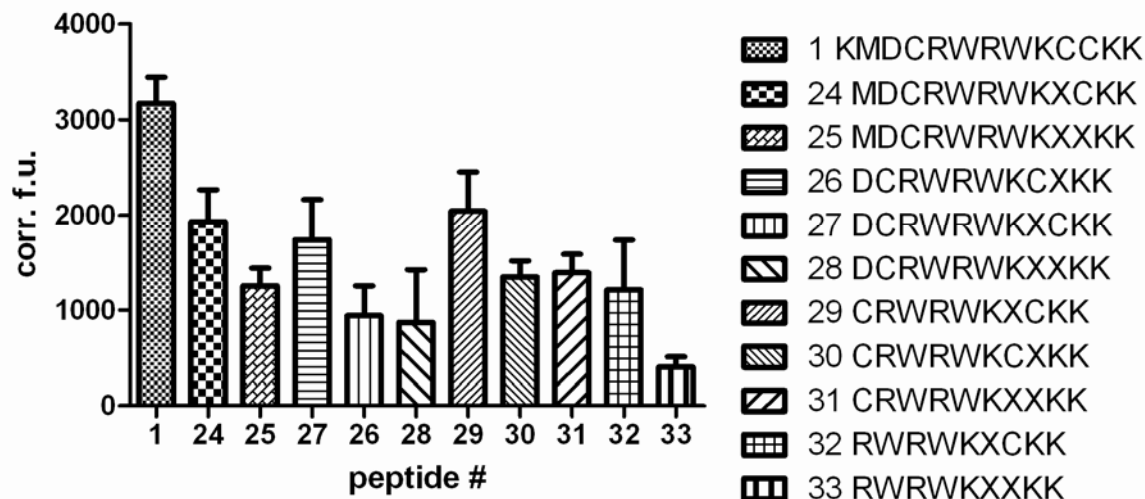
Figure 12: Influence of deletion and substitution on internalization

2.1.8.6 Deletions

Keeping the positively charged amino acids untouched, deletions of other amino acids like methionine or aspartic acid were investigated. Therefore mutants with deletion of methionine, aspartic acid and cysteine were synthesized and analyzed [peptide 34-36]. Similarly, systematic deletion of amino acid residues other than arginines and lysines one by one from the N-terminus in peptide 1 [peptides 37-40] were also done to get an idea about the minimal length required to maintain the uptake efficiency.

Difference in the uptake behaviour and cytosolic distribution were observed with the removal of amino acids one by one from N-terminus or randomly in the sequence. Deletion of methionine, aspartic acid and cysteine showed a decrease in internalization whereas in the case of systematic deletions variations in the uptake efficiency of these peptides was observed (Figure 13). One amongst these i.e. peptide 39 showed the highest uptake efficiency and cytosolic distribution pattern.
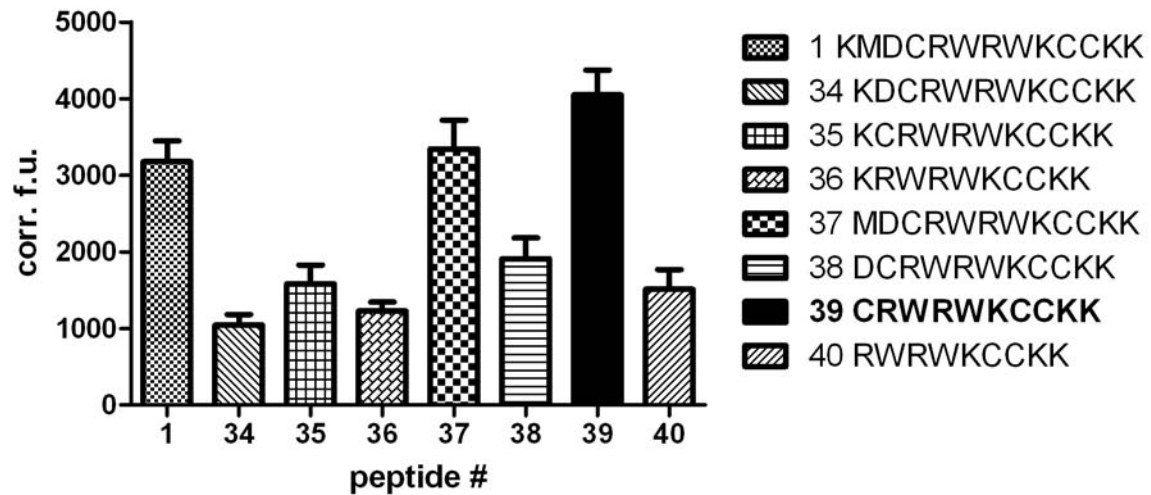
Figure 13: Influence of deletions on internalization

Screening of the peptides for their intracellular delivery and distribution figured out peptide 39 as the best mutant showing highest delivery efficiency. Therefore studies were further carried out to optimize this peptide. Peptide 39 will from now on be referred to as CyLoP-1 (Cytosol Localizing Peptide).

2.1.9 Distinct features of CyLoP-1

CyLoP-1 is a short cysteine rich peptide of ten amino acids showing the best internalization efficiency amongst all tested variants. This fragment was three amino acids shorter and more efficient than the initial starting sequence.
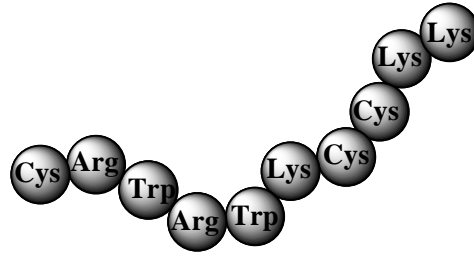
CyLoP-1 = Cytosol Localizing Peptide-1

- Short peptide **CRWRWKCCKK**
- Cysteine rich
- Best internalization efficacy (of all mutants)
- Mainly cytosolic (diffused) localization at 2.5 µM

Interestingly, CyLoP-1 showed an approximately 20% more efficient uptake compared to peptide 1 (Figure 14) and exhibited uniformly distributed cytoplasmic fluorescence along with endosomal, vesicular fluorescence (Figure 15) at concentration of 2.5 µM.
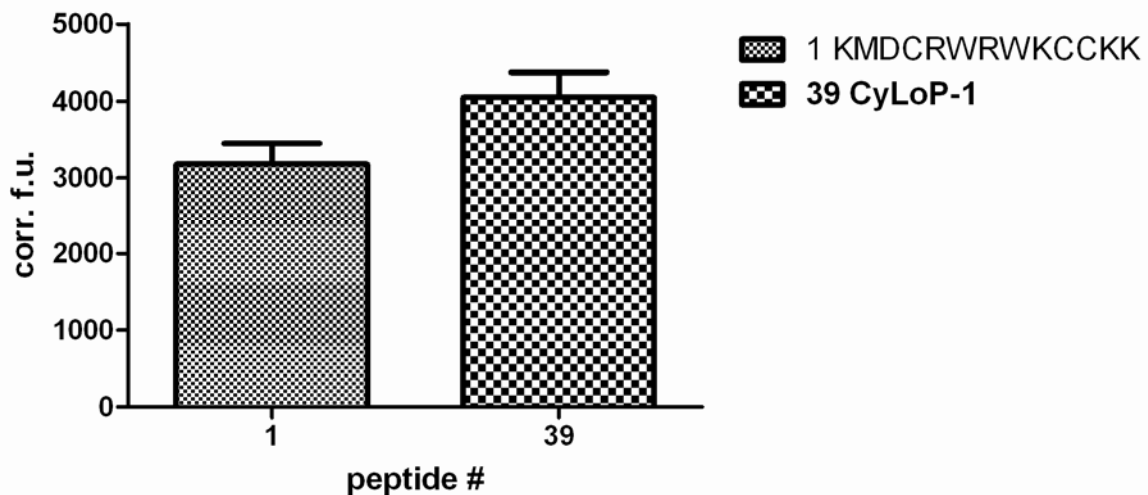
Figure 14: Comparison of intracellular uptake of Peptide 1 and CyLoP-1
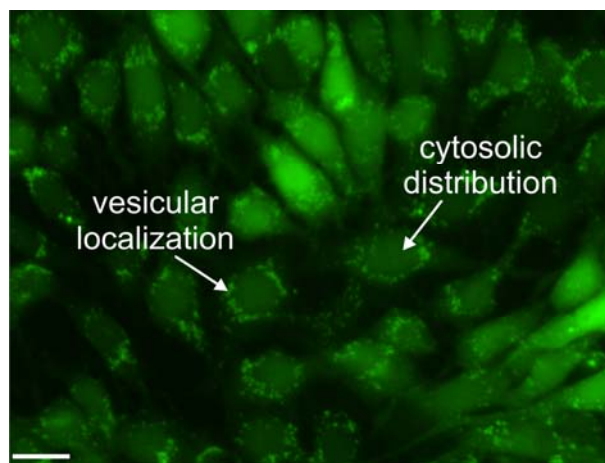
Figure 15: Intracellular fluorescence distribution of K(FITC)-coupled CyLoP-1 in 3T3 cells.

The bright punctate and encapsulated FITC fluorescence was categorized as vesicular uptake while fluorescence distributed in the entire cell with similar intensity was designated as diffused. The bar represents 20 μm.

2.1.10 Optimization of CyLoP-1

Since CyLoP-1 showed the best results in the initial screening, further studies were carried out to evaluate and eventually optimize this fragment. Here again more specifically substitution of cysteines and tryptophans were tested along with stereochemical modifications (Figure 16).

CRWRWKCCKK
CyLoP-1

⟱

Substitution of cysteine	**Stereochemical changes**	**Substitution of tryptophan**
CRWRWKCSKK	**crwrwkcckk**	
CRWRWKSSKK	**kcckwrwrck**	
SRWRWKSSKK	C**r**WRWKCCKK	CRFRWKCCKK
SRWRWKCSKK	CR**w**RWKCCKK	CRWRFKCCKK
SRWRWKSCKK	CRW**r**WKCCKK	CRFRFKCCKK
SRWRWKCCKK	CRWR**w**KCCKK	
	C**rwrw**KCCKK	
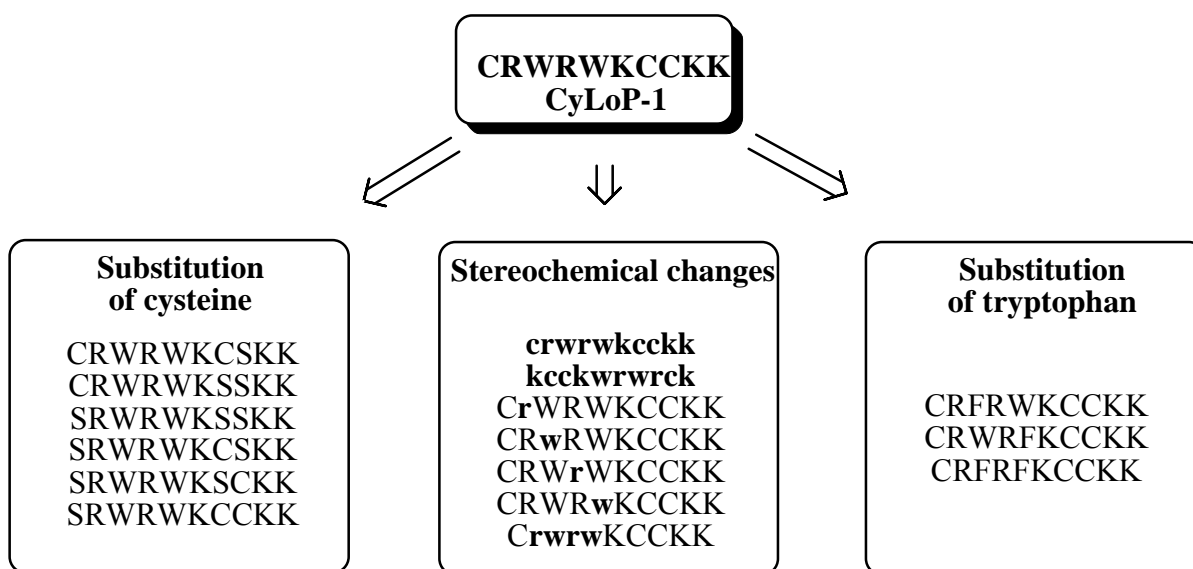
Figure 16: Various mutations included in CyLoP-1

2.1.10.1 Cysteine substitution by serine residue in CyLoP-1

The significance of cysteines for internalization in CyLoP-1 was determined by replacing cysteine residues with serine. Substitution of one to three cysteine(s) by serine(s) in CyLoP-1 [peptides 41-46] revealed a regular decrease in the uptake efficiency with the number of cysteines being replaced. Total exchange led to a nearly complete loss of activity (Figure 17). Therefore, the number of cysteines in CyLoP-1 is vital for internalization and especially for cytosolic diffusion.
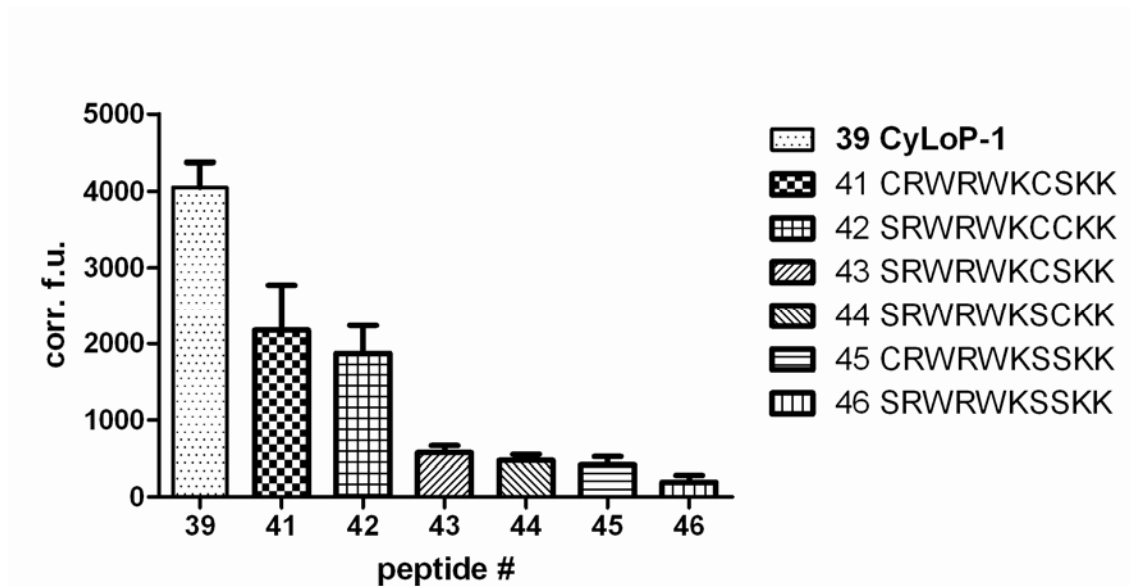
Figure 17: Influence of cysteine substitution by serine in CyLoP-1 on internalization

2.1.10.2 Tryptophan substitution

The presence of tryptophans had been illustrated to participate in membrane permeation. Dom *et al,* 2003 showed an effect of modulating the hydrophobicity, on the cellular uptake in case of penetratin. Almost complete loss of internalization was observed after the change of the tryptophan 6 residue (W6) into a phenylalanine (W6F mutant). Tryptophans are reported to destabilize the membrane once the peptide is adhered to the surface (Dom *et al.*, 2003).

To examine these effects in CyLoP-1, replacement of one or both tryptophans by phenylalanine was investigated [peptides 47-49]. A decreased uptake and almost complete loss of diffusion was observed (Figure 18).
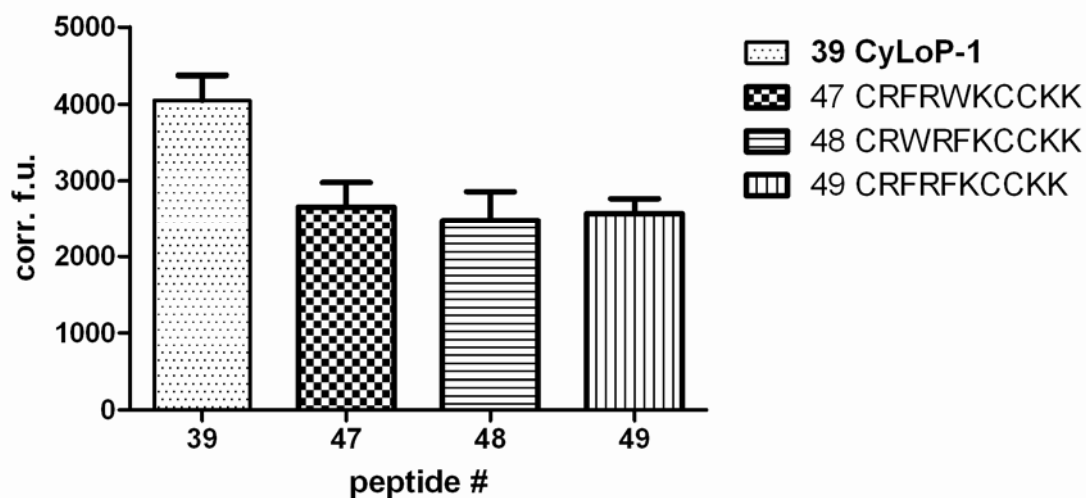
Figure 18: Influence of tryptophan substitution by serine in CyLoP-1 on internalization

2.1.10.3 Stereochemical effects

CPP based delivery approach is potentially hampered by the instability of the vector to endogenous peptidases (Wender *et al.*, 2000). A potential solution to this hurdle could be the use of D-amino acids instead of the naturally occurring L-amino acids, or the use of beta-peptides (Rueping *et al.*, 2002) or peptoids (Wender *et al.*, 2000) to enhance vector stability. In this concern we studied further analogues of CyLoP-1 to evaluate the influence of the stereochemistry of the peptide backbone (enantiomeric purity of CyLoP-1 was about 95% as shown by GC-MS analysis on chiral phase, C.A.T. GmbH&Co, Chromatographie und Analysentechnik KG**,** Tübingen, Germany) as well as the sequence alignment. The incorporation of D-amino acids and reversal of the sequence (inverse isomers) of the peptide is shown to increase the transmembrane delivery in the case of the Tat peptide (Wender *et al.*, 2000). Therefore, the D-isomer (peptide 50) and L-inverse as well as D-inverse isomers of CyLoP-1 (peptide 51, peptide 52) were synthesized. Unexpectedly, these analogues showed reduced uptake by about 50% (Figure 19).

In addition, the Arg-Trp-Arg-Trp domain of the peptide sequence seems to be a key feature in CyLoP-1 CPP paradigm, as indicated from the results of the SAR studies. Thus the effects of configurational changes were examined with restriction to this region [peptide 53-57, 102]. As a

result the internalization was reduced to about 40% accompanied with a decrease in cytoplasmic diffusion as compared to CyLoP-1. These results demonstrate that chiral inversion of the residues has a clear effect on cellular uptake of CyLoP-1. Unlike known CPPs, CyLoP-1 proved to be most efficient in its natural L-amino acid form.
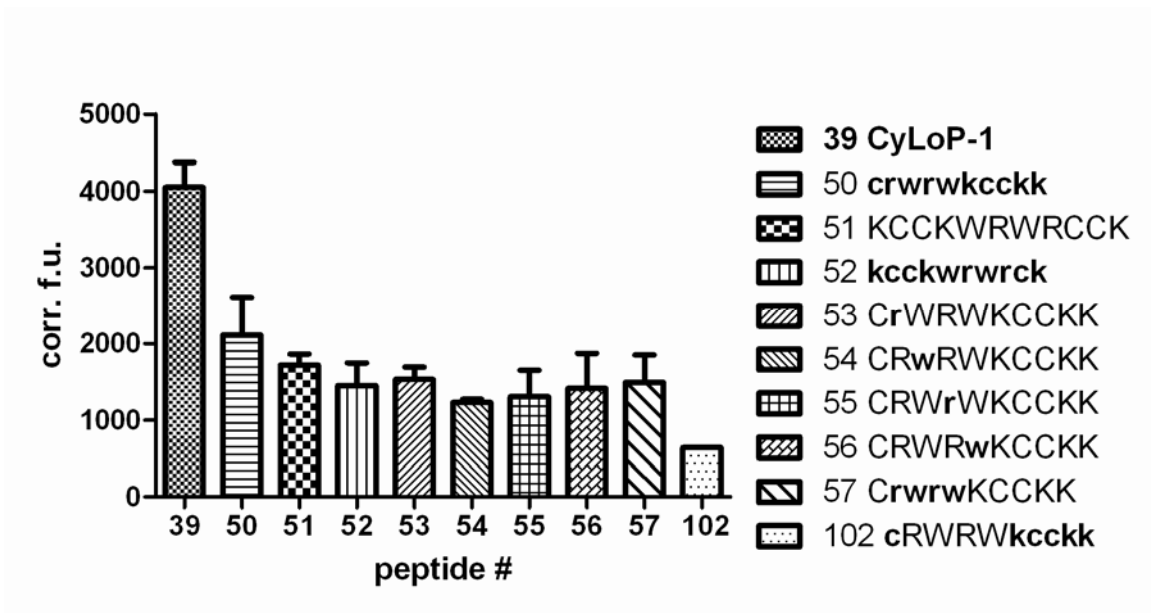
Figure 19: Influence of stereochemistry of CyLoP-1 on internalization

Table 3: List of all the synthesized peptides, the calculated and observed molecular masses are shown. X= α-amino-*n*-butyric acid. All peptides were elongated with K or k FITC at the N-terminus. Intracellular fluorescence intensity values in NIH/3T3 cells were measured after a labeling period of 18 h at 2.5 µM. D-amino acids are represented in lower case.

Peptide	Sequence	Molecular weight		Intracellular fluorescence intensity [corr. f.u.]		% of CyLoP-1
		Expected $(M+H)^+$	Observed $(M+H)^+$	Mean	SEM	
1	KMDCRWRWKCCKK	2288.7	2288.6	3176	271	78
	Peptide 1					
2	KMDCRWRWKCSKK	2272.7	2274	2335	99	58
3	KMDCRWRWKSCKK	2272.7	2274.4	1188	398	29
4	KMDSRWRWKCCKK	2272.7	2274.4	987	181	24
5	KMDCRWRWKSSKK	2256.6	2257.2	615	87	15
6	KMDSRWRWKSCKK	2256.6	2257.6	856	171	21
7	KMDSRWRWKCSKK	2256.6	2259	1244	350	31
8	KMDSRWRWKSSKK	2240.5	2240.8	496	156	12
9	KMDCRWRWKCXKK	2142.5	2143.6	1542	433	38
10	KMDXRWRWKCCKK	2270.7	2272	1943	114	48
11	KMDXRWRWKXCKK	2252.6	2253.2	734	149	18
12	KMDXRWRWKCXKK	2252.6	2253.8	2816	317	70
13	KMDXRWRWKXXKK	2234.6	2236	162	74	4
14	KMDCRWRWKCKK	2185.6	2186.4	1516	181	37
15	KMDCRWRWKKK	2082.4	2084.7	1202	218	30
16	KMDRWRWKKK	1979.3	1979.6	100	50	2
17	KMDCRWRPKCCKK	2199.6	2200	1272	255	31
18	KMDCRPRPKCCKK	2110.5	2110.8	347	68	9
19	KMDXRPRPKCCKK	2092.5	2092.8	251	62	6

20	KMDXRPRPKXCKK	2074.4	2074.6	222	8	5
21	KMDXRPRPKCXKK	2074.4	2075.8	257	12	6
22	KMDCRPRPKXCKK	2092.5	2093.6	294	33	7
23	KMDCRPRPKCXKK	2092.5	2092.8	353	15	9
24	MDCRWRWKXCKK	2142.5	2142	1937	335	48
25	MDCRWRWKXXKK	2124.5	2124.8	1256	187	31
26	DCRWRWKXCKK	2011.3	2013	1741	427	43
27	DCRWRWKCXKK	2011.3	2011.6	943	313	23
28	DCRWRWKXXKK	1993.3	1993.8	872	554	22
29	CRWRWKXCKK	1896.2	1897	2044	408	50
30	CRWRWKCXKK	1896.2	1896.6	1347	171	33
31	CRWRWKXXKK	1878.2	1880	1390	199	34
32	RWRWKXCKK	1793.1	1793.1	1211	529	30
33	RWRWKXXKK	1775	1776.2	405	109	10
34	KDCRWRWKCCKK	2157.5	2159.2	1043	137	26
35	KCRWRWKCCKK	2042.4	2043	1583	246	39
36	KRWRWKCCKK	1939.3	1940.8	1226	120	30
37	MDCRWRWKCCKK	2160.5	2162	3344	374	83
38	DCRWRWKCCKK	2029.3	2031	1909	272	47
39	CRWRWKCCKK CyLoP-1	1914.3	1914	4050	322	100
40	RWRWKCCKK	1809.1	1811.3	1511	256	37
41	CRWRWKCSKK	1898.2	1899	2172	597	54
42	SRWRWKCCKK	1898.2	1898.6	1867	367	46
43	SRWRWKCSKK	1882.1	1881.9	572	94	14
44	SRWRWKSCKK	1882.1	1882.4	475	77	12

45	CRWRWKSSKK	1882.1	1882.6	415	109	10
46	SRWRWKSSKK	1866.1	1866	193	89	5
47	CRFRWKCCKK	1875.2	1875.6	2656	320	66
48	CRWRFKCCKK	1875.2	1875.8	2476	382	61
49	CRFRFKCCKK	1836.2	1836.8	2569	197	63
50	KKCCKWRWRC	1914.3	1914.8	2109	503	42
51	crwrwkcckk	1914.3	1914.9	1713	148	52
52	kcckwrwrck	1914.3	1914.9	1449	295	36
53	CrWRWKCCKK	1914.3	1916	1529	163	38
54	CRwRWKCCKK	1914.3	1914.8	1229	40	30
55	CRWrWKCCKK	1914.3	1915	1304	345	32
56	CRWRwKCCKK	1914.3	1915.8	1412	456	35
57	CrwrwKCCKK	1914.3	1915	1488	360	37

2.2 Discussion

Different mutants of Peptide 1 were synthesized by Fmoc/tBu strategy. All variants were labeled with FITC at the N-terminus on the ε-amino group of the linker lysine. Synthesis was optimized to ensure minimal racemization which is a serious problem in case of cysteine rich peptides. Choice of coupling agents comprising of DIC/HOBt was suggested to minimize racemization (Hans *et al*, 1997) thus it was used in the synthesis of the peptides. In order to maintain the reduced state of cysteines, proper choice of the cleavage cocktail was also optimized. Thus, the choice of scavengers like EDT was considered. Apart from maintaining the reduced state it is also know to be an extremely good scavenger for tert-butyl cations released during the cleavage of the peptide. It also helps to remove the trityl protecting group and prevents acid catalyzed oxidation of tryptophan residues. On the other hand, prolonged exposure of tryptophan containing peptides to EDT/ TFA mixtures could lead to enhanced substitution of mercaptan into the indole nucleus (Johnson *et al*., 1991). Therefore exposure of the peptide to cleavage cocktail was limited to 60-90 min. As the peptide sequence is rich in tryptophan and cysteine one could

think about tert-butyl cation being scavenged by these residues. De La Torre and Andreu, 2008, showed the effect of the ether on alkylation of peptide and PNA sequences. They showed that the tert-butyl cation could be released from the butyl based protecting group but also during MTBE workup as MTBE can undergo cleavage under the strong prevailing acidic cleavage conditions. Thus, for sequences with increasing number of aromatic residues (PNA monomers) or alkylation prone residues (Trp, Tyr, Cys, and Met) the use of DEE over MTBE was strongly recommended. Therefore, DEE was preferred over MTBE as precipitating agents in our studies. However no significant difference was observed in the reduction if tBu cation irrespective of the used ether. Different methods to reduce the TFA content in the peptides were also optimized. FITC labeled mutants of peptide 1 were screened as crude products (purity >85%) for intracellular uptake and distribution by fluorescence spectroscopy and microscopy.

Peptide 1 consists of amino acids like methionine, cysteines, tryptophans that are more prone to side reactions like oxidation, racemization and tert-butylation (Siedler *et al*., 1996; Huang *et al*., 1999; Wünsch *et al*., 1977; Giraud *et al*., 1999). Thus, in order to reduce the side products, SAR studies were performed by substituting and/or deleting these amino acids to achieve and optimal sequence. Variants with cysteines substitutions (with serine or Abu) and deletions were synthesized. Serine is a highly isosteric analogue of cysteine in terms of geometry and volume occupancy therefore generally used as cysteine substituent for structure activity relationship studies (Moroder *et al*., 2005). Abu is also shown to be isosteric with cysteine (Karim *et al*., 2001) and generally used as a substituent for cysteines. Substitutions by serine or Abu reduced the cellular uptake and cytosolic distribution. These results were in concordance with the results obtained by deletion of cysteines. Thus it can be concluded that cysteines are important as well as their number and location in the peptide also plays an important role in maintaining their function. Replacement or deletion of amino acids like cysteine and tryptophans negatively affected uptake and distribution pattern indicating that these amino acids are substantial in the sequence. The considerable hydrophobicity provided by tryptophans adds to the positive charge of the sequence. The high intracellular delivery and distribution might be the combined effect of both factors and could be involved in the mechanism of membrane penetration.

SAR studies resulted in, CyLoP-1, showing the best cellular internalization and cytosolic diffusion at low concentrations of 2.5 µM. CyLoP-1, a small cysteine rich decapeptide, is active

in its native L-form. Contrary to the Tat peptide, where the incorporation of D-amino acids and reversal of the sequence (inverse isomers), showed increase in internalization (Wender *et al.*, 2000), CyLoP-1 showed reduction in the cellular uptake of such variants. Thus, a negative effect of the stereochemical modification and sequence reversal was observed in case of CyLoP-1. Reduced cytosolic distribution and uptake by substitution of tryptophan with phenylalanine also signifies the substantial role played by the tryptophan residues. Results suggest that not only the presence but also the number of tryptophans are inevitable to maintain the required hydrophobicity and well functioning of CyLoP-1

Assuming both positive charge and hydrophobicity as key requirement for the internalization, uptake of CyLoP-1 can be divided in a two step process. First, the interaction of the peptide with the cell surface which is dependent on the charge neutralization as well as hydrophobicity (Dom *et al.*, 2003) followed by membrane destabilization and penetration. Reduction in the uptake and distribution profiles of the stereochemical analogues of CyLoP-1 also gives an indication of the specific orientation required for the facile permeation or the involvement of the receptors in the uptake of CyLoP-1. The molecular mechanism for the uptake of CyLoP-1 has not been determined yet but cytosolic diffusion may be the result of either direct uptake of the peptide or due to release from endosomes because of membrane disruption.

Because of the high reactivity of the thiol side chain, cysteine constitutes an important structural and functional component of proteins. The disulphide linkages within a polypeptide chain offer a secondary structure to the protein. Thus the role of cysteine in the peptide sequence is of shell importance and should be well considered. Though cysteine containing peptides increases complexities during synthesis and storage but adds to the differences in the biological activity when they are present in reduced or oxidized forms. The replacement of cysteine residues in CyLoP-1 by its isosteric analogues serine and Abu, showed a significant decrease in the uptake and distribution inside the cell implying the importance of cysteine in CyLoP-1. Thus not only the number of cysteine but also the position of cysteine residues in the sequence is of paramount importance. Hence in our case, it has been found that CyLoP-1 actually requires all three cysteines and two tryptophans to show optimal internalization properties.

Therefore one could foresee the role played by the cysteine residues in membrane permeation. They could be involved in the cross linking with the serum proteins at physiological conditions

conferring a special structure enhancing the uptake. NMR studies however show that no definite structure was obtained by CyLoP-1 at pH 4 or pH 6.5 in aqueous solution. Presuming the effect of oxidation on the uptake mechanisms further studies were done to elucidate this concept.

2.3 OXIDATION STUDIES

Disulphide bonds are the essential structural element in extracellular peptides and proteins (eg. toxins, enzymes inhibitors, growth factors). They impart considerable conformational restraints and serve to induce and maintain bioactive foldings. Intramolecular disulphides could covalently crosslink the far regions of a linear polypeptide sequence giving it a close three-dimensional structure. Intermolecular cysteines lead to cysteine networks (from isomeric to polymeric products). Complexities increases with increasing the number of cysteines. Regioselective disulphide formation is still a challenge in the synthesis of cysteine containing peptides and proteins. Intermolecular oligomerizations often lead to low yields, disulphide scrambling as well as modifications of the side chain of sensitive amino acids. Careful experimental conditions are required for accomplishing the correct folding.

As CyLoP-1 is rich in cysteines there are number of potential intra and intermolecular cysteine connectivities. CyLoP-1 consists of three cysteines at positions 1, 7, 8 bearing a pair of adjacent cysteines. The chance of intramolecular disulphide linkage is relatively rare unless both the cysteines are present in the cis-form which is thermodynamically favorable. In order to comprehend the role of cysteine on the uptake efficiency various disulphide analogues of CyLoP-1 were synthesized (Table 4).

2.3.1 Results

2.3.1.1 Synthesis

The synthesis scheme was not changed to generate these peptides with the exception of the protecting groups used for the cysteine side chain protection. In case of the reduced peptides Fmoc-Cys(Trt)-OH was used as a common protecting group for sulphydryl groups. But in case of the oxidized peptides different protecting groups were used in order to specifically cleave and oxidize two cysteines without affecting the third one.

2.3.1.1.1 Synthesis of tBu protected CyLoP-1 peptides

Syntheses of tBu protected peptides were done on solid phase by the general scheme discussed in the experimental section. Different cysteine side chain protecting groups were used at different position in order to achieve the defined product. Fmoc-Cys(tBu)-OH is stable to TFA cleavage conditions, therefore, Fmoc-Cys(Trt)-OH along with the cysteine tert butyl derivative was used for this synthesis. After synthesis, peptides were cleaved off the resin by Reagent K, containing EDT, yielding the reduced protected product.

Table 4: Synthesized combinations of intramolecular disulphide linkages in CyLoP-1

S.No.	Sequence
1.	K(FITC)-C-R-W-R-W-K-C-C-K-K with S(tBu) on first C, and C-C bridge to S(tBu), S(tBu)
2.	K(FITC)-C-R-W-R-W-K-C-C-K-K S(tBu)
3.	K(FITC)-C-R-W-R-W-K-C-C-K-K S(tBu)
4.	K(FITC)-C-R-W-R-W-K-C-C-K-K S(tBu)
5.	K(FITC)-C-R-W-R-W-K-C-C-K-K S————S S(tBu)
6.	K(FITC)-C-R-W-R-W-K-C-C-K-K S————-S S(tBu)
7.	K(FITC)-C-R-W-R-W-K-C-C-K-K S(tBu) S–S
8.	K(FITC)-C-R-W-R-W-K-C-C-K-K S————S
9.	K(FITC)-C-R-W-R-W-K-C-C-K-K S————S
10.	K(FITC)-C-R-W-R-W-K-C-C-K-K S–S

On the other hand, for the synthesis of oxidized protected peptides oxidation has to be performed on resin before cleavage. Therefore the side chain protecting groups of cysteines were changed.

Synthesis was performed by using two Fmoc-Cys(Acm)-OH which can be oxidized on resin by iodine treatment and the third cysteine was still protected by Fmoc-Cys(tBu)-OH which is stable to iodine treatment. Finally; after oxidation peptide was cleaved by TFA: TIPS: water (Figure 20). The cleavage cocktail was changed here in order to maintain the oxidized state of the cysteine which is not possible in case of Reagent K due to the presence of EDT.
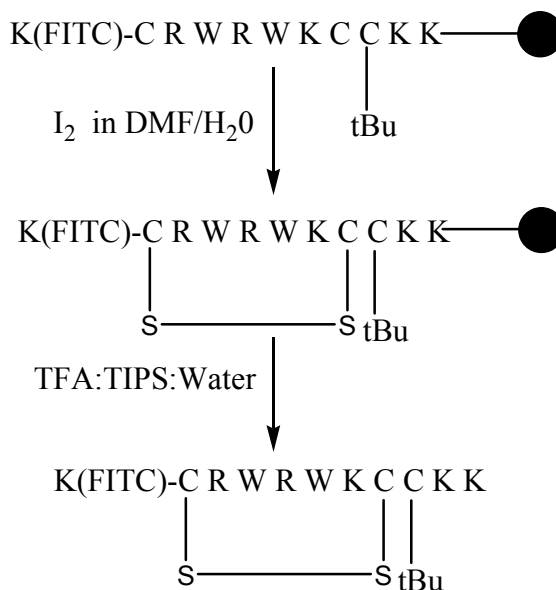
Figure 20: Scheme for the synthesis of protected oxidized peptides

2.3.1.1.2 Synthesis of the oxidized peptides

Syntheses of defined oxidized peptides were done by two different schemes discussed individually:

2.3.1.1.2.1 Scheme 1

In this case Fmoc-Cys(Mmt)-OH and Fmoc-Cys(Acm)-OH were used in order to achieve defined disulphide linkages. Fmoc-Cys(Acm)-OH can be selectively oxidized by iodine in DMF/water and finally the peptide was cleaved from the resin by TFA:TIPS:water (95:2.5:2.5) (Figure 21).

K(FITC)-C R W R W K C C(Mmt) K K━━━━●

$\downarrow$ I$_2$ (10 eq) DMF/H$_2$0

K(FITC)-C R W R W K C C(Mmt) K K━━━━●
         | |
         S━━━━━━━S

$\downarrow$ TFA:TIPS:Water

K(FITC)-C R W R W K C C K K
         | |
         S━━━━━━━S
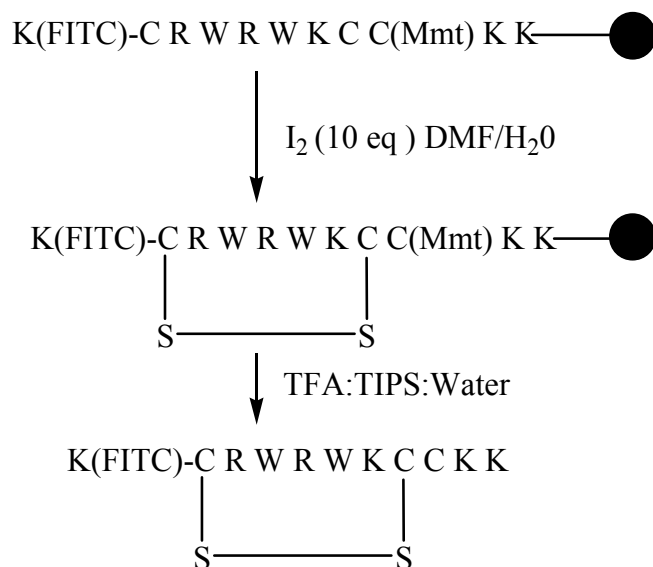
Figure 21: Schematic representation of defined disulphide linkages

2.3.1.1.2.2 Scheme 2

Peptides were synthesized with cysteines protected with two Mmt groups and one trityl group at indicated positions (Figure 22). Mmt group can be selectively cleaved by 1% TFA whereas trityl group is cleaved only under 95% TFA. Therefore, Mmt group was cleaved with DCM/TFA/TIPS (94:1:5) in nitrogen atmosphere for 5 min (3×). As reported by Wacker *et al.*, 2008, cyclization was performed by air oxidation, bubbling air through the resin in N-methylpyrrolidone with 0.1 TEA for 3 days. Peptides were cleaved from the resin by TFA: TIPS: water (95: 2.5: 2.5) for 2 h, followed by purification and analysis. Cyclized fractions were identified by ESI-MS showing reduction of molecular mass by two units compared to the reduced form.

Trt
|
K(FITC)-C R W R W K C C K K—●
| |
Mmt   Mmt   Mmt Removal
                  DCM/TFA/TIPS(94:1:5)

Trt
|
K(FITC)-C R W R W K C C K K—●
| |
SH   SH

                  Cyclization by air oxidation
                  Cleavage

K(FITC)-C R W R W K C C K K
        | |
        S————————S
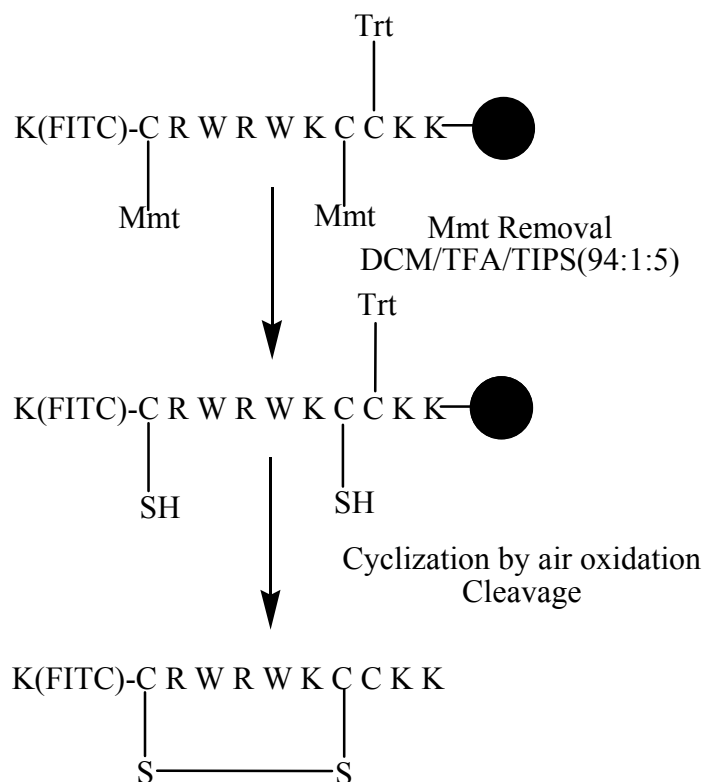
Figure 22: Schematic representation of defined disulphide linkages

2.3.2 Internalization studies

The cellular uptake and cytosolic distribution was reduced for the tBu protected CyLoP-1 compounds compared the cyclized tBu CyLoP-1 analogues (data not shown). However tBu protected CyLoP-1 (cyclized or noncyclized) showed comparatively lower internalization in comparison to the CyLoP-1 itself.

The three combinations with specific disulphide bridges CyLoP-1 (S_1-S_7), CyLoP-1 (S_1-S_8), and CyLoP-1 (S_7-S_8) were synthesized. Results show better internalization of the oxidized forms compared to the reduced CyLoP-1. Amongst the three oxidized mutants of CyLoP-1 the compounds S_7 (ox. CyLoP-1(C_1-C_7)) and S_8 (ox. CyLoP-1(C_7-C_8)) showed significantly higher uptake and exclusively high cytosolic distribution compared to the other analogues (Figure 23).
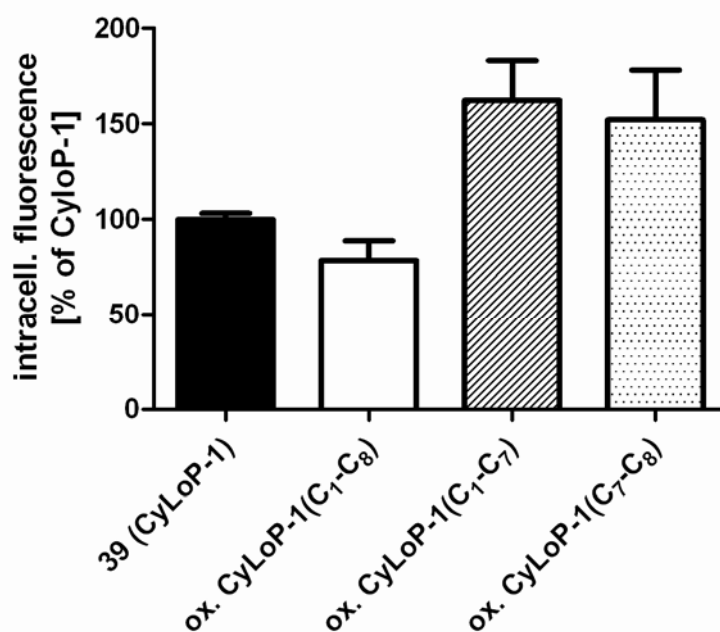
Figure 23: Comparison of internalization efficiency of reduced and oxidized analogues of CyLoP-1

2.3.3 Discussion

As concluded from the SAR studies cysteines were inevitable in CyLoP-1 for the internalization. Therefore, cysteines might be involved in the mechanism of uptake. To visualize the role of oxidation in uptake and distribution inside the cell, participation of the cysteine residues in the cystine formation need to be investigated. Due to the presence of three cysteines there are considerable chances of disulphide scrambling at physiological conditions. Thus, studies were initiated with one cysteine selectively protected with tBu amongst three in CyLoP-1 and the other two involved in disulphide formation. This will reduce the chance of disulphide scrambling.

Various combinations with one cysteine protected with tBu were synthesized in reduced and oxidized form and tested for their uptake. Cellular uptake as well as cytosolic gain of the peptide was reduced when cysteines were present in protected form. Nevertheless, the peptides with intramolecular disulphide bonds were better internalized and distributed in cytoplasm compared to its reduced form, thus, highlighting the participation of oxidation in the uptake process. Though the scheme of synthesis was directed for the defined cysteine linkages, still the

46

formation of inter-molecular disulphides could not be excluded, thus, increasing the complexity of purification and analysis.

2.4 EFFECT OF FLUOROPHORES ON INTERNALIZATION

In order to quantify the import efficiency of CPPs, fluorophores generally serve as the reporter unit. Fluorophores covering the visible spectral range with different spectral properties are available. The differences in the spectral characteristics also provide an opportunity for dual or triple labeling of the peptides. For the purpose of tracking the intracellular distribution of CPPs dyes like fluorescein or TAMRA are generally used. Therefore, studies were carried out with FITC, carboxyfluorescein (CF), TAMRA derivatives of CyLoP-1 in order to study the influence of position and nature of fluorophore on internalization.

2.4.1 Results

2.4.1.1 Fluorophore at N or C terminus

To investigate the effect of dye in the sequence, FITC was coupled to CyLoP-1 at N-terminus and C-terminus [sample 1 and 2, Table 5]. A significant reduction in the internalization was observed for the C-terminal labeled peptide (Figure 24). Thus, fluorophore location affected significantly the cellular uptake and cytosolic localization.
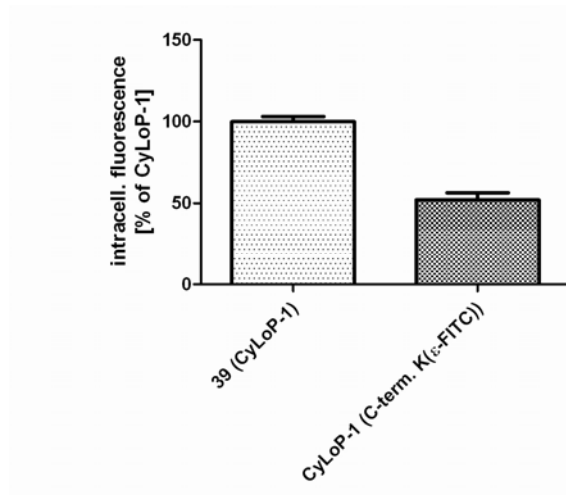
Figure 24: Influence of location of fluorophore (terminus) in CyLoP-1 on internalization

Table 5: List of CyLoP-1 coupled to various fluorophores

S. No.	Fluorophore	Terminus	Sequence
1	FITC	N-terminal(ε-position of lysine)	K(FITC)-CRWRWKCCKK
2	FITC	C-terminal (ε-position of lysine)	KCRWRWKCCK(FITC)K
3	Carboxyfluorescein(CF)	N-terminal (α-position)	(CF)-KCRWRWKCCKK
4	Carboxyfluorescein	N-terminal (ε-position of lysine)	K(CF)-CRWRWKCCKK
5	FITC	N-terminal(ε-position of lysine)	K(FITC)-CRWRWKCCKK
6	TAMRA	N-terminal (α-position)	(TAMRA)-KCRWRWKCCKK
7	TAMRA	N-terminal (ε-position of lysine)	K(TAMRA)-CRWRWKCCKK
8	FITC, TAMRA	TAMRA-N-terminus, FITC-C-terminus	K(TAMRA)-CRWRWKCCK(FITC)K

2.4.1.2 Position of fluorophore (amino group of N-terminal lysine)

To determine the optimal position i.e. α- or ε-position of N-terminal lysine of CyLoP-1 conjugates with carboxyfluorescein labeled at either one position were synthesized [sample 3, 4, Table 5]. A significant influence of the position of selected amino group on the intracellular delivery was observed (Figure 25). K(ε-CF)-CyLoP-1 showed higher uptake compared to similar FITC analogue. Comparison of CF labeled peptides with and without a linker lysine, CF-K-CyLoP-1 and CF-CyLoP-1, a strong reduction in the activity was observed in case of CF-

CyLoP-1. Thus all the analogues were synthesized with labeling at the ε-position of lysine to keep the α-amino group free for the attachment of the cargos to the peptide.
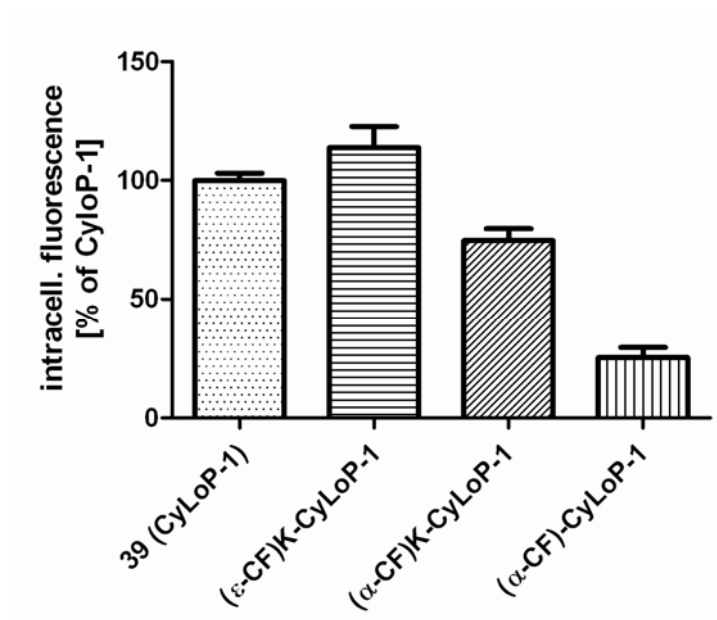
Figure 25: Influence of the fluorophore position in CyLoP-1 on internalization

2.4.1.3 Nature of fluorophore

Charge and hydrophobicity of fluorophore is known to have an impact on the efficiency of internalization (Derossi *et al*., 1994; Futaki *et al*., 2001). On this basis the effect of dyes with different physicochemical properties on the ability of penetration was investigated. A set of analogues of CyLoP-1 with different reporters (FITC, carboxyfluorescein, TAMRA) were synthesized. A significant difference was observed in the distribution pattern of CyLoP-1 labeled with FITC, carboxyfluorescein or TAMRA indicating the dependence of the physiochemical properties of the dyes on the uptake of the CPP conjugates.

The cytosolic distribution pattern was different for fluorescein and TAMRA conjugates. FTIC and carboxyfluorescein labeled peptides were distributed both in cytosol as well as embraced in the vesicles whereas TAMRA labeled peptides were exclusively entrapped in the endosomes. This observation was in accordance with results reported by Fischer *et al*. 2002.

The distribution pattern differed according to the structure of the dye as seen in case of FITC, CF, and TAMRA labeled peptides. A switch to exclusively vesicular uptake was observed with the TAMRA labeled peptide.

2.4.1.4 Dual labeling

Dual labeling of the CPP was described for the simultaneous detection of two fluorophore on a CPP with within a single cell (Fischer *et al* 2006). Here they visualize the concept of protease activity in the endosomal pathway with the help of two reporter units. Based on similar concept CyLoP-1 was synthesized with two fluorophores at both ends in order to study the degradation of the peptide. Chasing experiments were performed by incubating peptides with FITC or TAMRA labeled peptide alone as well as with the dual labeled peptide and various time points.

2.4.2 Discussion

Fluorescence based methods suffer from various drawbacks questioning their utility. For example fluorophore affects the intracellular distribution (Fisher *et al*., 2002), uptake and cytotoxicity (Andaloussi *et al*., 2007). Localization of fluorophore peptide conjugate within the cell does not necessarily correlate with the actual bioavailability of the cargo inside the cell (Lundberg *et al*., 2007; Lundin *et al*., 2008). Nevertheless fluorescence based techniques are equally applied to track the intracellular distribution of the molecules covering the wide spectral range. The uptake and distribution of the fluorescein (FITC, CF) and TAMRA conjugates of CyLoP-1 was studied. The fluorescein differs from TAMRA in being negatively charged whereas the latter being zwitter ionic.

Position of the fluorescein in the peptide seems to be important as indicated by the uptake studies. K(ε-CF)-CyLoP-1 was better internalized compared to K(ε-FITC)-CyLoP-1. On the other hand when position of CF was changed to α-amino group the uptake efficiency decreased indicating an effect of the position of the fluorophore position on the uptake. FITC was substituted by carboxyfluorescein as the former is prone to Edman Degradation if coupled at the α-NH$_2$ group and when treated with TFA. Upon comparison of carboxyfluorescein labeled peptides CF-K-CyLoP-1 and CF-CyLoP-1 a reduction in the activity was observed for CF-CyLoP-1. The cysteine side chain adjacent to the bulky and hydrophobic fluorescein group might hinder the function of the cysteine thiol group which is not the case in CF-K-CyLoP-1 where a

lysine linker separates the peptide and the dye. Influence of the dye on the structure of CyLoP-1 was observed in the NMR spectra of CyLoP-1 and K(FITC)-CyLoP-1: They indicated that the introduction of the dye orients the peptide to a spatial arrangement. A well defined structure was not obtained in both the cases. But an effect on the internalization behavior was observed. Internalization as well as cytosolic diffusion is more pronounced with the dye conjugated at N-terminus of the peptide compared to the C-terminus. These results indicate that not only the terminus but also the availability of the α-amino group influences the uptake and intracellular distribution of the peptide.

The distribution pattern differed according to the nature of the dye as seen in the cases of FITC, CF, and/or TAMRA labeled peptides. A switch to exclusively vesicular uptake was observed in case of all TAMRA labeled peptide. Fluorophores might differ in their physicochemical properties rendering the difference in their uptake behavoiur.

2.5 COMPARISON OF UPTAKE EFFICIENCY OF CyLoP-1 WITH OTHER CPPs

CPPs like Tat, penetratin and oligoarginines are widely studied as delivery vectors for a variety of cargos (Dietz *et al.*, 2004). Tat and octaarginines are highly cationic whereas penetratin and CyLoP-1 apart from being positively charged are rich in hydrophobic residues. Verification of the carrier ability of CyLoP-1 was done by comparing with the well characterized CPP (Tat, penetratin, octaarginines) (Table 6). Accumulative evidences showed D-Tat $_{49-57}$, D-Tat $_{57-49}$ and D-R$_8$ to be better internalized in comparison to their native L-form (Wender *et al.*, 2000). Therefore, these peptides were synthesized as their D-analogues. To avoid the discrepancies of the results all peptides were synthesized in parallel and analysed under similar experimental conditions.

Table 6: List of the CPPs synthesized

S. No.	CPP	Sequence
1	Octaarginine	rrrrrrrr
2	D-Tat $_{49-57}$	rkkrrqrrr
3	D-Tat $_{57-49}$	rrrqrrkkr
4	Penetratin	RQIKIWFQNRRMKWKK

These most studied CPPs were less internalized compared to CyLoP-1 at 2.5 µM and with predominantly vesicular distribution. At concentrations above 10 µM, cytosolic distribution was also seen in such peptides (Duchardt *et al.*, 2007) whereas CyLoP-1 was proficiently taken up by cells at a subtoxic concentration of 2.5 µM (Figure 26), interestingly showing cytosolic distribution along with vesicular uptake. Other distinctive features were the influence of the chirality of amino acids as well as the sequence order on the cellular uptake. The L-amino acid stereoisomer of CyLoP-1 was better internalized and localized in the cells compared to the D-isomer analogues with reversed sequence.
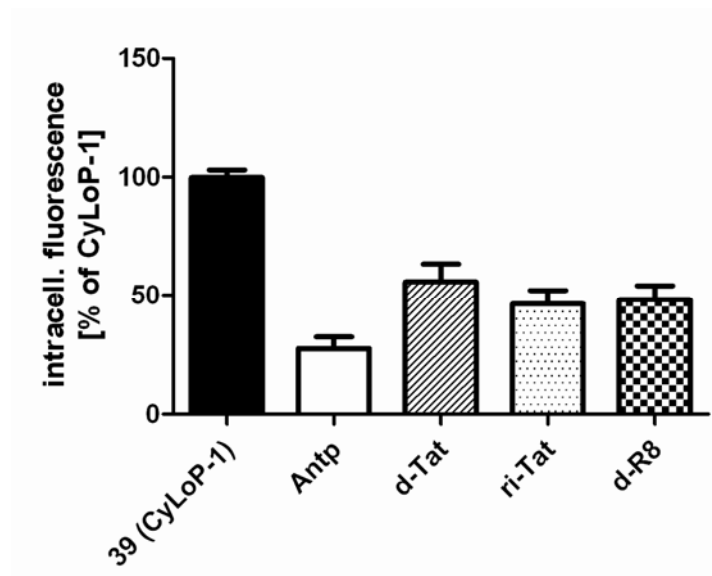

Figure 26: Comparison of internalization efficiency of CyLoP-1 and other known CPPs

2.6 SUMMARY

A series of peptides was synthesized by continuous solid phase peptide synthesis. FITC was coupled to each peptide as optical reporter for the detection of intracellular uptake and distribution by fluorescence spectroscopy and microscopy. The influence of chemical properties of the side chain functionalities of amino acids on internalization and distribution was compared in SAR studies. SAR studies resulted in CyLoP-1, showing the best intracellular delivery in NIH/3T3 cells at 2.5 µM and specifically cytosolic diffusion along with vesicular uptake. The role of amino acids like cysteine and tryptophan in peptides was critical for biological effects. Complete removal of cysteines resulted in almost complete loss of cellular uptake and cytosolic diffusion. Similar behavior was observed by substitution of tryptophans by phenylalanine.

CyLoP-1 was better internalized in its native L-form compared to its stereochemical analogues stating the influence of the role of chirality of peptide backbone on the internalization ability. Modifications of the peptide sequence had a direct effect on the uptake and distribution indicating the participation of the chemical properties of different side-chains of the amino acids. Not only the chemical nature but also the spatial arrangement of these amino acids played a significant role in maintaining the properties of CyLoP-1.

The role of cysteines was further elucidated by comparing the internalization efficiency of the reduced as well as oxidized CyLoP-1. Therefore, the three possible intramolecular cystine bridges of CyLoP-1 were synthesized and it was observed that the oxidized form of CyLoP-1, especially Ox-CyLoP-1 (C_1-C_7), was better taken up and distributed when compared to its reduced analogue.

When compared to other well studied CPPs like Tat, penetratin, oligoarginines, CyLoP-1 showed proficient uptake and cytosolic distribution with endosomal uptake at concentrations as low as 2.5 µM accompanied by cytosolic distribution unusual for other CPPs at this concentration.

The application of CyLoP-1 as a delivery vector to transport different sizes of cargos inside the cell was further studied and is discussed in the next part of the thesis.

PART 3

APPLICATION OF CyLoP-1 AS A DELIVERY TOOL

3.1 EFFICIENT INTRACELLULAR DELIVERY OF A MR IMAGING PROBE BY CyLoP-1

3.1.1 Introduction

Magnetic Resonance Imaging (MRI) has emerged as an important noninvasive medical diagnostic tool for molecular imaging in the past decades. In order to amplify the differences in signal intensities from normal and diseased tissues, so-called contrast agents (CAs) are used. MRI CAs are usually compounds capable of altering the relaxation times of the water protons in the surrounding they are taken up. The term relaxivity is generally used to express the efficiency of an MRI CA. By definition, relaxivity is the ability of 1 mM CA to shorten the relaxation time (Frullano *et al*, 2004). Relaxivity results from an electron-nuclear dipolar interaction between the paramagnetic metal complex and the water molecules either bound in the inner coordination sphere of the metal ion (inner-sphere relaxivity) or due to the bulk water in the vicinity of the complex (outer-sphere relaxivity). The contribution of the inner-sphere is influenced by the rotational correlation time, the water/proton exchange rate, the hydration number and the longitudinal and transverse relaxation rates of the Gd(III) electron spin. Generally used CAs are complexes of Gd(III) because of its high magnetic moment and long relaxation times. Due to the toxic nature of free Gd(III) it is complexed with suitable ligands to avoid free Gd(III) and by this reduce toxicity. In this respect, macrocyclic metal chelates are often used in order to study *in vivo* pharmacokinetics.

Common CAs are restricted to extra-organ and extracellular regions. Nevertheless, various intracellular CAs with a variety of applications were also reported (Su *et al*., 2007; Wolf *et al*., 2007; Mier *et al*., 2004, Hyodo *et al*., 2006). The major hurdle in the development of MR contrast agents for the detection of intracellular processes is the intracellular delivery of the agent. In order to facilitate intracellular delivery, MR reporters (i.e. the Gd(III)-complex) could be coupled to so-called cell penetrating peptides (CPPs). Gd-DOTA or Gd-DTPA conjugated bound to CPPs like arginines and Tat have been widely studied (Pranter *et al*., 2003; Allen *et al*., 2004).

Other than these, numerous other applications have been investigated for multimodality imaging studies (Zhang *et al*., 2005).

Intracellular targeted CAs not only requires a high intracellular accumulation, high relaxivity but also specific biochemical interactions. As a proof of principle, one of the first examples was "EgadMe", a β–galactosidase responsive CA (Louie *et al*., 2000). With "EgadMe" an increase in relaxivity was observed as result of the removal of galactopyranose by the activity of the beta-galactosidase enzyme. This allowed an exposure to an additional coordination site for water exchange in the Gd-complex, thus increasing relaxivity. As mentioned above, this model suffered from the limitation of intracellular delivery which is one of the prerequisite for the success of this model. Such obstacles can be overcome by CPPs that have been proben to be efficient carriers for transmembrane delivery for a variety of cargoes attached to them (Zorko *et al*. 2005; Langel *et al*. 2001).

In order to simplify the concept of intracellular delivery, CPPs with a MR-reporter were first standardized without a targeting moiety. In these cases the intracellular delivery and relaxivity studies were performed with several CPPs (Allen *et al*., 2004; Pranter *et al*., 2003). Although, such conjugates showed sufficiently high relaxivities, they were mostly restricted to cellular vesicles, i.e endosomes and lysosomes. This endosomal entrapment is a major hurdle for a molecule with a cytosolic target. Therefore, next to intracellular delivery it is also desirable to achieve access to the cytosol.

In this second part of the study, the work is focused on the synthesis of a bimodal intracellular CA applying CyLoP-1 as a delivery tool coupled to DOTA as gadolinium chelator for MRI and FITC as an optical reporter molecule. The coupling of a fluorophore allows the visualization of intracellular uptake and distribution via fluorescent microscopy while the MR reporter enables target tracking by MRI. Confirmations of intracellular delivery by fluorescence spectroscopy and microscopy and relaxivity-studies are discussed herein.

3.1.2 Results

3.1.2.1 General synthesis

Continuous Fmoc SPPS was used to synthesize CyLoP-1 on preloaded 2-chlorotrityl resin using DIC/ HOBT mediated coupling chemistry (Figure 27). Fmoc deprotection was performed twice by 20 % piperidine in DMF for 10 min. CyLoP-1 was N-terminally elongated by Fmoc-Lys (Dde) for orthogonal coupling of two different reporter molecules. To synthesize the peptide-based intracellular CA, carboxylate of DOTA was coupled to the free alpha amino group of the

peptide at the N-terminus after removal of the Fmoc protecting group. Similarly, selective removal of the Dde group by 2% hydrazine in DMF resulted in a free amino group, now readily available to couple a fluorescein moiety. FITC was coupled in the presence of TEA (FITC: TEA, 1:2) in DMF overnight. Completeness of coupling and deprotection was confirmed by the Kaiser Test. The peptide was cleaved from the resin with a cleavage cocktail of TFA (8.5 ml), Reagent K (1.45 ml) and TMSBr (0.05 ml) for 2 h. The filtrate was triturated in DEE two times and then freeze-dried. Finally the conjugate was purified by preparative HPLC and the product was analysed by ESI-MS.
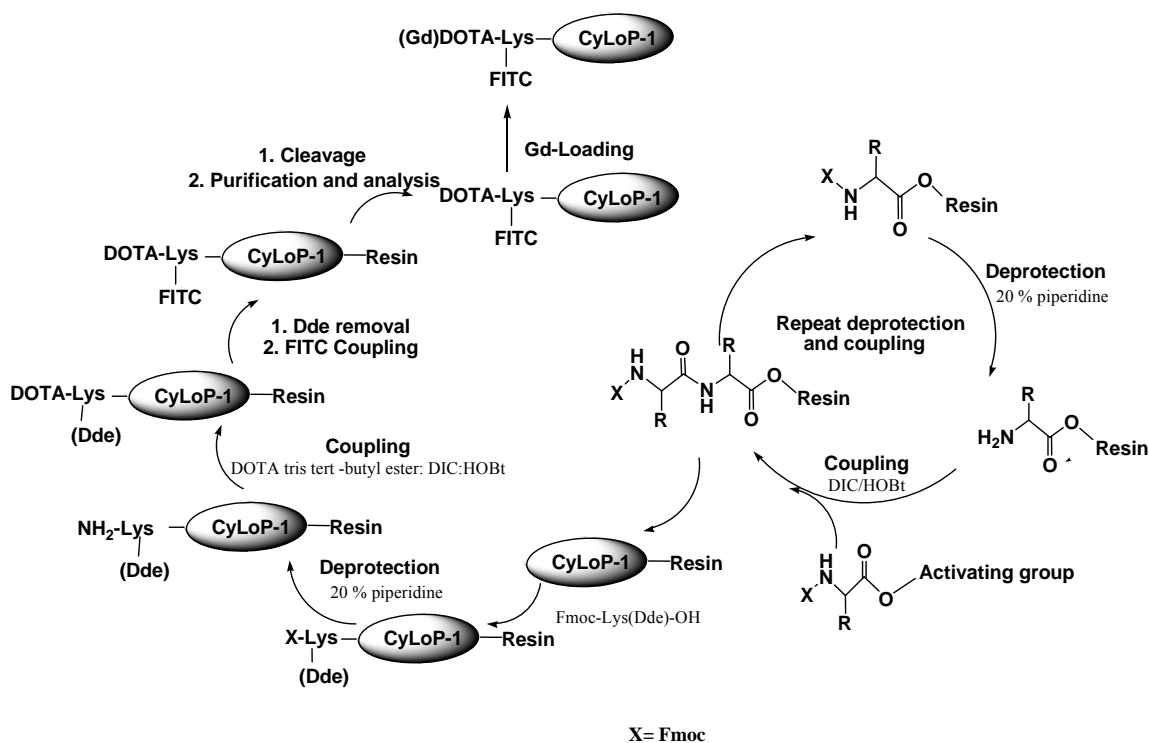
Figure 27: Route for synthesis of (Gd)-DOTA-K(FITC)-CyLoP-1.

3.1.2.2 Gadolinium loading

The purified ligand was dissolved in water and the pH was adjusted to ~ 6.5 with NaOH followed by addition of GdCl$_3$.6H$_2$O. The solution was stirred for 8 h at 45 °C and then overnight at room temperature. The pH was periodically checked to be maintained between 6-6.5 with 1 N NaOH or 1N HCl as required. After Gadolinium loading the sample was purified again by HPLC with 0.05 % TFA in ACN/water and then analysed with ESI-MS. The samples were freeze dried yielding an orange powder. Since the samples were purified under TFA conditions it

is likely for TFA to bind to the positively charged amino acids. Therefore the concentration of the peptide was determined by UV-Vis absorption of FITC at 485nm. The similar scheme and the analytical conditions were adapted to synthesize octaarginine- and Tat-based CAs.

3.1.2.3 Structure

CyLoP-1 was covalently attached to the chelate framework to hold Gd(DOTA) and FITC at the α- and the ε-position, respectively of the N-terminal lysine (Figure 28).
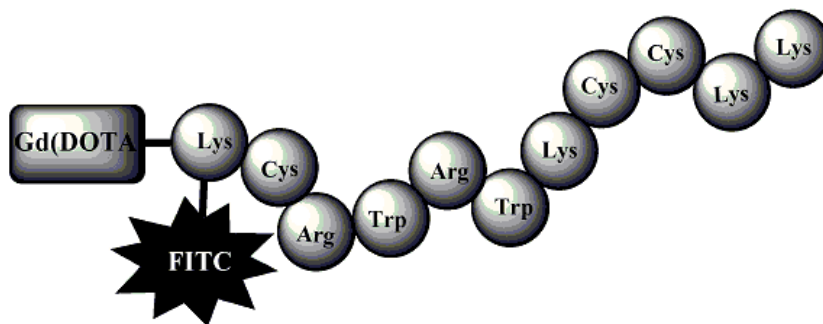
Figure 28: Schematic structure of Gd-DOTA-K(FITC)-CyLoP-1

The success of the synthesis and purification of the CA was determined by ESI-MS and analytical HPLC. The detected purity was >90%. The analytical data (Figure 29) show the successful incorporation of gadolinium into the ligand. The molecular ion peak corresponds to a single gadolinium in the molecules also shown by gadolinium isotopic pattern obtained (insert).
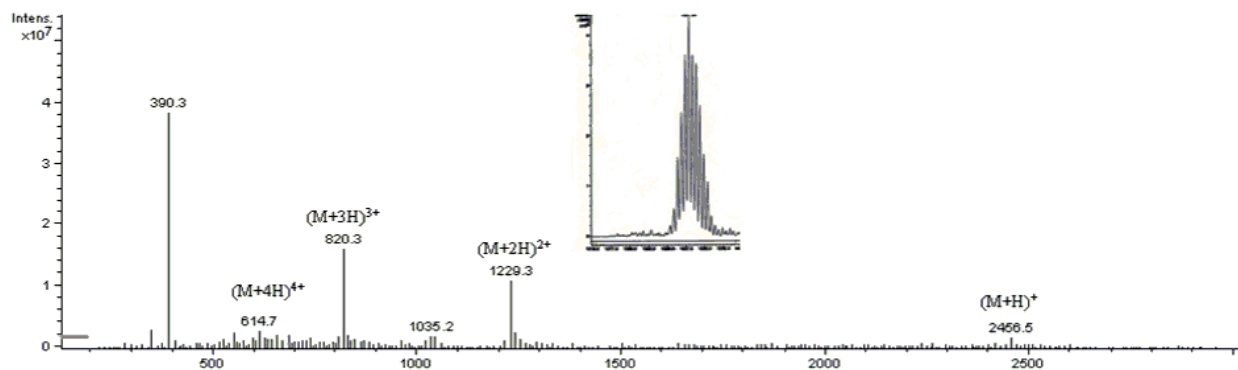
Figure 29: ESI-MS of purified Gd-DOTA-K(FITC)-CyLoP-1. The detected molecular ions for Gd-DOTA-K(FITC)-CyLoP-1 were (M+H) $^+$= 2456.5, (M+2H) $^{2+}$= 1229.3, (M+3H) $^{3+}$= 820.3, (M+4H) $^{4+}$= 614.7. They were consistent with the calculated mass of the desired product (2454.9). Peaks of 390.1 and 1035.2 are fragment ions. The insertion in Figure 29 shows the gadolinium isotopic pattern confirming the presence of one gadolinium in the peptide construct.

3.1.2.4 Internalization studies

Coupling of Gd-DOTA to K(FITC)-CyLoP-1 only slightly decreased the uptake compared to the CyLoP-1 itself whereas the cytosolic localization of the conjugate was maintained (Figure 30).
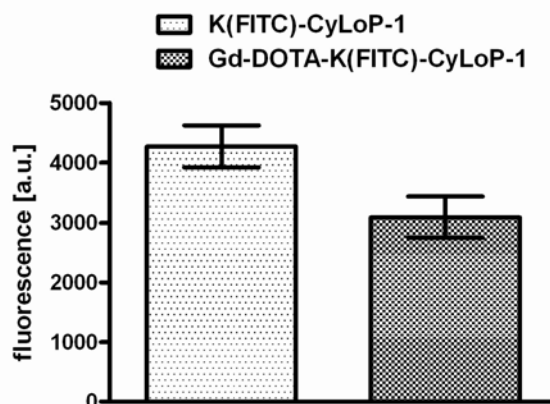
Figure 30: Cellular internalization of K(FITC)-CyLoP-1 with and without coupling of Gd-DOTA.

The uptake of the conjugate, Gd-DOTA-K(FITC)-CyLoP-1 (Figure 28) was tested in NIH/3T3 mouse fibroblast (Figure 31). Fluorescence microscopic images showed efficient uptake of this compound into the cells, indicating cytosolic targeting along with vesicular entrapment.
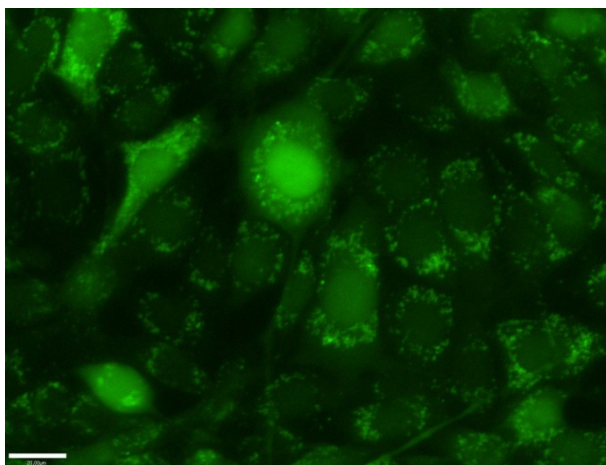
Figure 31: Intracellular fluorescence distribution of Gd-DOTA-K(FITC)-CyLoP-1 in NIH/3T3 cells after incubation of 2.5 µM for 18 h. The bright punctate and encapsulated FITC fluorescence was categorized as vesicular uptake while fluorescence distributed in the entire cell with similar intensity was designated as diffused. The bar represents 20 µm.

Furthermore, uptake efficacy of D-octaarginine (Gd-DOTA-K(FITC)-D-R$_8$), D-Tat (Gd-DOTA-K(FITC)-D-Tat) and CyLoP-1 (Gd-DOTA-K(FITC)-CyLoP-1) based CAs were compared at 2.5 µM concentration (Figure 32).
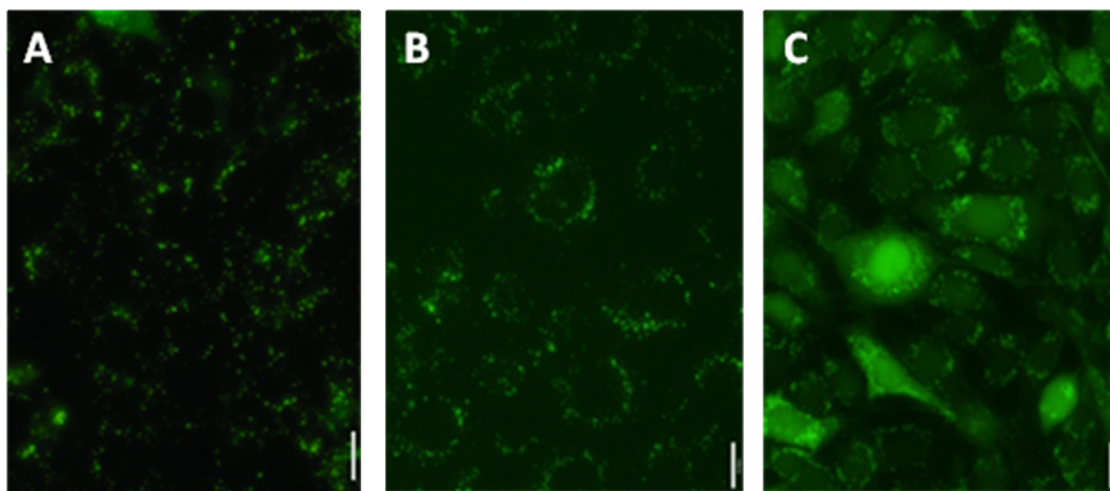
Figure 32: Microscopic images of NIH-3T3 cells after loading with 2.5 µM of contrast agents A (Gd-DOTA-K(FITC)-D-R$_8$), B (Gd-DOTA-K(FITC)-D-Tat), C (Gd-DOTA-K(FITC)-CyLoP-1) for 18 hours. The bright punctate and encapsulated FITC fluorescence was categorized as vesicular uptake while fluorescence distributed in the entire cell with similar intensity was designated as diffused. The bar represents 20 µm. Bars represent 20 µm

Lower and exclusively vesicular uptake was observed in case of D-octaarginine- and Tat-based CAs whereas diffused along with endosomal uptake was visualized for CyLoP-1 based CA. Compared to another well-known CPP (D-form of the Tat-peptide) the uptake of the CyLoP-1-coupled version was significantly higher (Figure 33). Thus, our CyLoP-1 conjugate showed a better uptake and a distinct distribution pattern when compared to other CPP- constructs.

Figure 33: Intracellular flurescence of NIH-3T3 cells after loading with 2.5 μM of contrast agents Gd-DOTA-K(FITC)-D-Tat and Gd-DOTA-K(FITC)-CyLoP-1 for 18 hours. **, p<0.01, significantly different compared to CyLoP-1 (student's t-test).

3.1.2.5 Relaxivity studies

Measurements in an aqueous solution were performed for the CyLoP-1-coupled CA at a magnetic field strength of 3T at room temperature. The relaxivity obtained in solution for Gd-DOTA-K(FITC)-CyLoP-1 was 16.8 $\pm$0.7 mM^{-1}s^{-1} at 2.5 μM. It is measured by taking the slope of the plot of R1 relaxation rate versus concentration.

Cellular relaxation rates of Gd-DOTA-K(FITC)-CyLoP-1 were determined by *in vitro* MR studies. Labeling of NIH/3T3 cells with 2.5 μM of gadolinium containing conjugate was done in tissue culture flasks for 18 h and MR analysis of labeled cells was performed in Eppendorf tubes (1×10^7 cells /tube). Relaxation rates were obtained from axial slices as well as T1-weighted images of saggital slices. A continuous increase in the cellular relaxation rates was observed with increasing concentrations. The cellular relaxation rate $R_{1,\,cell}$ was increased to 245 and 425% of control at 2.5 and 5 μM, respectively (Figure 34). This resulted in a highly significant contrast

enhancement in MR images already at low micromolar concentrations (Figure 35) clearly visible in the T1-weighted images of labeled cells compared to cells without CA (tube C in Figure 35). Control cell images are comparatively darker than the images of the cells loaded with CA at different concentrations.
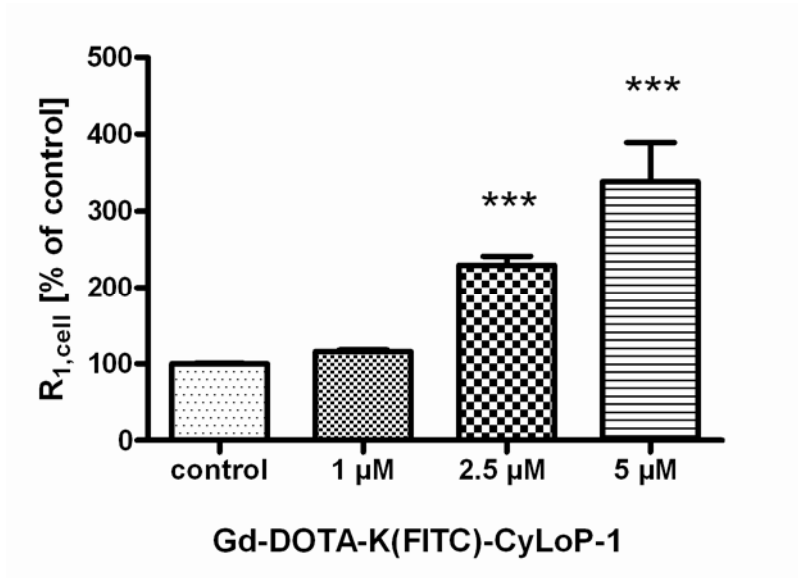
Figure 34: Cellular relaxation rate $R_{1,cell}$ after labeling for 18 hours at indicated concentrations in µM. ***, $p < 0.001$ significantly different compared to control (ANOVA, Bonferroni's Multiple Comparison Test).
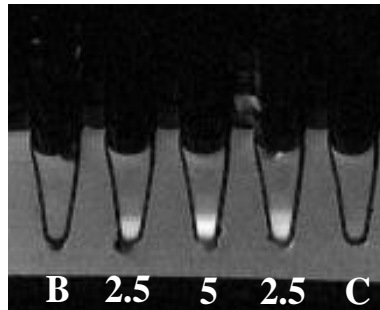
Figure 35: Contrast enhancement of Gd-DOTA-K(FITC)-CyLoP-1 in 3T3 cells at 2.5 and 5 µM. T1-weighted images. B: medium blank without cells, C: unlabelled control cells.

3.1.2.6 Comparison with other CPP-conjugates

The intracellular relaxation rates of the D-octaarginine-, l-Tat- and D-Tat-coupled CAs were also measured under the same experimental conditions like before. The CyLoP-1 conjugate showed a significantly higher contrast enhancement than the other CAs (Figure 36).
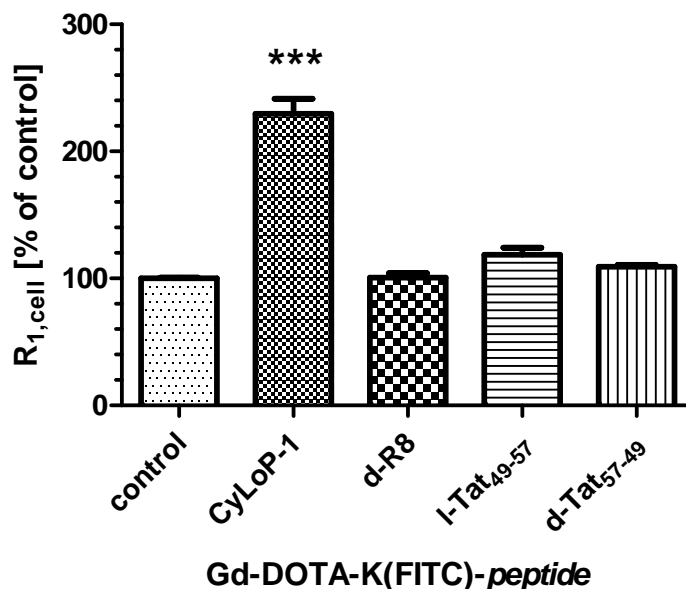
Figure 36: Contrast enhancement of Gd-DOTA-K(FITC)-CyLoP-1 compared to three other well-known CPP-conjugates in 3T3 cells. Cellular relaxation rate $R_{1, cell}$ after labeling for 18 hours at 2.5 µM. ***, $p < 0.001$ significantly different compared to CyLoP-1 (ANOVA, Bonferroni's Multiple Comparison Test).

3.1.3 Discussion

3.1.3.1 Tert-Butylation

Tert-butylation was a problem during the synthesis of Gd-DOTA-K(FITC)-CyLoP-1 and affected the yield of the product. Various conditions were tested to reduce the extent of side product formation.

- *Choice of cleavage cocktail-*
  Use of two different cleavage cocktails (Reagent K and TFA: TMSBr: Reagent K). Reagent K alone gave a continuation of symmetrical peaks in ESI-MS spectra of the

product corresponding to +1tBu, +2tBu whereas this side product could be reduced by substituting reagent K with TFA: TMSBr: Reagent K.

- *Choice of ether*

  Another aspect was the choice of the ether when DEE was applied as a precipitating agent. It showed reduction in the side product formation compared to MTBE.

- *Resin quantity*

  Another way to reduce the tert-butylated product is the cleavage of the resin in small portions.

The above optimizations resulted in significant decrease in the tert-butylated side product.

3.1.3.2 Removal of excess gadolinium

Excess gadolinium was a problem in context of cytotoxicity and erroneous high relaxivity values. Therefore, in order to assure complete removal of unbound gadolinium various purification techniques were tested.

3.1.3.2.1 HPLC purification

Gadolinium containing compounds are sensitive to low pH which increases the probability of gadolinium leaching from the ligand. Gd-DOTA complexes are reported to be stable at pH 2 with a half–life of about 4,000 h (Lukeš *et al*., 2001; Sturzu *et al*., 2009). In order to avoid the release of toxic free gadolinium, purification of the gadolinium loaded compounds was conducted in low percentage of TFA (0.05% TFA in water/ ACN) (pH= ~3) unlike 0.1 % TFA (pH= ~1) used for normal purifications.

3.1.3.2.2 Dialysis

After HPLC-purification the samples were further purified by dialysis in order to remove free gadolinium and other inorganic impurities. Dialysis was performed for 48 h after which samples were freeze-dried and obtained as an orange powder.

3.1.3.2.3 Varian Solid Phase Extraction

Another procedure that was used for the complete removal of excess gadolinium was Solid Phase Extraction, by passing the samples through the Varian ABS ELUT- NEXUS, 500 MG, 12 ML.

The relaxivity measurements were then done with the samples just after HPLC-purification, HPLC followed by dialysis and HPLC followed by Solid Phase Extraction. No significant differences were obtained showing the efficiency of HPLC purification for removal of excess or loosely bound gadolinium (data not shown).

3.1.3.3 Factors influencing the uptake

In order to achieve a detectable contrast enhancement by MRI cells have to be efficiently labeled with at least 10^7-10^8 Gd(III) complexes per cell (Cabella *et al.*, 2006). Most of the current intracellular CAs for MRI uses CPPs like penetratin, Tat, or oligoarginines as delivery vectors. However, differences in the delivery have been observed with different CPPs owing to the cargo as well as to the chemical structure (e.g. position or type of the chemical connection between CPP and Gd-complex). Peptide length and sequence, and choice of the chelating agent seem to have an influence on the intracellular delivery of the CA. For example, Sturzu *et al.* demonstrated a difference in the uptake behavior of penetratin- and Tat- based bimodal CAs in U373 glioma cells. A reduced internalization was observed with both CAs when compared to the respective monolabeled conjugates, thus highlighting that two reporter molecules impair the internalization capacity of the CPPs.

Our previous screening of CAs based on Tat and octa-arginine coupled with Gd-DTPA or Gd-DOTA as gadolinium chelators also supported the influence of the CPP and chelator on internalization (Jha *et al.*, 2007; Su, 2007). DTPA-based CAs were better taken up better by cells when compared to DOTA when conjugated to octa-arginines whereas in Tat-based CAs the internalization seemed to be independent of the type of the conjugated chelator. However, on increasing the concentration the cellular uptake of the CAs was enhanced, but also accompanied by higher cytotoxicity. Similar results were obtained in a study from Endres *et al.*, 2006 where a higher uptake for DTPA compared to DOTA based CA was reported. Inspite of all these observations proving DTPA to be the superior CA over DOTA-based CA one cannot ignore the lower thermodynamic stability of Gd-DTPA complexes (Crich *et al.*, 2006). Leaching of gadolinium could lead to cytotoxicity. Therefore, based on these discussions in our studies DOTA was selected as gadolinium chelator to avoid the cytotoxicity issues. Intracellular fluorescence of Gd-DOTA-K(FITC)-CyLoP-1 in NIH/3T3 cells at 2.5 μM after 18 h incubation showed both cytosolic diffusion as well as vesicular entrapment whereas in the case of Gd-

DOTA-K(FITC)-D-Arg and Gd-DOTA-K(FITC)-D-Tat the distribution was exclusively vesicular (under the same experimental conditions). This difference of the intracellular localization can be attributed to the disparity in the chemical structure of the CPPs. Arginines and Tat are positively charged peptides whereas CyLoP-1 also constitutes hydrophobic moieties along with positively charge amino acids. Apart from this, CyLoP-1 also contains three cysteines which may lead to aggregation in physiological media that could influence the import into the cell.

3.1.3.4 High relaxivity

Commercially available CAs like Dotarem, Prohance, Magnevist and Omniscan have relaxivities in the range of 3.4-3.5 $mM^{-1}sec^{-1}$ at 20 MHz and 39° C (Cabella *et al.*, 2006). Achievement of high relaxivities is the key objective of the researchers working with CAs for MRI. Efforts have been made to increase the sensitivity of CAs by either increasing the number of gadolinium per molecule or by optimizing the parameters that have a direct influence on the relaxation-enhancement like the rotational correlation time or the hydration number (Zhang *et al.*, 2005). For example, coupling of gadolinium chelates to polymeric materials seems to influence the rotational correlation time and hence increases the relaxivity per gadolinium atom (Caravan et al., 1999). Another aspect of such a concept was also shown by the Gd-DTPA derivative of MS-325, targeting serum albumin. Albumin binding increases the rotational correlation time and thus increasing the relaxivity (Caravan *et al.*, 2002).

Similarly, Gd-DOTA conjugated to CPPs like oligoarginines and Tat has been widely studied (Allen *et al.*, 2004; Pranter *et al.*, 2003; Sturzu *et al.*, 2009). The values for the longitudinal relaxivity (r1) of such conjugates have been observed in the range of 6-9 $mM^{-1}s^{-1}$. In detail, a relaxivity of 6.8 $mM^{-1}s^{-1}$ at 3T for Gd-DOTA-(R_8) (Allen *et al.*, 2004) and 7.94 $mM^{-1}s^{-1}$ at 4.7 T for Gd-DOTA-D-Tat (Pranter *et al.*, 2003) were determined. R1 relaxivities can also vary depending on the molecular weights of the compound (Ranganathan *et al.*, 1998). Generally, molecular weights of most of the CPP conjugates of Gd-DOTA or Gd-DTPA are in the range of 2200 to 2400 Daltons. High values of relaxivities are also reported for the DOTA-based prochelater conjugated to a Bombesin analogue. Furthermore, a two-fold increase in relaxivity was observed for a divalent analogue compared to the monovalent compound (Keelara *et al.*, 2008).

Gd-DOTA-K(FITC)-CyLoP-1, discussed here showed a relaxivity r1 of 16.8 ±0.7 mM^{-1}s^{-1} at 3T in water, which is about a factor of two higher than for the above mentioned similar CAs coupled to CPPs. This could be attributed to an increase in rotational correlation time which is influenced by the molecular weight (Caravan *et al*., 2002). Since the molecular weight of Gd-DOTA-K(FITC)-CyLoP-1 is in a similar range as that for other CPP-conjugates, the difference in the chemical structure of CyLoP-1 could be another reason for the higher relaxivity. Rigidity of a molecule is also known to have a positive impact on relaxivity (Aime *et al*., 1999; Ranganathan *et al*., 1998).

Apart from the differences seen in the solution-measurements the intracellular relaxation rates were also higher for the CyLoP-1-conjugated CA compared with the other CPP-analogues at concentrations of 2.5 and 5 μM. We demonstrated, that Gd-DOTA-K(FITC)-CyLoP-1 was better accumulated inside the cells leading to a higher intracellular gadolinium concentration. We also observed a difference in the distribution pattern between the CyLoP-1-CA (diffused as well as vesicular) and the octaarginine- and Tat-based CA (both exclusively vesicular) at 2.5 μM concentrations. Confinement of the CA in vesicles decouples it from the cytosol resulting in a high local relaxation rate and a slow water exchange rate because of the small volume, thus decreasing the relaxivity. On one hand vesicular entrapment results in quenching, on the other hand cytosolic diffusion leads to a higher accumulation inside the cell as well as access to a larger pool of water molecules, thus increasing the relaxivity (Terreno *et al*., 2006; Crich *et al*., 2006; Strijkers *et al*., 2009). Another aspect in case of CyLoP-1 based CA could be the increase in molecular weight by formation of aggregrates due to the presence of three cysteines in the molecule. High intracellular relaxation rates may also result from the binding of this CA with macromolecules inside the cell.

3.1.3.4 Summary and conclusion

This study focused on the synthesis and characterization of Gd-DOTA-K(FITC)-CyLoP-1. The intracellular uptake and distribution of this new CA was determined by fluorescence spectroscopy and microscopy. Cytosolic diffusion with vesicular uptake, high relaxivity in solution and extremely high intracellular longitudinal relaxation rates at low micromolar concentrations differentiate this CA from other CPP-based probes for MRI.

This work illustrates the potential of utilizing CyLoP-1 as a transporter for optical and MR reporters. Such combination of a fluorescent dye and Gd-DOTA makes the compound very useful for bimodal imaging. Thus, the novel peptide CyLoP-1 proved to be efficient in transmembrane delivery of imaging agents and is expected also to be useful as a vector for delivery of probes specifically targeted to cytosolic constituents. This will be discussed in the next chapter.

3.2 CyLoP-1 AS CARRIER FOR PEPTIDES

3.2.1 Introduction

The application of Cell Penetrating Peptides (CPPs) for transmembrane delivery of hydrophilic drugs and gene delivery is getting increasing attention. Covalent coupling of such agents to CPPs helps to circumvent limitations in their application. Although delivery of biologically active proteins into cells and still retaining biological functions is a challenging task, it has been shown that the fluorescence of the Green Fluorescent Protein (GFP) coupled to the CPP transportan was maintained when delivered intracellularly (Pooga *et al*., 2001). Similarly, activity of β-galactosidase coupled to Tat could be detected *in vivo* (Fawell *et al*., 1994). Not only proteins but also antibodies have been successfully delivered with CPPs like Tat or transportan (Pooga *et al*., 2001). CPPs conjugated to inhibitory peptides can be easily prepared using SPPS by conjugation via disulphide bonds (Gil-Parrado *et al*., 2003). However, the intracellular uptake can vary from cargo to cargo (Fischer *et al*., 2002).

In order to establish the delivery capacity of CyLoP-1 for different cargo-peptides, it was conjugated to SmacN7 and penetratin (Antp) at its N-terminus. SmacN7 (AVPIAQK) is a small bioactive pro-apoptotic peptide derived from the N-terminus of the so-called second mitochondria-derived activator of caspase (Smac) protein. Smac is released from mitochondria in response to apoptotic stimuli and promotes caspase activation by binding to the inhibitor of apoptosis proteins (IAPs) and abolishes their inhibitory activity (Sun *et al*., 2008; Fandy *et al*., 2008). Alone SmacN7 cannot pass through the membrane of cells and was therefore coupled to other CPPs in order to achieve its apoptotic effect (Duchardt *et al*., 2007). It was shown that the derived sequence SmacN7 is sufficient enough to maintain the original function of SmacN7, also clear signs of cell death were observed after coupling SmacN7 to polyarginines (Heckl *et al*., 2008).

Another example of a peptide used in this study is Antp, a CPP derived from the third helix of antennapedia. Antp is known to deliver numerous molecules through the plasma membrane (Derossi *et al*., 1994; Derossi *et al*., 1998). Antp, a 16 amino acid long peptide (RQIKIWFQNRRMKWKK), shows similarity with CyLoP-1 with respect to the amino acid

composition. Except cysteine residues all amino acids are common in both peptides. These two peptides are different in size as well as function. The effect of conjugating CyLoP-1 on the cell penetration of SmacN7 and Antp was studied to evaluate the influence of size as well as type of cargo on the internalization of peptidic CyLoP-1 conjugates.

3.2.2 Results

3.2.2.1 Synthesis Considerations

The peptide-CyLoP-1 conjugate with SmacN7 or Antp were synthesized on 2-chloro-trityl resin by continuous solid phase synthesis with DIC/HOBt- mediated coupling starting with the sequence of CyLoP-1. Each coupling was followed by a capping to block the unreacted reactive sites on the resin. Fmoc-Lys(Dde)-OH was introduced as a linker in between CyLoP-1 and the other peptide for further coupling to the fluorophore FITC. FITC was coupled after removal of the Dde protecting group by 2% hydrazine in DMF. On completion of the synthesis the conjugate was cleaved from the resin by Reagent K for 3 h followed by precipitation in MTBE and centrifugation. Conjugates were purified and analyzed by ESI-MS.

Penetratin CyLoP-1 conjugate-

Ac-RQIKIWFQNRRMKWK-K(FITC)-CRWRWKCCKK

SmacN7 CyLoP-1 conjugate-

Ac-AVPIAQK-(FITC)-CRWRWKCCKK

3.2.2.2 Uptake Studies

Successful synthesis of K(FITC)-SmacN7, Smac-N7-K(FITC)-CyLoP-1, K(FITC)-Antp, and Antp-K(FITC)-CyLoP-1 were performed. K(FITC)-SmacN7 was synthesized as a control as SmacN7 itself cannot penetrate the cells alone. The intracellular fluorescence distribution in NIH/3T3 cells showed an increase in intracellular import when peptides like Antp and SmacN7 were coupled to CyLoP-1 and when compared to peptides without CPP at 2.5 μM concentration (Figure 37). Nevertheless, a lesser uptake as well as intracellular cytosolic distribution (Figure 38) was observed when compared to CyLoP-1 alone.
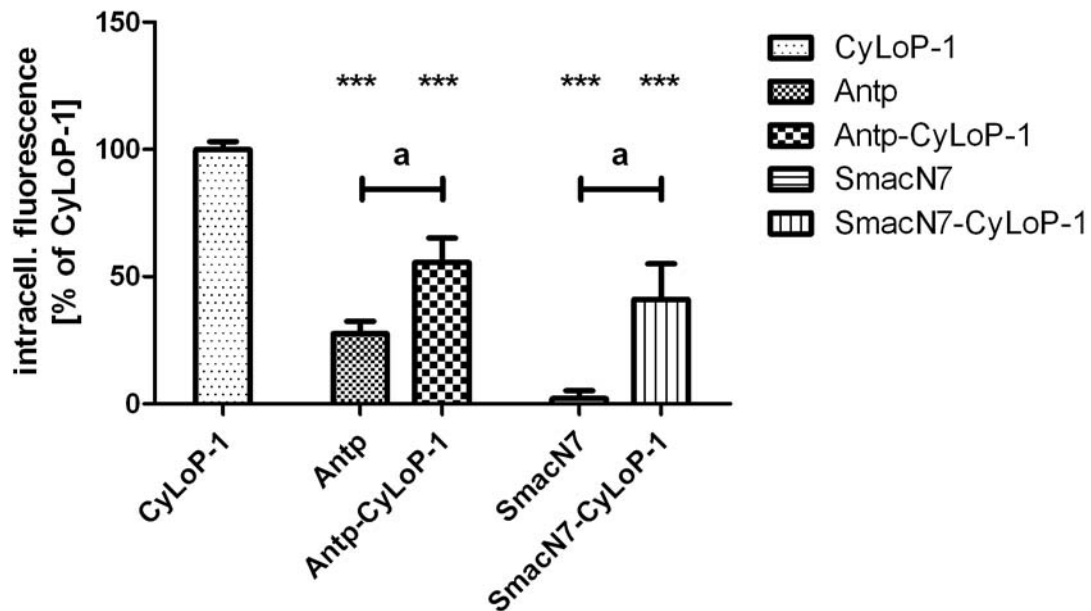
Figure 37: Intracellular fluorescence of peptide CyLoP-1 conjugates. ***, $p < 0.001$ significantly different compared to K(FITC)-CyLoP-1 (ANOVA, Bonferroni's Multiple Comparison Test). a, $p < 0.05$ significant difference between cargo alone and cargo CyLoP-1 conjugate. All conjugates were also coupled to FITC.

For Antp less uptake was observed compared to CyLoP-1 at 2.5 µM. When coupled to CyLoP-1 the uptake efficiency was enhanced and fluorescence appeared in the cytosol though not as much as with CyLoP-1 alone (Figure 38). Thus, a combined effect of the two peptides was detected regarding internalization and distribution inside the cell.

CyLoP-1	Antp	Antp-CyLoP-1
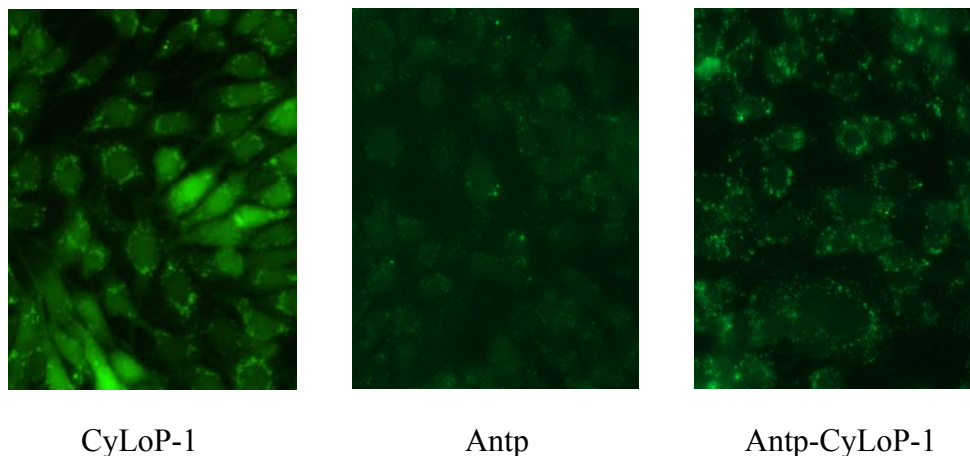
Figure 38: Intracellular fluorescence and distribution pattern of CyLoP-1, Antp and Antp-CyLoP-1 conjugate. The bright punctate and encapsulated FITC fluorescence was categorized as vesicular uptake while fluorescence distributed in the entire cell with similar intensity was designated as diffused.

When SmacN7 was coupled to CyLoP-1 there was an efficient intracellular delivery along with cytosolic diffusion (Figure 39). Internalization as well as cytosolic distribution was reduced when compared to CyLoP-1 alone (Figure 36) and showing the effect of cargo on the internalization properties of CyLoP-1.

CyLoP-1	SmacN7	SmacN7-CyLoP-1

Figure 39: Intracellular fluorescence and distribution pattern of CyLoP-1, SmacN7 and SmacN7-CyLoP-1 conjugate. The bright punctate and encapsulated FITC fluorescence was categorized as vesicular uptake while fluorescence distributed in the entire cell with similar intensity was designated as diffused.

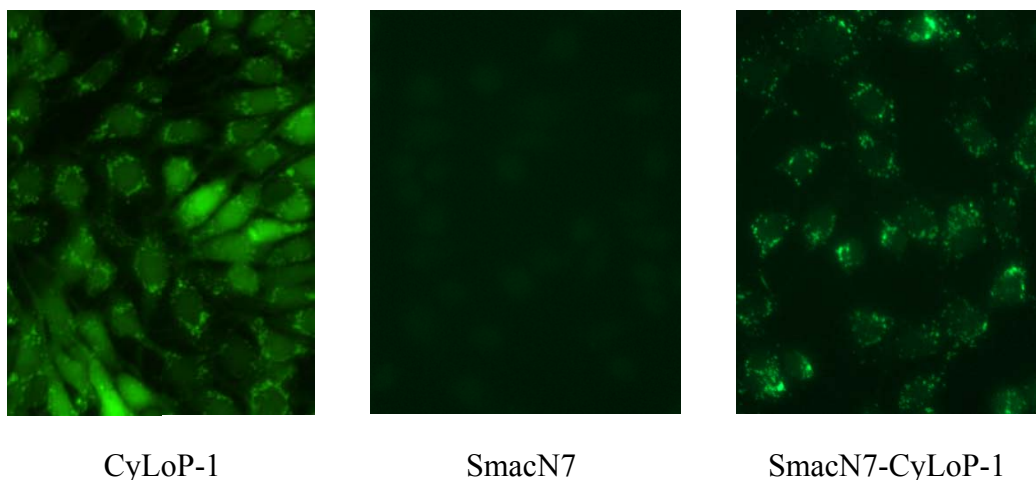### 3.2.3 Discussion

In order to be bioactive, SmacN7 peptide requires the successful delivery into the cytosol. Duchardt *et al.*, 2007 showed the ability of Antp and nonaarginines (R9) to deliver SmacN7 into the cytoplasm at various concentrations. When coupled to Antp, a concentration dependent vesicular staining was observed. In case of SmacN7-R9 conjugate an exclusively vesicular confinement was observed at 5 µM which shifted to an efficient delivery into the cytoplasm and the nucleus at 20 µM. An increase in the apoptotic activity was also observed with increasing concentrations, by this showing the biological activity of SmacN7. In our system, an access to cytosol was observed with SmacN7-CyLoP-1 at 2.5 µM which was observed for other CPP conjugates only above 10 µM (Duchardt *et al.*, 2007) highlighting the efficient cytosolic delivery of CyLoP-1 at low concentrations. Experiments will have to be undertaken to determine the apoptotic effect of SmacN7-CyLoP-1.

Our results indicate a strong influence of the cargo type on the cellular uptake. Antp though longer in sequence was better internalized and distributed into the cytosol compared to the shorter SmacN7 sequence. Reduction in delivery efficiency of both the conjugates could be the effect of difference in lipophilic nature of the cargo or the rigidity of the molecule induced by the coupling of the cargo to CyLoP-1. Assuming the role of aggregation in the pronounced uptake of CyLoP-1, attachment of the cargo might hinder this effect and result in reducing the import and cytosolic diffusion.

3.2.4 Summary and Conclusion

The effect of two peptides (Antp and SmacN7) of different lengths and nature on the uptake efficiency of CyLoP-1 was studied. Reduction in intracellular uptake and distribution into the cytosol was observed compared to CyLoP-1 alone. However, this effect was more pronounced in case of the smaller SmacN7-CyLoP-1 conjugate compared to the Antp-CyLoP-1 conjugate indicating the dominance of the nature of the cargo peptide on internalization rather on its size. The cytosolic distribution of the SmacN7-CyLoP-1 conjugate already at 2.5 µM can prove it to be an efficient carrier peptide to study its pro-apoptotic activity at low incubation concentrations and without the use of endosomolytic agents. Summarizing, CyLoP-1 has an enormous potential to deliver a range of small peptides attached to it into the cell and possibly into the cytosol.

3.3 APPLICATION OF CyLoP-1 AS A CARRIER FOR ANTISENSE TARGETING

3.3.1 Introduction

Antisense technology emerged as a powerful tool in therapeutics owing to its potential to down regulate any desired gene. In such cases an oligonucleotide analogue (so-called silencing RNA or siRNA) binds to the matching mRNA sequences in a specific manner interfering with the expression of the respective proteins. Peptide Nucleic Acids (PNAs) are nucleic acid analogues with an uncharged pseudopeptide backbone and are extensively used in antisense and antigene applications (Nielson, 1995). PNAs are DNA-mimics because of their hybridization abilities with complementary DNA sequences following Watson and Crick base pairing rules (Larsen *et al*. 1999). Under physiological conditions PNAs have a better binding affinity with DNA/RNA compared to DNA/DNA counterparts, mainly because of the lack of electrostatic repulsive forces that are acting between DNA/DNA or DNA/RNA (Díaz-Mochón *et al*., 2005). PNAs are also extremely stable against enzymatic degradation. However, poor solubility in physiological buffers, inefficient internalization, poor biodistribution due to rapid excretion limits the application of unmodified PNAs.

Adequate *in vivo* bioavailability of the antisense-molecules inside the cells is one of the major challenges in intracellular targeted approaches using antisense techniques. PNA-molecules are large (MW>2000) and neutral molecules that a very poorly taken up by cells (Nielson *et al*., 2005). It has been shown, that intracellular DNA-delivery can be achieved by applying a number of transfection agents (e.g. formation of lipoplexes). However, such delivery approaches are restricted in case of PNA as they lack formal charges present in DNA (Díaz-Mochón *et al*., 2005). In order to deliver PNAs into cells inclusion of multiple positive charges into the PNA backbone (Barawkar *et al*., 1998) or conjugating PNAs to CPPs were employed (Koppelhus *et al,* 2003). Various CPPs like Transportan (Pooga *et al*., 1998) or penetratin (Braun *et al*., 2002) have been used for PNA delivery.

Our results (see Part I) showed efficient intracellular delivery properties of CyLoP-1. Therefore, CyLoP-1 was tested for its potential in antisense targeting. The prerequisite for such an approach is the abundant cytosolic accumulation of PNA for high and selective binding to the desired

mRNA target. The antisense PNA chosen for this study targets a unique part in the mRNA sequence of the red fluorescent DsRed protein. The gene coding for the DsRed protein originates from a coral of the *Discosoma* genus and is commonly used as a transfection marker (Baird *et al.*, 2000). In order to investigate the ability of CyLoP-1 to enhance the intracellular delivery of PNA, a conjugate to a 12mer PNA targeting a unique region of the DsRed mRNA (Su *et al.*, 2007) was studied.

3.3.2 Results

3.3.2.1 Synthesis Considerations

PNA-peptide conjugation was achieved by continuous Fmoc solid phase synthesis (Figure 40). The peptide was synthesized on Rink amide MBHA resin at 0.2mmol/g scale by DIC/ HOBt-mediated coupling. Fmoc-Lys(Dde)-OH was introduced as a linker for further coupling of the PNA monomers and the fluorophore. The PNA chain was elongated by continuous coupling of the respective PNA monomers, HATU, DIPEA (1:0.9:2) for 1h, followed by acetylation at each step. Fmoc was removed by 20% piperidine for 5 min two times. Regular washing with DMF/NMP, DCM, methanol, DCM, DMF/NMP was done to ensure the removal of the reacting reagents from the reaction vessel. At the end the fluorophore FITC was attached to the linker (lysine) after the removal of Dde by 2% hydrazine in DMF. Once the synthesis of the PNA-peptide-conjugate was complete, the resin was thoroughly washed by DMF, DCM, and methanol, dried and cleaved by reagent K for 3 h. The filtrate was collected and precipitated twice with MTBE. The pellet was collected by centrifugation and lyophilized in water: *tert*-butanol (1:4) containing 5% acetic acid. The crude Peptide-PNA-conjugate was then purified by HPLC and analyzed by ESI-MS.

PNA CyLoP-1 conjugate-

Ac-tccgtgaacggc-K(FITC)-CRWRWKCCKK-CONH$_2$
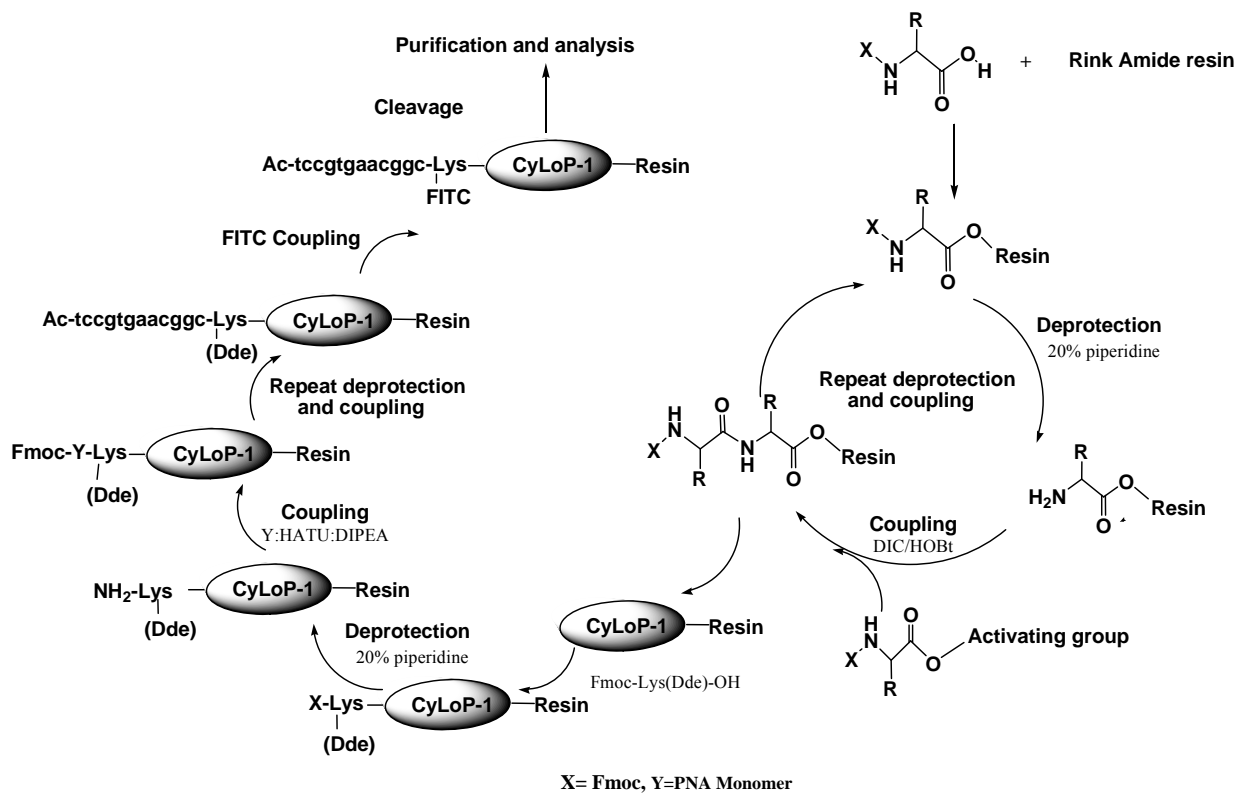
Figure 40: Synthesis scheme for PNA-CyLoP-1 construct

3.3.2.2 Uptake Studies

Fluorescence microscopic images demonstrated an intracellular distribution pattern for the PNA-CyLoP-1 construct in NIH/3T3 cells at 2.5 µM concentrations (Figure 41). The cytosolic diffusion was considerably lowered after coupling of the neutral PNA sequence in comparison to CyLoP-1 alone. The overall import efficiency as well as the distribution pattern of the PNA-CyLoP-1 construct was considerably reduced compared to CyLoP-1 itself.
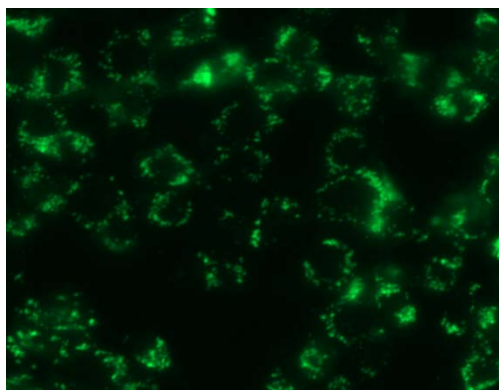
Figure 41: Fluorescence microscopic image showing intracellular distribution of PNA-CyLoP-1 conjugate in NIH/3T3 cells at 2.5 µM. The bright punctate and encapsulated FITC fluorescence was categorized as vesicular uptake while fluorescence distributed in the entire cell with similar intensity was designated as diffused.

3.3.3 Discussion

Reduction in the cellular uptake and cytosolic distribution could be attributed to a shift in the uptake mechanism to a more vesicular mechanism on elongation of the peptide chain with the PNA sequence. The rigidity introduced by the PNA sequence might hinder the specific orientation of the peptide conjugate in physiological media limiting endosomal release or direct uptake of the construct. Another aspect could be the C-terminal amide group that prevents the enzymatic degradation of the peptide by exopeptidases. As observed in case of CyLoP-1 changes of the C-terminus from acid to amide leads to a significant decrease in the intracellular uptake as well as the cytosolic diffusion of the peptide. In order to test the role of the functional group at the C-terminus on the uptake and distribution behavior PNA-CyLoP-1 conjugate with a free C-terminal end has to be compared for its import properties.

3.3.4 Summary and Conclusion

Herein we showed the efficient synthesis and internalization of a PNA-CyLoP-1-conjugate. Though the reduction in the cytosolic distribution and instead promotion of vesicular entrapment was dominant, CyLoP-1 proved to be an efficient carrier for cargos of high molecular weights as well.

3.4 SUMMARY OF THE CARGO STUDIES

In order to address the influence of the cargo on the uptake and the distribution of CyLoP-1-coupled compounds, CyLoP-1 was covalently conjugated at the N-terminus to a panel of cargos of different sizes: different fluorophores, the magnetic resonance imaging agent (Gd)-DOTA, the bio-active peptide SmacN7, the peptide Penetratin or to the PNA molecule (Table 7).

Table 7: List of various cargoes that were attached to CyLoP-1

S.No.	Cargo	Sequence
1.	Fluorophores (FITC, CF, TAMRA)	Optical reporter-CyLoP-1
2.	Gd-DOTA	MR reporter- CyLoP-1
3.	SmacN7	AVPIAQK - CyLoP-1
4.	Penetratin	RQIKIWFQNRRMKWKK(FITC)- CyLoP-1
5.	PNA	tccgtgaacggc K(FITC)- CyLoP-1

Small and medium sized cargos were selected for this study. They are different not only in their size but also in their nature and are otherwise impermeable through the plasma membrane. They were covalently linked to CyLoP-1 by a peptide bond via a lysine residue with a fluorophore (FITC) attached to it. Thus, the distribution of the payload inside the cell can be ascertained by the localization of the fluorophore. Successful delivery of cargos of various sizes attached to CyLoP-1 was achieved after incubation of NIH/3T3 cells with these peptide conjugates at the concentration of 2.5 µM for 18 h (Figure 42).

Nevertheless, with the increase in size of the cargo a decreased intracellular uptake and a tendency to more vesicular uptake was observed thus promoting the endocytosis of high molecular weight cargos.
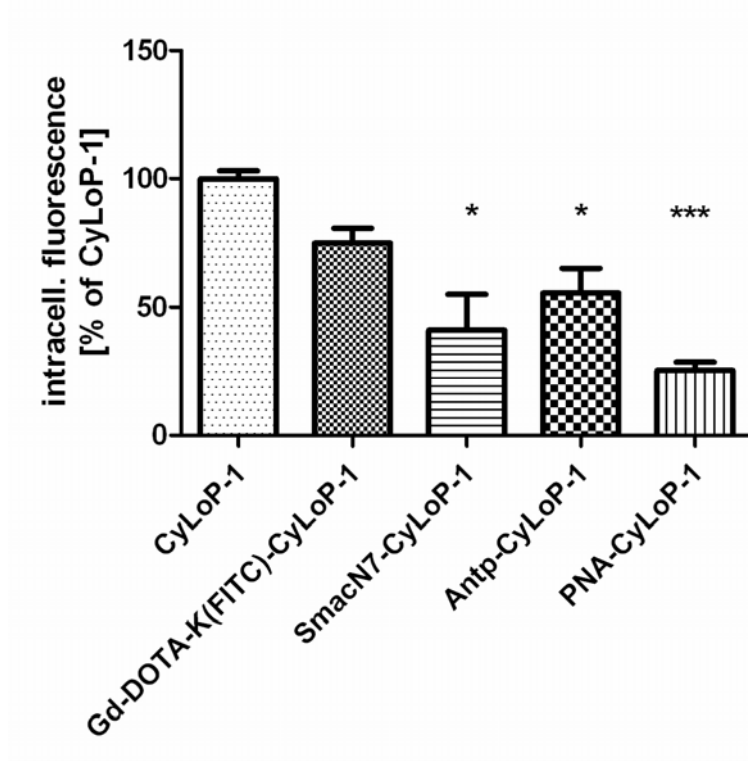
Figure 42: Intracellular fluorescence of various cargoes of different molecular weight attached to CyLoP-1. *, $p<0.05$, ***, $p<0.001$ significantly different compared to CyLoP-1 (ANOVA, Bonferroni's Multiple Comparison Test). All conjugates were coupled to FITC.

Conjugation of the payload to CyLoP-1 changes the cellular uptake and intracellular distribution of the construct. This observation was in accordance with studies from Zorko *et al*, where they also showed no effect of small sized cargo on rate of internalization but a substantial decrease in uptake with the increase in size of the cargo. The decrease in the uptake concomitant with the increase in the cargo size may also be induced by the nature and size of the cargo. However, the differences in the distribution pattern indicated to the delivery of intact molecule into the cell. But degradation of the peptide inside the cells could not be ruled out releasing the cargo. Nevertheless, our preliminary results with one of the CyLoP-1 cargo conjugate (Gd-DOTA-K(FITC)-CyLoP-1) showed cargo and FITC were colocalized in the cytoplasm.

Considering the importance of cysteines in the proficient uptake and significant cytosolic diffusion, the attachment of the cargo may induce conformational changes preventing formation of disulphide bridges. Though CyLoP-1 alone is unstructured in solution conjugation of the cargo might give a stable structure to the peptide in a physiological environment thus altering its

function. In addition, different internalization routes could be responsible for diffused and vesicular uptake whose predominance might be depending on nature of cargo coupled to CyLoP-1.

4   SUMMARY, CONCLUSION AND OUTLOOK

A potent delivery agent CyLoP-1 was designed, synthesized and characterized which is active in its natural form at concentrations as low as 2.5 μM. CyLoP-1 not only possesses the ability of intracellular access but also distributes easily into the cytosol. CyLoP-1 has a net positive charge and is of lipophilic nature. Any alterations introduced into the peptide sequence had a direct effect on the intracellular localization indicating the role played by the chemical properties of different side-chains of the amino acids. Cytosolic targeting (as evidenced by diffuse fluorescence) was a prominent characteristic of CyLoP-1. This feature is also observed with other CPPs but only at higher concentrations and short incubation times, and only in serum free medium (which is a non-physiological condition). Thus, efficient intracellular delivery, low cytotoxicity and high cytosolic appearance make CyLoP-1 an appropriate candidate for cytosolic delivery of small sized cargo molecules. The heterogeneous distribution pattern in the cell might allow some part of the CPP-cargo conjugate to reach its destination in either the cytosol or the nucleus. As CyLoP-1 was better internalized in its natural form, the possibility of degradation of the peptide cannot be ruled out. The reason for cytosolic gain could not be determined conclusively but escape from the endosomes also has to be considered (instead of direct cytosolic delivery). Also, the mechanism of internalization needs to be investigated further. Despite these unknown facts, continued rational design and combinatorial approaches will undoubtly result in further improvements of this peptide in the near future.

PART 5

EXPERIMENTAL PROCEDURES

5. EXPERIMENTAL PROCEDURES

5.1 Apparatus

Peptide Synthesizers

Automatic peptide synthesizer

Prelude^{TM}, Peptides&Elephants (Germany)

Manual peptide synthesizer

Heidolph Synthesis 1 synthesizer (Schwabach, Germany)

HPLC

Analytical and semipreparative RP-HPLC was performed at room temperature on a Varian PrepStar Instrument (Australia) equipped with PrepStar SD-1 pump heads. UV absorbance was measured using a ProStar 335 photodiode array detector at 214 nm and 260 nm. A Varian Polaris C18-Ether column (4.6 × 250 mm, particle size 5 μm, particle pore diameter 100 Å) was used for analytical RP-HPLC. For semipreparative HPLC, a Varian Polaris C18-Ether column (21.2 × 250 mm, 5 μm, 100 Å) was used.

ESI-MS

ESI-MS was performed on ion trap SL 1100 system (Agilent, Germany) with detection in positive and negative ion mode.

Varian Solid Phase Extraction

Varian ABS ELUT- NEXUS, 500 MG, 12 ML

Dialysis

Spectra/Pro, Float-A-Lyzer with Biotech, Cellulose Ester Membranes, MWCO: 1,000; Diameter-10mm, Volume- 10 ml. Spectrum Laboratories, Inc.

5.2 Chemicals

All solvents were of peptide synthesis grade. DMF, DCM, TFA, FITC, methanol, HOBt, DIPEA, DIC, piperidine, carboxyfluorescein (CF) were purchased from Acros Organics (Belgium). Protected Fmoc-amino acids as well as resins were obtained from Novabiochem (United Kingdom). The side chains of lysine and tryptophan were protected by Boc, cysteine by Trt, and arginine by Pbf. 1,4,7,10-tetraazacyclododecane (cyclen) was obtained from Strem Chemicals (Newburyport, USA). PNA monomers (Fmoc-PNA-T-OH, Fmoc-PNA-A(Bhoc)-OH, Fmoc-PNA-C(Bhoc)-OH, Fmoc-PNA-G(Bhoc)-OH) were purchased from Link technologies Ltd (Scotland). HATU was bought from Applied Biosystems (Darmstadt, Germany), TAMRA (Fluka, Germany).

5.3 Synthesis

5.3.1 Peptide Synthesis

(A1) Automatic synthesizer (At EMC microcollections)

Peptides were prepared by fully automated solid-phase peptide synthesis using the Fmoc/*t*Bu-strategy on α-Fmoc-(ε-Boc)-lysine-TCP resin. The resin was distributed in 30 mg aliquots (15 μmol) into filter tubes, which were positioned in the format of a microtiter plate on valve blocks. Fmoc deprotection was carried out two times, 10 min each, with 30% piperidine in DMF (300 μl). Nine washing steps were done with DMF (300 μl). Fmoc-amino acids (0.5 M) were dissolved with HOBt (0.5 M) in DMF. Amino acids were introduced into the reaction vessels in a two step procedure using a sevenfold molar excess of the respective Fmoc-amino acid. First coupling step with Fmoc-amino acids (200 μl), DIC (3 M in DMF, 50 μl) for 1h. Then, coupling reagents were filtered off and the resin was washed with DMF [1 x 200 μl] followed by the second coupling step with Fmoc-amino acids (100 μl) with TCTU (0.5 M in DMF, 200 μl) for next 1h. After washing with DMF [4 x 400 μl] Fmoc deprotection was carried out two times, 10 min each, with 30% piperidine in DMF (300 μl). Nine washing steps were done with DMF (300 μl). All peptides were elongated with Boc-L-Lys(Fmoc)-OH followed by Fmoc deprotection. Completeness of thiourea formation was monitored with the Kaiser Test.

*(A2) Automatic synthesizer (*Prelude^{TM}*)*

Peptides were prepared by continuous automated solid-phase peptide synthesis using the Fmoc/*t*Bu-strategy on Fmoc-(ε-BOC)-lysine-2-chlorotrityl resin (0.66 mmol/g). 50 mg of the resin was distributed in each of the reaction vessel. Fmoc deprotection was carried out two times, 10 min each, with 30% piperidine in DMF (2000 µl) followed by DMF washings (4x, 2000 µl). Fmoc protected amino acids (4 fold excess) were coupled with DIC/HOBT activation. Solutions of Fmoc-amino acids (1000µl, 136 mM), DIC (300 µl, 906 mM) and HOBt (500 µl, 272 mM) were prepared in DMF. Amino acids were first introduced in the reaction vessel with subsequent addition of HOBt and DIC respectively and allowed to stir for 90 min. Coupling reagents were filtered off and the resin continued by DMF washings [4x 2000 µl]. Fmoc deprotection was carried out two times, 10 min each, with 30% piperidine in DMF (2000 µl) followed by DMF washings (2000 µl). All peptides were elongated with Boc-L-Lys(Fmoc)-OH followed by Fmoc deprotection. Completeness of thiourea formation was monitored with the Kaiser Test.

Similar synthesis was performed for CyLoP-1 elongated by Penetratin and Smac peptides. Each coupling was followed by capping to block the unreacted active sites. Fmoc-Lys(Dde)-OH was introduced as a linker in between CyLoP-1 and cargo (penetratin and Smac) for the further coupling of the fluorophore. On completion of the synthesis the conjugate was cleaved from the resin by reagent K for 3 h followed by precipitation in MTBE and centrifugation.

B) Manual Peptide Synthesis:

The synthesis of selected peptides was carried out by solid phase Fmoc chemistry using a manual multiple peptide synthesizer (Heidolph Synthesis 1 synthesizer). Peptides were synthesized on α-Fmoc-(ε-BOC)-lysine-2-chlorotrityl resin (0.83 mmol/g). Fmoc protected amino acids (4 fold excess) were coupled with DIC/ HOBT activation for 60 min. Fmoc was removed with 30% piperidine in DMF (2 x 10 min). The resin was washed after each cycle of coupling and deprotection with DMF (4x). Completeness of coupling and deprotection was monitored with the Kaiser Test. Peptides were washed with DMF, DCM, and methanol (4 x each) and dried. The peptides were cleaved off the resin and side-chain deprotected with Reagent K (500 µl).

Further on, this cleavage reaction was optimized, in particular for the synthesis of DOTA-based compounds, by using TFA: Reagent K: TMSBr (8.5:1.45:0.05) for 2 hr instead of Reagent K alone. For the oxidized peptides a different cleavage cocktail consisting of TFA:TIPS:H_2O was used for 1 h followed by the addition of DMSO (5:1) at 0°C for 30 min and stirring for 1 h at RT.

Coupling of FITC to ε-amino group:

For structure activity relationship studies all peptides were coupled to FITC through a Boc-Lysine (Fmoc)-OH as a linker. The ε-group of N-terminal lysine was labeled with FITC (4 fold excess) with triethylamine (1:2) in DMF overnight. Peptides were washed with DMF, DCM, and methanol (4 x each), dried and cleaved from the resin with Reagent K (500 µl).

Coupling of TAMRA and carboxyfluorescein:

Different dyes were coupled at ε-amino group to study the effect of cargo on internalization. TAMRA or carboxyfluorescein (CF) were coupled both at α-amino and ε-amino group by DIC, HOBt activation for 8h.

5.3.2 PNA Synthesis

The selected antisense PNA targets the mRNA of the red fluorescent dsRed protein (Su et al, 2007). PNA peptide conjugation was achieved by continuous Fmoc synthesis. Peptide was synthesized on Rink Amide MBHA resin at 0.2mmol/g scale by continuous solid phase peptide synthesis followed by the Fmoc-Lys(Dde)-OH as a linker for further coupling with the fluorophore. The PNA-chain was elongated by regular coupling of the respective PNA monomers (Fmoc-PNA-T-OH, Fmoc-PNA-A(Bhoc)-OH, Fmoc-PNA-C(Bhoc)-OH, Fmoc-PNA-G(Bhoc)-OH) using Fmoc/Bhoc chemistry. Coupling with the PNA monomers HATU, DIPEA (1:0.9:2) was done for 1h, followed by acetylation after each step. Fmoc-deprotection was performed with 20% piperidine for 5 min two times. Washing with DMF/NMP, DCM, methanol, DCM, DMF/NMP was done to ensure removal of the reacting reagents from the reaction vessel. Completeness of coupling and deprotection was confirmed with the Kaiser Test. FITC was attached to the linker (lysine) after removal of Dde with 2% hydrazine in DMF two times. Once the synthesis of PNA peptide conjugate was complete, the resin was thoroughly washed with DMF, DCM, and methanol, dried and then cleaved by reagent K for 3 h.

5.3.3 Synthesis of Gd-DOTA-K(FITC)-CyLoP-1

Continuous Fmoc SPPS was exploited to synthesize CyLoP-1 on preloaded 2-chlototrityl resin using DIC/ HOBT mediated coupling chemistry (Scheme 1). Fmoc deprotection was performed twice by 20 % piperidine in DMF for 10 min. CyLoP-1 was N-terminally elongated by Fmoc-Lys(Dde) for orthogonal coupling of two different reporter molecules. To synthesize the peptide based intracellular CA, carboxylate of DOTA (Synthesis of 1,4,7-Tris(*tert*-butoxycarbonylmethyl)-1,4,7,10-tetraazacyclododecane-10-acetic acid was done as shown by Mizukami et al., 2008) have been coupled to the free alpha amino group of the peptide at N-terminus by removal of Fmoc protecting group. Similarly selective removal of Dde group by 2% hydrazine in DMF resulted in free amino group readily available to couple a fluorescein moiety. FITC was coupled in the presence of TEA (FITC: TEA, 1:2) in DMF overnight. Completeness of coupling and deprotection were confirmed by Kaiser Test. Peptide was cleaved from the resin in a cleavage cocktail comprising of TFA (8.5 ml), Reagent K (1.45 ml), and TMSBr (0.05 ml) for 2 h. The filtrate was triturated in DEE two times and freeze-dried.

Finally the ligand was purified by HPLC and the product was analysed by ESI-MS.

Purified ligand was dissolved in water and pH was adjusted to ~ 6.5 by NaOH followed by addition of corresponding lanthanides (GdCl$_3$.6H$_2$O or EuCl$_3$.6H$_2$O). Solution was stirred for 8 h at 45 °C and then overnight at room temperature. pH was periodically checked to be maintained between 6-6.5 by 1 N NaOH or 1N HCl as per requirement.

After Gadolinium loading the sample was purified again by HPLC with 0.05 % TFA in ACN/water and analysed by ESI-MS. Samples were freeze dried and obtained as orange powder.

As samples were purified under TFA conditions one could expect binding of TFA to the positive charged amino acids. Therefore the concentration of the peptide was determined by UV-Vis absorption of FITC at 485nm. Similar scheme and analytical conditions were adopted to synthesize octaarginine and Tat based CA.

5.3.4 SAR studies

To evaluate the uptake efficiency for all 60 peptides they were screened in their crude form. As the purity of the crude peptide [Fig. 43 (a), (b)] was considerable, only some selected peptides were purified and reevaluated.

Analytical data of a crude peptide 49

(a)
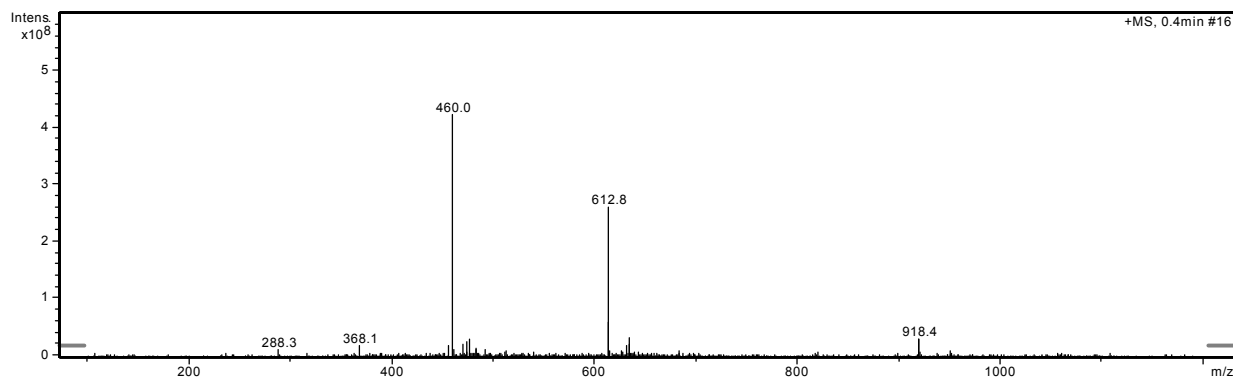
(b)

Figure 43: ESI-Mass spectra (a) and HPLC chromatogram (b) of crude peptide 49.

The amino acid sequence of Peptide **49** is CRFRFKCCKK. The peptide was characterized by ESI-MS. The detected molecular ions for peptide 49 conjugated with a lysine linker and 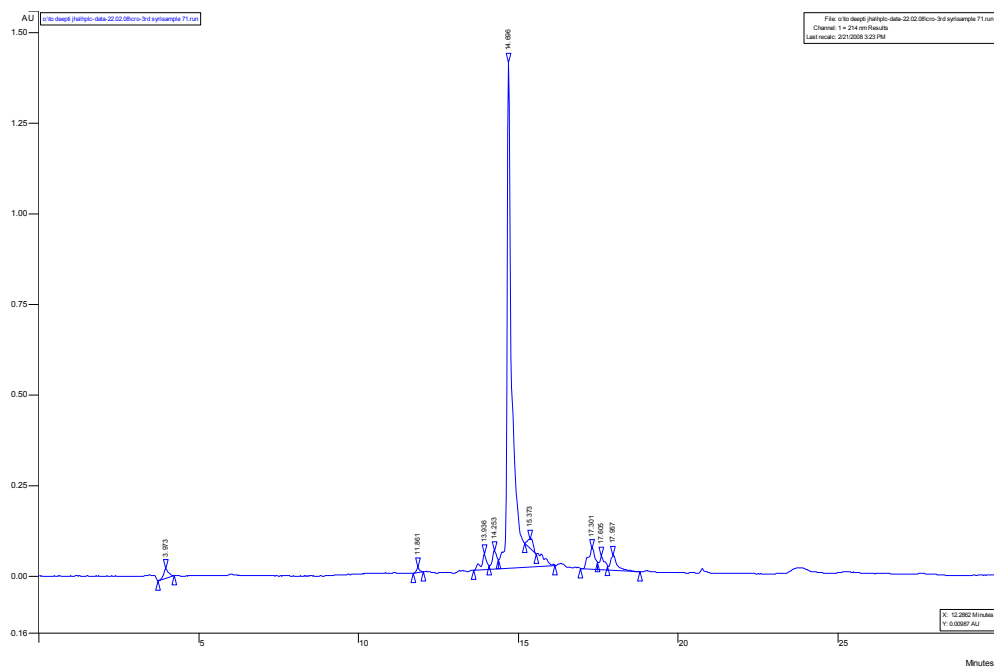FITC were (M+2H) $^{2+}$= 918.4, (M+3H) $^{3+}$= 612.8, (M+4H) $^{4+}$= 460.0, (M+5H) $^{5+}$ =368.1. They were consistent with the calculated mass of the desired product 1836.2.

5.4 Purification and characterization

All peptides were precipitated with MTBE. Precipitates were collected by centrifugation and resuspended in cold MTBE two times. The pellet was dissolved in a mixture of water, *tert*-butyl alcohol (1:4) and 2% acetic acid, and then lyophilized. CPP and PNA conjugates were purified by semi-preparative RP-HPLC using a gradient of water (0.1% TFA) (solvent A)/ACN (0.1% TFA) (solvent B) from 20% B to 90% B within 30 min (flow rate: 1 ml/min for analytical and 10 ml/sec for semipreparative HPLC). The gradient systems were adjusted according to the elution profiles and peak profiles obtained from the analytical HPLC chromatograms.

Mass spectrometry (ESI-MS, Nebulizer, 20.0 psi; Dry gas, 5.0 L/min; Dry temperature 250°C) was used for further characterization of the samples. The purified product was dissolved in water and *tert*-butyl alcohol (1:4) with 5% acetic acid, and lyophilized.

5.4.1 Storage

Peptides containing cysteines are prone to formation of disulphide bonds due to oxidation, which can be formed either intramolecularly, resulting in a cyclic peptide, or intermolecularly, forming oligomers or aggregates. As most of the CPPs that were used in this work are cysteine rich peptides, care had to be taken during synthesis and storage of the peptides. After lyophilization, the peptides were stored under nitrogen at acidic pH. Dissolved aqueous stock solutions for internalization studies were aliquoted and stored at -80°C. Dilutions for cell studies were prepared fresh.

5.4.2 GC-MS analysis for enantiomeric purity

The optical purity of amino acid derivatives and peptides was determined with GC-MS analysis by the external company C.A.T. GmbH&Co, Chromatographie und Analysentechnik KG, Tübingen, Germany. The exact quantitation of racemate involves hydrolysis with 6N D_2O/DCl. The amino acids are derivatized using deuterated reagents. Racemization during this sample

preparation is accompanied by deuterium exchange in the α-position (deuterium label). The proportion of D-amino acid originally present in the peptide is thus represented by the relative amounts of the unlabeled form which is monitored by mass spectrometry. The limit of quantitation is 0.1% of the optical antipode. The standard deviation is <0.1%.

5.4.3 Varian Solid Phase Extraction

Column was conditioned first with 2 ml MeOH then with 1% HCOOH in water avoiding the complete dryness of the column. Sample was prepared in 0.1% HCOOH in water (Solvent A) and loaded on the cartridge (1-2 ml/min) and washed with solvent A. Later the cartridge was washed with Solvent A and 0.1% HCOOH in ACN (Solvent B) 50:50 and with Solvent B. The sample was eluted in 50:50 solvent conditions. This fraction was collected and freeze-dried to obtain the dried product.

5.5 Analytical data

1. K-(FITC)-CyLoP-1

Chemical Formula: $C_{88}H_{120}N_{24}O_{17}S_4$
Exact Mass: 1912.81
Molecular Weight: 1914.31
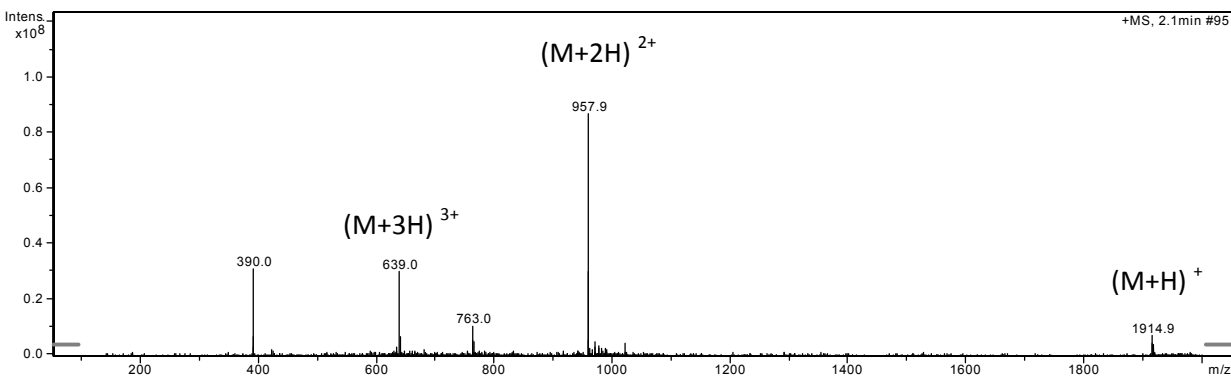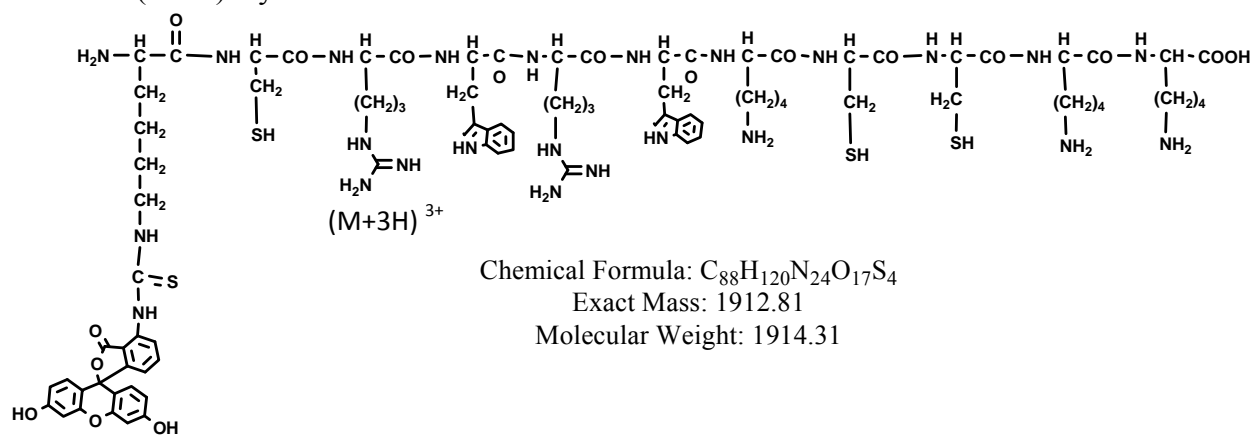
The detected molecular ions for CyLoP-1 with FITC in positive mode were $(M+H)^+ = 1914.9$, $(M+2H)^{2+} = 957.9$, $(M+3H)^{3+} = 639.0$. They were consistent with the calculated mass of the desired product 1914.3. Peaks 390.0 and 763 are fragment ions.
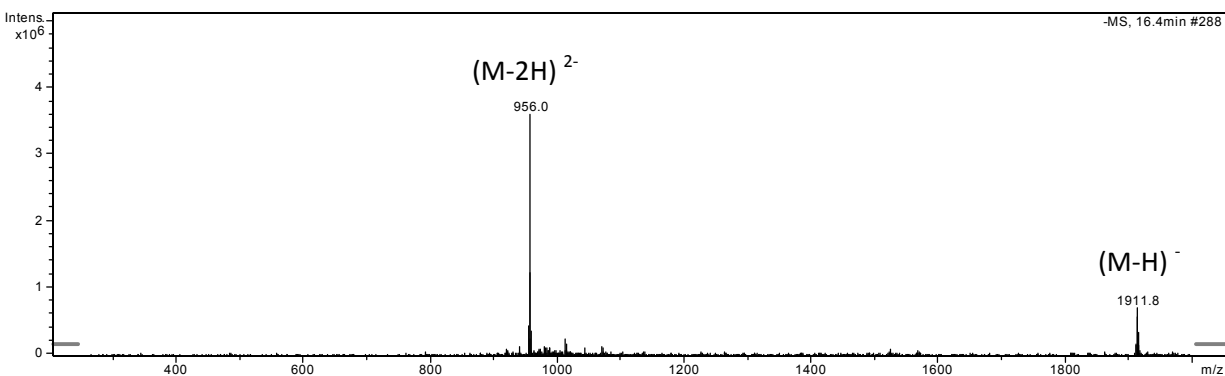
The detected molecular ions for CyLoP-1 with FITC in negative mode were $(M-H)^- = 1911.8$, $(M-2H)^{2-} = 956.0$. They were consistent with the calculated mass of the desired product 1912.

2. DOTA-K(FITC)-CyLoP-1 (Ligand)

Chemical Formula: $C_{104}H_{146}N_{28}O_{24}S_4$
Exact Mass: 2298.99
Molecular Weight: 2300.71
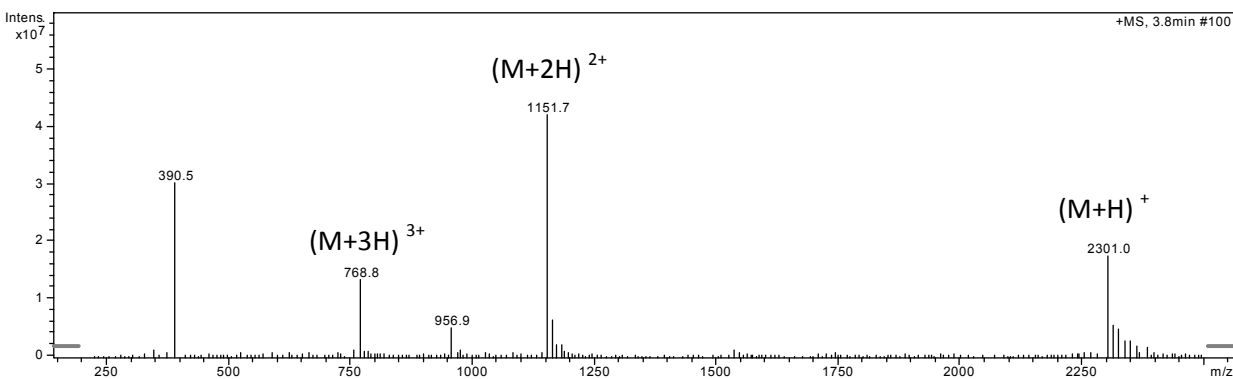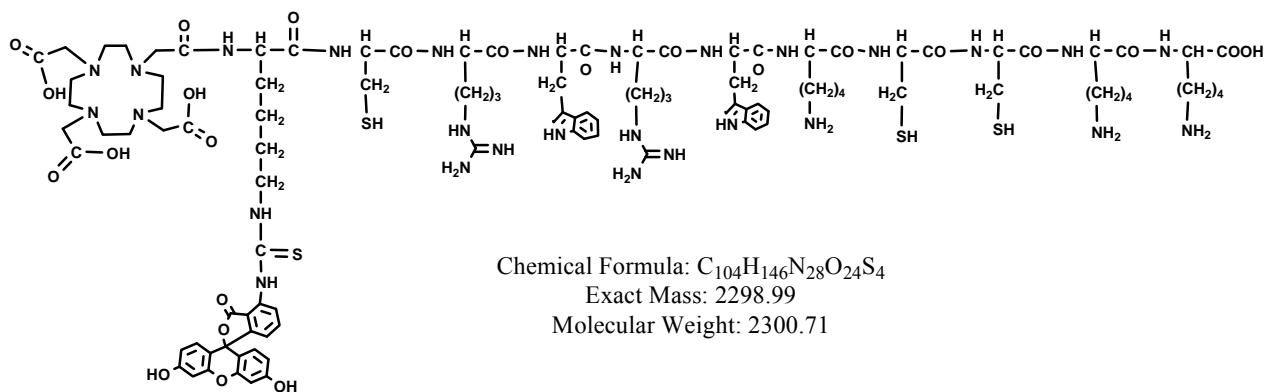
The detected molecular ions for DOTA-K(FITC)-CyLoP-1 were $(M+H)^+ = 2301.0$, $(M+2H)^{2+} = 1151.7$, $(M+3H)^{3+} = 768.8$. They were consistent with the calculated mass of the desired product 2300.7. Peaks 390.0 and 763 are fragment ions.

Gd-DOTA-K(FITC)-CyLoP-1

Chemical Formula: $C_{104}H_{143}GdN_{28}O_{24}S_4^{3+}$
Exact Mass: 2453.89
Molecular Weight: 2454.93

The detected molecular ions for Gd(DOTA)-K(FITC)-CyLoP-1 were $(M+H)^+ = 2456.5$, $(M+2H)^{2+} = 1229.3$, $(M+3H)^{3+} = 820.3$. They were consistent with the calculated mass of the desired product 2454.9. Peaks 390.0, 614.7 and 1035 are fragment ions.

DISTRIBUTION OF ISOTOPES CALCULATED BY 'ISOFORM' PROGRAM FOR
Formula : C104H143GdN28O24S4
Factor : 100   Nominal MW = 2453   Exact MW = 2453.89526   Average MW =   2454.96
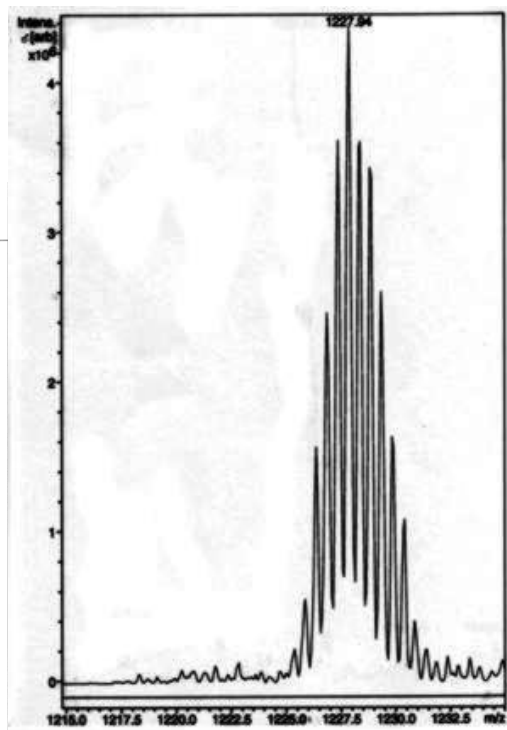
Figure 1   Figure 2

Isotopic pattern simulated by NIST, Formula and Isotopic Pattern Generator (United States
Department of Commerce) for Gd(DOTA)-K(FITC)-CyLoP-1 is shown in Figure 1 which
corresponds to the measured distribution (Figure 2)

3. SmacN7-CyLoP-1

Chemical Formula: $C_{117}H_{167}N_{31}O_{25}S_4$
Exact Mass: 2534.16
Molecular Weight: 2536.03
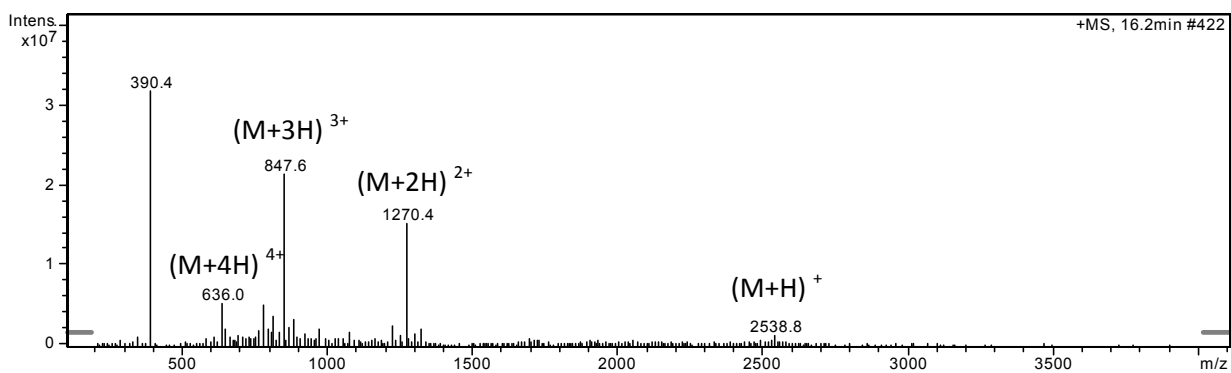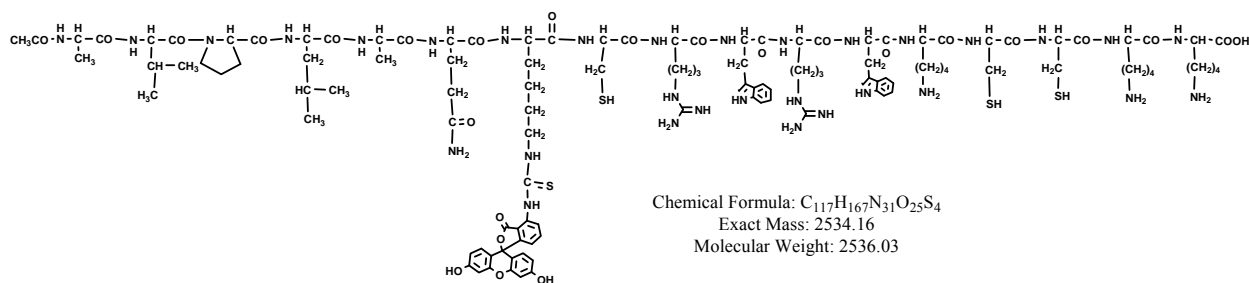
The detected molecular ions for Smac-CyLoP-1 were $(M+H)^+ = 2538.8$, $(M+2H)^{2+} = 1270.4$, $(M+3H)^{3+} = 847.6$, $(M+4H)^{4+} = 636.0$. They were consistent with the calculated mass of the desired product 2536.03. Peak of 390.0 is due to fragment ion.
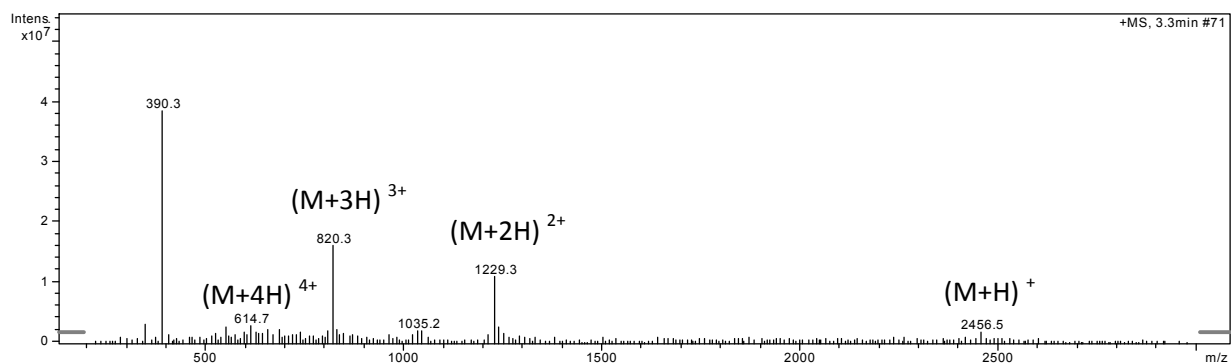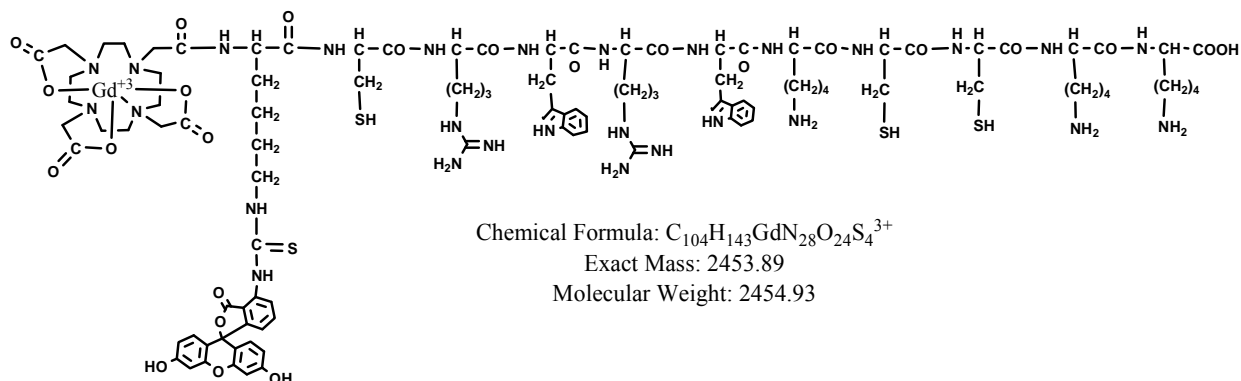
4. Antp-CyLoP-1

CH$_3$CO-RQIKIWFQNRRMKWKK (FITC)-CRWRWKCCKK
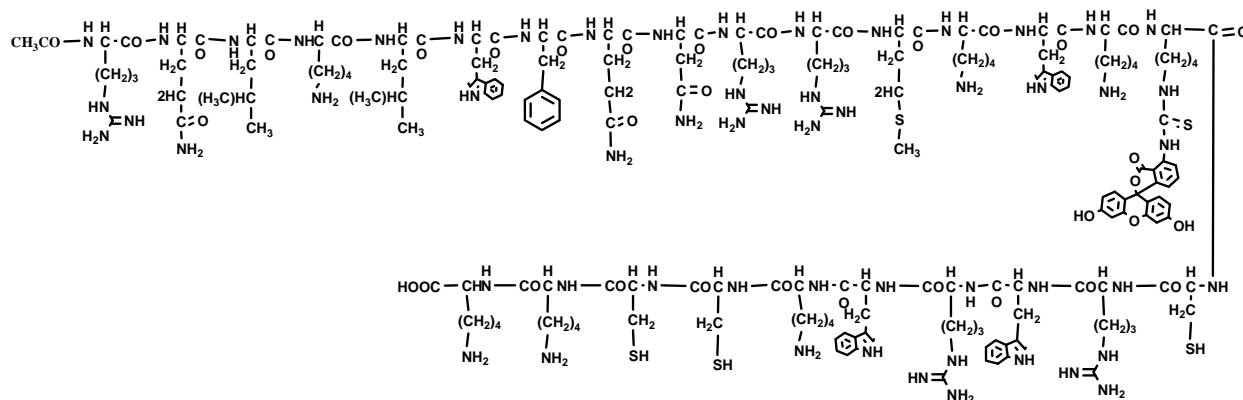
Chemical Formula: C$_{188}$H$_{276}$N$_{56}$O$_{36}$S$_5$
Exact Mass: 4054.01
Molecular Weight: 4056.88
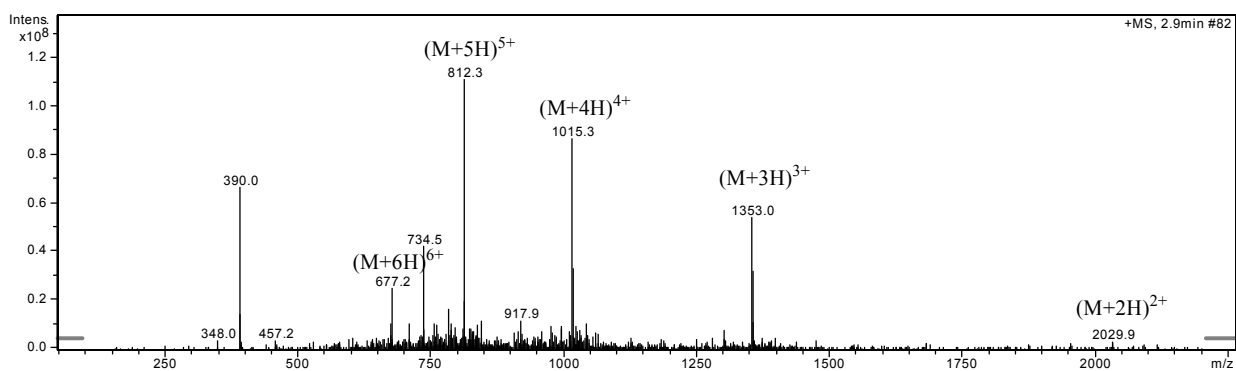
The detected molecular ions for Pen +15 conjugated with a lysine linker and FITC were (M+2H) $^{2+}$= 2029.9, (M+3H) $^{3+}$= 1353.0, (M+4H) $^{4+}$ =1015.3, (M+5H) $^{5+ =}$ 812.3, (M+6H) $^{6+ =}$ 677.2. They were consistent with the calculated mass of the desired product 4056.9. Peaks 390.0, 734.5 and 917.9 are fragment ions.
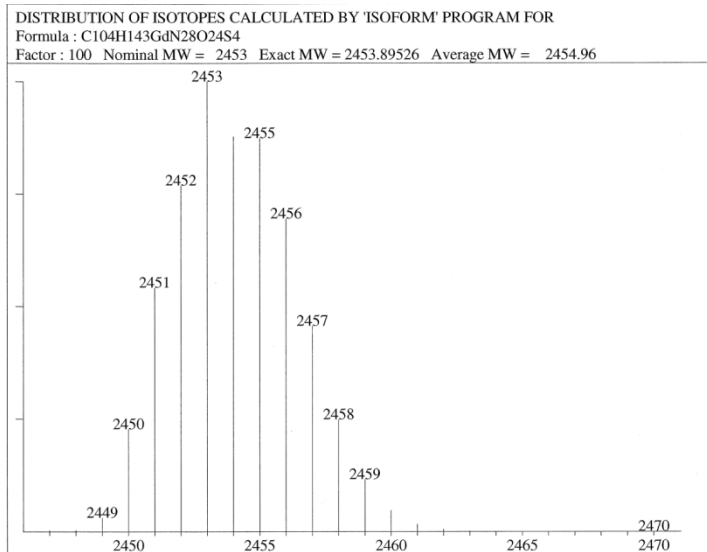
5. PNA-CyLoP-1

Ac-tccgtgaacggc-K(FITC)-CRWRWKCCKK

Chemical Formula: $C_{218}H_{281}N_{95}O_{53}S_4$
Exact Mass: 5205.11
Molecular Weight: 5208.43
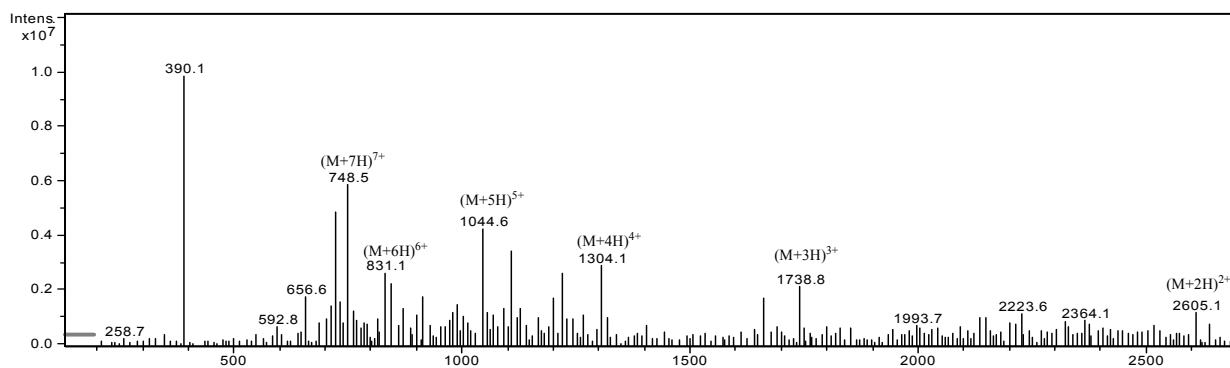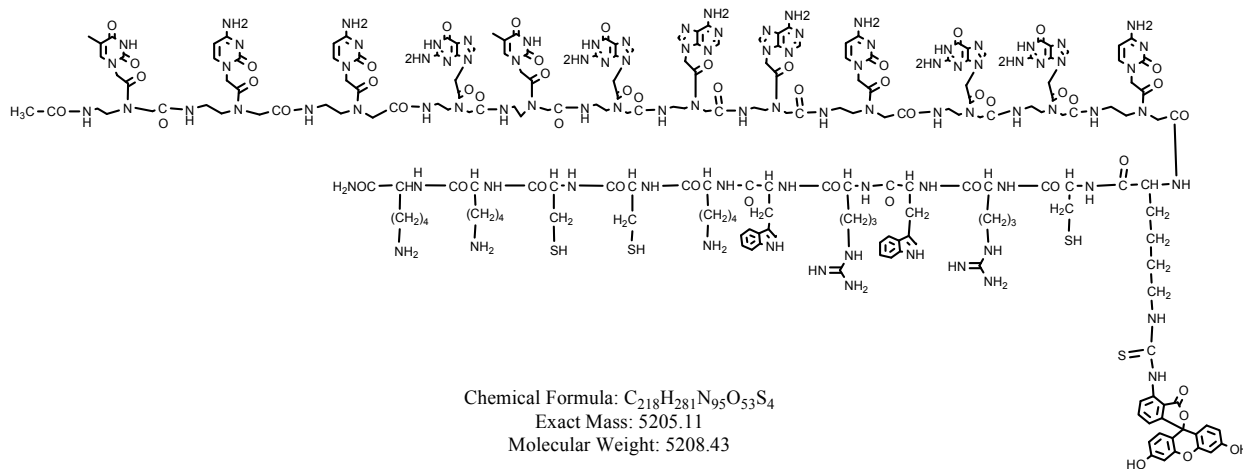
The detected molecular ions for PNA +15 conjugated with a lysine linker and FITC were $(M+2H)^{2+} = 2605.1$, $(M+3H)^{3+} = 1738.8$, $(M+4H)^{4+} = 1304.1$, $(M+5H)^{5+} = 1044.6$, $(M+6H)^{6+} = 869.2$, $(M+7H)^{7+} = 748.5$. They were consistent with the calculated mass of the desired product 5208.4. A peak of 390.0 is due to fragmentation.

5.6 Uptake studies

5.6.1 Concentration estimation of FITC-labeled compounds

Compounds were dissolved in purified water (Milli-Q, Millipore) to obtain a 10 mM solution by weight. The pH was adjusted to 6.5 with 0.1M NaOH and 0.1M HCl. Especially for peptide conjugates this had to be done carefully since pH values >7 led to poorly reversible precipitation of the compounds, For the determination of the actual concentration, the stock solutions were diluted (1:100) in Dulbecco's Modified Eagle's Medium (DMEM; Biochrom AG, Germany). The absorbance of the diluted solutions was measured in a multiplate reader (BMG Labtech, Germany) at 485 nm with ratiometric correction of turbidity at 690 nm. The concentrations of the stock solutions were calculated assuming $\varepsilon_{carboxyfluorescein\ 485\ nm}$=81,000 l/(mol·cm) and all further dilutions of the stock solutions for cell incubations and relaxivity studies were done according to this calculated concentration.

5.6.2 Cell Culture

The NIH 3T3 embryonic mouse fibroblast cells (obtained from DSMZ, Germany) and C6 rat glioma cells (a kind gift from Prof. B. Hamprecht, University of Tuebingen, Germany) and PANC-1 human pancreatic carcinoma cells (obtained from ATCC, USA) were grown as monolayers in Dulbecco's Modified Eagle's Medium (DMEM) supplemented with 10% fetal bovine serum, 4 mM L-glutamine, 100 µg/ml streptomycin and 100 U/ml penicillin (all purchased from Biochrom AG, Germany) at 37°C with 10% CO_2. Confluent cultures were split using trypsin/EDTA 0.05/0.02% (w/v) in phosphate-buffered saline (PBS; Biochrom AG, Germany) every second to third day, depending on the cell line.

CCL-11 mouse fibrosarcoma cells (obtained from ATCC, USA) were cultured in an antibiotic-free mixture of NCTC135 medium supplemented with 10% heat inactivated donor horse serum at 37°C with 5% CO_2. Subculturing was performed two times a week by trypsinization.

5.6.3 Internalization

Internalization experiments on cells were performed in 96 well microplates. At 70-80% confluency (after 24 – 48h), cells were incubated with different concentrations of the compounds in complete culture medium for the indicated time points (2 – 18h) at routine culture conditions.

After incubation, the medium was removed and cells were incubated with Bisbenzimid 33342 (Hoechst 33342), a nuclear stain, in complete medium for 30 min (100µl/well) in order to estimate the cell number. Afterwards, the supernatant was removed and extracellular fluorescence was quenched by incubation with cold trypan blue (0.05% (w/v) in PBS, 100µl/well) for 3 min (*ref*) followed by two washes with 200µl cold HBSS (Biochrom AG, Germany) and the addition of 200µl pre-warmed (37°C) HBSS. Cell-related FITC fluorescence (Ex 485 nm/Em 530 nm) and cell number (Ex 346 nm/ Em 460 nm) were evaluated in the multiplate reader. The internalized fluorescence was corrected by the cell number according to the following equation and called Corrected fluorescence units (corr. f.u.):

$$fluorescence_{(FITC)}/fluorescence_{(Hoechst)} \times 1000.$$

Cells incubated in absence of CA were used as control and wells without cells but treated with Hoechst, Trypan Blue and washed as described above were used as blank.

Hoechst fluorescence could also be used for the evaluation of cytotoxicity of compounds.

The cells in plates processed for fluorescence spectroscopic measurement, as mentioned above, were used for complementary fluorescence microscopy. Microscopy was performed without fixation using a Zeiss Axiovert 200 M microscope (Germany) with an LD Plan NeoFluor 40X objective. The imaging conditions were kept constant for all different samples. Cellular localization and distribution of the peptide was observed by irradiating with blue light (Ex 470/40 nm) and observing at the emission (Em) at 525/50 nm. Apart from FITC fluorescence, the nuclear staining with Hoechst was observed using Ex 365/15nm and Em 460/50 nm. Furthermore, trypan blue fluorescence was viewed at Ex 535/50 and Em 645/75 nm. Phase contrast images with differential interference contrast (DIC) microscopy of the same areas were made to verify if the cells maintain their normal morphology. Volocity Acquisition and Visualization software (Improvision, England) was used for high speed image capture and high resolution rendering of data sets as images.

5.6.4 Statistical analysis

Data were expressed as means with standard errors of the mean (SEM) for the various statistical groups (three or more experiments with six replicate each). To find out whether the two mean

values of interest were significantly different, unpaired Student's t-tests were performed using GraphPad Prism version 5.00 for Windows (GraphPad Software, USA). When comparing more than two values, a one-way analysis of variance (ANOVA) with Bonferroni's post test for multiple comparisons was performed using GraphPad Prism.

5.7 Relaxation rates in cells

For MR imaging of cells, exponentially growing cells were labeled with different concentrations of CAs in 175 cm^2 tissue culture flasks for 2, 4, or 18h. After two times washing with HBSS and once with PBS, cells were trypsinated, centrifuged and re-suspended in 1.5 mL Eppendorf tubes to a density of 2×10^7 cells in 500 µl complete medium. Cells were allowed to settle before MR measurements. Tubes with medium only and tubes with cells without CA were used as controls. MR imaging of the cell pellets at room temperature (~21 °C) was done using a 3 T (123 MHz) human MR scanner (MAGNETOM Tim Trio, Siemens Healthcare, Germany), with a 12-channel RF Head coil and slice selective measurements from a slice with a thickness of 1 mm positioned through the cell pellet. T_1 was measured using an inversion-recovery sequence, with an adiabatic inversion pulse followed by a turbo-spin-echo readout. Between 10 and 15 images were taken, with the time between inversion and readout varying from 23 ms to 3000 ms. With a repetition time of 10 s, 15 echoes were acquired per scan and averaged six times. For T_2, a home written spin-echo sequence was used with echo times varying from 19 ms to 1000 ms in about 10 steps and a repetition time of 8 s. Diffusion sensitivity was reduced by minimizing the crusher gradients surrounding the refocusing pulse. All experiments scanned 256^2 voxels in a field-of-view of 110 mm in both directions resulting in a voxel volume of $0.43 \times 0.43 \times 1$ mm^3. Data analysis was performed by fitting to relaxation curves with self-written routines with the software MATLAB 7.1 R14 (The Mathworks Inc., United States). The series of T_1 and T_2 relaxation data were fitted to the following equations:

   a) *T_1 series with varying $t = T_I$*: $S = S_0 (1 - \exp(-t / T_1) + S(T_I = 0) \exp(-t / T_1)$.

   b) *T_2 series with varying $t = TE$*: $S = S_0 \exp(-t / T_2)$.

Nonlinear least-squares fitting of three parameters S_0, $S_{(TI = 0)}$, and T_1/T_2 was done for manually selected regions-of-interest with the Trust-Region Reflective Newton algorithm implemented in MATLAB. The quality of the fit was controlled by visual inspection and by calculating the mean

errors and residuals. The obtained T_1 and T_2 values of the pellets were converted to $R_{1,cell}$ (= $1/T_1$) and $R_{2,cell}$ (=$1/T_2$). These were expressed in % of control ($R_{1,cell}$ and $R_{2,cell}$ of cells incubated similar in absence of CA): $R_{1,cell\,(sample)}/R_{1,cell\,(control)} \times 100$

5.8 Relaxivity in solution

Three to five concentrations in the range of $5 - 40$ µM were prepared in 800 µl purified (Milli-Q, Millipore,) water. Water was used as blank. Two times 200µl of each sample were transferred to a 96well plate and the absorbance was measured at 485nm to verify the exact concentration. Afterwards, samples for each concentration were combined and 380µl aliquots were transferred into Eppendorf cups for MR measurement (two replicates per concentration). Parameters and evaluation were the same as for measurements of relaxations rates in cells. Relaxation rate values were plotted versus the exact concentration (in mM) and linear regression was done. The slope of the obtained curve is the corresponding relaxivity. Alternatively, relaxivity can also be calculated for each concentration according to the following equation:

$(R_{1,conc.} - R_{1,blank})/c$

$R_{1,conc}$, relaxation rate for sample with CA at concentration c (in mM)

$R_{1,blank,}$ relaxation rate for blank

C, concentration of CA in mM

PART 6

REFERENCES

Aime S., Botta M., Geninatti Crich S., Giovenzana G., Palmisano G., Sisti M. (1999). A macromolecular Gd(III) complex as pH-responsive relaxometric probe for MRI applications *Chem. Commun.*, 1577–1578.

Allen M. J., Mac Renaris K. W., Venkatasubramanian P. N, and Meade T. J., (2004). Cellular Delivery of MRI Contrast Agents, *Chemistry & Biology, 11*: 301–307.

Anderson, C. J. and Welch M. J., (1999). Radiometal-Labeled Agents (Non-Technetium) for Diagnostic Imaging, *Chem. Rev., 99*: 2219-2234.

Andreu D., Albericio F., Solé N. A., Munson M. C., Ferrer M., and Barany G. in *Peptide Synthesis Protocols, Methods Mol. Biol.,* Vol.35 (Eds: M. W. Pennington, B. M. Dunn), Humana Press Inc., Totowa, NJ (1994), 91-169.

Andrushchenko V. V., Vogel H. J., Prenner E. J., (2007). Optimization of the hydrochloric acid concentration used for trifluoroacetate removal from synthetic peptides, *J. Pept. Sci. 13*: 37–43.

Angell Y. M., Alsina. J., Albericio F., and Barany. G. (2002), Practical protocols for stepwise solid-phase synthesis of cysteine-containing peptides, *J. Peptide Res., 60*: 292-299.

Baird G. S., Zacharias D. A., Tsien R. Y. (2000). Biochemistry, mutagenesis, and oligomerization of DsRed, a red fluorescent protein from coral, *PNAS, 97*: 11984–11989.

Barawkar D. A., Bruice T. C. (1998). Synthesis, biophysical properties, and nuclease resistance properties of mixed backbone oligodeoxynucleotides containing cationic internucleoside guanidinium linkages: Deoxynucleic guanidine/ DNA chimeras, *Proc. Natl. Acad. Sci., 95*: 11047–11052.

Braun K., Peschke P., Pipkorn R., S. Lampel, Wachsmuth M., Waldeck W., Friedrich E., Debus J. (2002). A Biological Transporter for the Delivery of Peptide Nucleic Acids (PNAs) to the Nuclear Compartment of Living Cells, *J. Mol. Biol., 318*: 237–243.

Bulmus V., Woodward M., Lin L., Murthy N., Stayton P., Hoffman A., (2003). A new pH-responsive and glutathione-reactive, endosomal membrane-disruptive polymeric carrier for intracellular delivery of biomolecular drugs, *Journal of Controlled Release*, *93*: 105– 120.

Cabella C., Geninatti Crich S., Corpillo D., Barge A., Ghirelli C., Bruno E., Lorusso V., Uggeri F., Aime S. (2006). Cellular labeling with Gd(III) chelates: only high thermodynamic stabilities prevent the cells acting as 'sponges' of Gd^{3+} ions, *Contrast Med. Mol. Imaging, 1*: 23–29.

Caplen N.J., Parrish S, Imani F, Fire A., Morgan R.A. (2001). Specific inhibition of gene expression by small double-stranded RNAs in invertebrate and vertebrate systems, *PNAS, 98*: 9742-9747.

Caravan P., Cloutier N. J., Greenfield M. T., McDermid S. A., Dunham S. U., Bulte J.W. M., Amedio J. C., Looby R. J., Supkowski R. M., Horrocks W. D., McMurry T. J., Lauffer R B. (2002)**.** The Interaction of MS-325 with Human Serum Albumin and Its Effect on Proton Relaxation Rates, *J. Am. Chem. Soc.*, *124*: 3152-3162.

Caravan P., Ellison J. J., McMurry T. J., Lauffer R. B. (1999). Gadolinium(III) Chelates as MRI Contrast Agents: Structure, Dynamics, and Applications, *Chem. Rev., 99*: 2293-2352.

Chaloin L., Vidal P., Heitz A., Van Mau N., Méry J., G. Divita, Heitz F. (1997). Conformations of primary amphipathic carrier peptides in membrane mimicking environments, *Biochemistry*, *36*: 11179– 11187.

Chen L.L., Frankel A.D., Harder J.L., Fawell S., Barsoum J., Pepinsky B. (1995). Increased cellular uptake of the human immunodeficiency virus-1 Tat protein after modification with biotin. *Anal Biochem., 227*:168-75.

Cioca D. P., Aoki Y., Kiyosawa K. (2003). RNA interference is a functional pathway with therapeutic potential in human myeloid leukemia cell lines, *Cancer Gene Therapy, 10*: 125-33.

Cornish J., Callon K. E.,. Lin C. Q.-X, Xiao C. L., Mulvey T. B., Cooper G. J. S., Reid I. R. (1999). Trifluoroacetate, a contaminant in purified proteins, inhibits proliferation of osteoblasts and chondrocytes, *Am J Physiol Endocrinol Metab, 277*:779-783.

Crich G., Cabella C., Barge A., Belfiore S., Ghirelli C., Lattuada L., Lanzardo S., Mortillaro A., Tei L., Visigalli M., Forni G., Aime S. (2006). In Vitro and in Vivo Magnetic Resonance Detection of Tumor Cells by Targeting Glutamine Transporters with Gd-Based Probes, *J. Med. Chem.*, *49*: 4926-4936.

Crombez L., Charnet A., Morris M.C., Aldrian-Herrada G., Heitz F., Divita G., (2007). A non-covalent peptide-based strategy for siRNA delivery, *Biochemical Society Transactions, 3:* 44-46.

Czajlik A., Meskó E., Penke B., Perczel A. (2002). Investigation of Penetratin Peptides Part 1. The Environment Dependent Conformational Properties of Penetratin and Two of its Derivatives, *J. Peptide Sci, 8*: 151–171.

De La Torre B. G., Andreu D., (2008), On choosing the right ether for peptide precipitation after acid cleavage, *J. Pept. Sci.*, *14*: 360-363.

De Sousa-e-Silva M.C.C., Tomy S.C., Tavares F.L., Navajas L., Larsson M.H.M.A., Lucas S.R.R., Kogika M.M., Sano-Martins S. (2003). Hematological, hemostatic and clinical chemistry disturbances induced by *Crotalus durissus terri.cus* snake venom in dogs, *Human & Experimental Toxicology, 22*: 491- 500.

Delgado R., Felix *V.*, *Lúı*s M. P. Lima and Price D. W. (2007), Metal complexes of cyclen and cyclam derivatives useful for medical applications: a discussion based on thermodynamic stability constants and structural data. *Dalton Trans.*, 2734–2745.

Derossi D, Chassaing G, Prochiantz A. (1998), Trojan Peptides - the Penetratin System for Intracellular Delivery. *Trends in Cell Biology, 8*: 84-87.

Derossi D, Joliot A.H., Chassaing G., Prochiantz A. (1994), The third helix of the Antennapedia homeodomain translocates through biological membranes. *Journal of Biological Chemistry, 269*: 10444-50.

Deshayes S., Morris M. C., Divita G., and Heitz F (2005). Cell-penetrating peptides: tools for intracellular delivery of therapeutics. *Cell. Mol. Life Sci.***, *62:* 1839–1849.

Díaz-Mochón J. J., L. Bialy, J. Watson, Sánchez-Martín R. M., Bradley M. (2005). Synthesis and cellular uptake of cell delivering PNA–peptide conjugates *Chem. Commun.*, 3316–3318.

Dietz G.P.H. and Bähr M. (2004). Delivery of bioactive molecules into the cell: the Trojan horse approach, *Mol. Cell. Neurosci., 27:* 85–131.

Dom G., Shaw-Jackson C., Matis C., Boufoux O., Picard J. J., Prochiantz A., Mingeot-Leclercq M.-P., Brasseur R. and Rezsohazy R. (2003). Cellular uptake of Antennapedia Penetratin peptides is a two-step process in which phase transfer precedes a tryptophan-dependent translocation, *Nucleic Acids Research, 31*: 556-561.

Duchardt F., Fotin-Mleczek M., Schwarz H., Fischer R. and Brock R. (2007). A comprehensive model for the cellular uptake of cationic cell-penetrating peptides. *Traffic. 8*: 848-866.

El-Andaloussi S., Järver P., Johansson H. J., Langel Ü, (2007). Cargo-dependent cytotoxicity and delivery efficacy of cell-penetrating peptides: a comparative study, *Biochem. J., 407*: 285–292.

Endres P. J., MacRenaris K. W., Vogt S., Allen M. J., Meade T. J. (2006). Quantitative Imaging of Cell-Permeable Magnetic Resonance Contrast Agents Using X-Ray Fluorescence., *Molecular Imaging, 5*: 485–497.

Fadel V., Bettendorff P., Herrmann T., de Azevedo Jr W. F., Oliveira E. B., Yamane T., Wüthrich K. (2005). Automated NMR structure determination and disulfide bond identification of the myotoxin crotamine from Crotalus durissus terrificus: *Toxicon, 46*: 759–767.

Fandy T. E, Shankar S., Srivastava R. K. (2008). Smac/DIABLO enhances the therapeutic potential of chemotherapeutic drugs and irradiation, and sensitizes TRAIL-resistant breast cancer cells, *Molecular Cancer*, 7:1-10.

Faure, G., Choumet, V., Bouchier, C., Camoin, L., Guillaume, J.L., Monegier, B., Vuilhorgne, M., Bon, C. (1994). The origin of the diversity of crotoxin isoforms in the venom of Crotalus durissus terrificus, *Eur. J. Biochem., 223*: 161–164.

Fawell S., Seery J., Daikh Y., Moore C., Chen L. L., Pepinsky B., Barsoum J. (1994). Tat-mediated delivery of heterologous proteins into cells. *Proc. Natl. Acad. Sci., 91*: 664-668.

Fischer P. M., (2006). Cellular Uptake Mechanisms and Potential Therapeutic Utility of Peptidic Cell Delivery Vectors: Progress 2001-2006, *Medicinal Research Reviews, 27*, 755-795.

Fischer R., Bächle D., Fotin-Mleczek M., Jung G., Kalbacher H., Brock R. (2006). A Targeted Protease Substrate for a Quantitative Determination of Protease Activities in the Endolysosomal Pathway, *ChemBioChem, 7*: 1428 – 1434.

Fischer R., Waizenegger T., Köhler K., Brock R. (2002). A quantitative validation of fluorophore-labelled cell-permeable peptide conjugates: fluorophore and cargo dependence of import, *Biochimica et Biophysica Acta, 1564*: 365– 374.

Fittipaldi A., Ferrari A., Zoppé M., Arcangeli C., Pellegrini V., Beltram F., and Giacca M., (2003). Cell Membrane Lipid Rafts Mediate Caveolar Endocytosis of HIV-1 Tat Fusion Proteins, *J. Biol. Chem., 36*: 34141–34149.

Foerg C., Ziegler U., Fernandez-Carneado J., Giralt E., Rennert R., Beck-Sickinger A.G. and Merkle H.P. (2005). Decoding the entry of two novel cell penetrating peptides in HeLa cells: lipid raft-mediated endocytosis and endosomal escape, *Biochemistr., 44:* 72–81.

Frankel A. D., Bredt D. S., Pabo C. O. (1988), Tat Protein from Human Immunodeficiency Virus Forms a Metal-Linked Dimer, *Science*, *240*: 70-73.

Frullano L., Rohovec J., Aime S., Maschmeyer T. Prata M. I., Pedroso de Lima J. J., Geraldes C. F. G. C., Peters J. A. (2004).Towards Targeted MRI: New MRI Contrast Agents for Sialic Acid Detection, *Chem. Eur. J., 10*: 5205 – 5217.

Fujihara S.M., Cleaveland J. S., Grosmaire L. S., Berry K. K., Kennedy K. A., Blake J. J., Loy J, Rankin B. M., Ledbetter J. A., and Nadler S. G., (2000). A D-Amino Acid Peptide Inhibitor of NF-kB Nuclear Localization Is Efficacious in Models of Inflammatory Disease, *The Journal of Immunology,* 165: 1004–1012.

Futaki S., Suzuki T., Ohashi W., Yagami T., Tanaka S., Ueda K., and Yukio S. (2001). Arginine-rich Peptides - An abundant source of membrane-permeable peptides having potential as carriers for intracellular protein delivery, *J Biol Chem.*, *276*: 5836–5840.

Gait M.J. (2003). Peptide-mediated cellular delivery of antisense oligonucleotides and their analogues, *Cell. Mol. Life Sci., 60*: 844–853.

Gaussier H., Morency H., Lavoie M. C., Subirade M. (2002). Replacement of Trifluoroacetic Acid with HCl in the Hydrophobic Purification Steps of Pediocin PA-1: a Structural Effect *Applied and Environmental Microbiology*, 4803–4808.

Gil-Parrado S., Assfalg-Machleidt I., Fiorino F., Deluca D., Pfeiler D., Schaschke N., Moroder L., Machleidt W. (2003). Calpastatin Exon 1B-Derived Peptide, a Selective Inhibitor of Calpain: Enhancing Cell Permeability by Conjugation with Penetratin, *Biol. Chem., 384*: 395 – 402.

Giraud M., Cavelier F., and Martinez J. (1999). A Side-reaction in the SPPS of Trp-containing Peptides, *J. Pept. Sci., 5*: 457-461.

Green M. and Loewenstein P. M. (1988). Autonomous Functional Domains of Chemically Synthesized Human lmmunodeficiency Virus Tat Trans-Activator Protein, *Cell, 55*: 1179-l 188.

Gupta B., Levchenko T. S., and Torchilin V. P. (2005). Intracellular delivery of large molecules and small particles by cell-penetrating proteins and peptides, *Adv. Drug Delivery Rev.*, *57*: 637– 651.

Han Y., Albericio F., and Barany G. (1997). Occurrence and Minimization of Cysteine Racemization during Stepwise Solid-Phase Peptide Synthesis, *J. Org. Chem.*, *62:* 4307-4312.

Hayashi M. A. F., Nascimento F. D., Kerkis A., Oliveira V., Oliveira E. B., Pereira A., Rádis-Baptista G., Nader H. B., Yamane T., Kerkis I., and Tersariol I. L. S. (2008). Cytotoxic effects of crotamine are mediated through lysosomal membrane permeabilization, *Toxicon, 52*: 508–517.

Heckl S., Sturzu A., Regenbogen M., Beck A., Feil G., Gharabaghi A., Echner H. (2008). A novel polyarginine containing Smac peptide conjugate that mediates cell death in tumor and healthy cells, Med Chem. 4: 348–354.

Hemann M.T., Fridman J.S., Zilfou J.T., Hernando E., Paddison P.J., Cordon-Cardo C., Hannon G.J., Lowe S.W., (2003), An epi-allelic series of p53 hypomorphs created by stable RNAi produces distinct tumor phenotypes in vivo. *Nat. Genet.*, *33*: 396-400.

Henriques S. T., Costa J., Castanho M. A.R.B., (2005), Re-evaluating the role of strongly charged sequences in amphipathic cell-penetrating peptides A fluorescence study using Pep-1, *FEBS Letters*, *579*: 4498–4502.

Huang H., and Rabenstein D. L. (1999). A cleavage cocktail for methionine-containing peptides, *J. Peptide Res., 53*: 548-553.

Hyodo F., Matsumoto K., Matsumoto A., Mitchell J. B., Krishna M. C. (2006), Probing the Intracellular Redox Status of Tumors with Magnetic Resonance Imaging and Redox-Sensitive Contrast Agents, *Cancer Res, 66:* 9921-9928.

Jha, D., Su W., Mishra R., Engelmann J., Wiesmüller K-H., Maier M. E., Pfeuffer J. and Ugurbil K., (2007), Cell internalizing conjugates for MR/Optical Imaging: CPP cargo relationship affects uptake for optical and MR imaging techniques. *Joint Molecular Imaging Conference,* 1032.

Johnson T. and Sheppard R. C., (1991), Resin Effects in Solid-phase Peptide Synthesis. Enhanced Purity of Tryptophan-containing Peptides through Two-step Cleavage of Side Chain Protecting Groups and Peptide-Resin Linkage, *J. Chem. Soc., Chem. Commun,* 1653-1655.

Joliot A., Pernelle C., Deagostini-Bazin H., Prochiantz A. (1991). Antennapedia homeobox peptide regulates neural morphogenesis, *Proc. Natl. Acad. Sci.*, *88*: 1864-1868.

Karim C. B., Paterlini M. G., Reddy L. G., Hunter G. W., Barany G., and Thomas D. D. (2001). Role of Cysteine Residues in Structural Stability and Function of a Transmembrane Helix Bundle, *Journal of Biological Chemistry, 276*: 38814–38819.

Keelara A., Jaccard H., Kretzschmar M., Helm L. and Maecke H. R. (2008), Novel DOTA-based prochelator for divalent peptide vectorization: synthesis of dimeric bombesin analogues for multimodality tumor imaging and therapy, *Chem. Commun.,* 3248–3250.

Kerkis A., Hayashi M. A. F., Yamane T. and Kerkis I. (*2006),* Properties of Cell Penetrating Peptides (CPPs), *IUBMB Life, 58*: *7-13.*

Kerkis A., Kerkis I., Rádis-Baptista G., Oliveira E. B., Vianna- Morgante A. M., Pereira L. V., and Yamane T. (2004). Crotamine is a novel cell-penetrating protein from the venom of rattlesnake *Crotalus durissus terrific*us, *FASEB J., 18*: 1407-1409.

Koppelhus U., P. E. Nielsen (2003). Cellular delivery of peptide nucleic acid (PNA). *Advanced Drug Delivery Reviews, 55*: 267–280.

Langel U., (2001), Cellular translocation of proteins by transportan, *FASEB J.,* 15: 1451-3,

Larsen H. J., Bentin T., Nielsen P. E. (1999). Antisense properties of peptide nucleic acid, *Biochimica et Biophysica Acta, 1489*: 159-166.

Lewin M., Carlesso N., Tung C.-H., Tang X.-W., Cory D., Scadden D.T., Weissleder R. (2000). Tat peptide-derivatized magnetic nanoparticles allow in vivo tracking and recovery of progenitor cells, *Nature Biotechnology, 18*: 410-414.

Liu S., and Edwards D. S. (2001), Bifunctional Chelators for Therapeutic Lanthanide Radiopharmaceuticals, *Bioconjugate Chem.*, *12:* 734 7.

Louie A.Y., Hüber M.M., Ahrens E. T., Rothbächer U., Moats R., Jacobs R. E., Fraser S. E., Meade T. J. (2000). In vivo visualization of gene expression using magnetic resonance imaging *Nature Biotechnology,18*: 321-325.

Lukeš I., Kotek J., Vojtíšek P., Hermann P. (2001) Complexes of tetraazacycles bearing methylphosphinic/phosphonic acid pendant arms with copper(II), zinc(II) and lanthanides(III). A comparison with their acetic acid analogues, *Coordination Chemistry Reviews,* 216–217:287–312.

Lundberg P. and Langel U. (2003). A brief introduction to cell-penetrating peptides, *J. Mol. Recognit., 16*: 227–233.

Lundberg P., El-Andaloussi S., Sütlü T., Johansson H., and Langel Ü, (2007). Delivery of short interfering RNA using endosomolytic cell-penetrating peptides, *The FASEB Journal*, 21: 2664-2671.

Lundin P., Johansson H., Guterstam P., Holm T., Hansen M., Langel Ü, EL Andaloussi S., (2008). Distinct Uptake Routes of Cell-Penetrating Peptide Conjugates, *Bioconjugate Chem.*, *1:* 2535–2542.

Mae M., and Langel U. (2006). Cell-penetrating peptides as vectors for peptide, protein and oligonucleotide delivery. *Curr Opin Pharmacol., 6*: 509–514.

Magzoub M. and Graslund A. (2004). Cell-penetrating peptides: small from inception to application, *Quart Rev Biophys., 37*: 147–195.

Mai J. C., Shen H., Watkins S. C., Cheng T. and Robbins P. D. (2002). Efficiency of protein transduction is cell type-dependent and is enhanced by dextran sulfate, *J. Biol. Chem., 277*: 30208–30218.

Maiolo J. R., M. Ferrer, E. A. Ottinger, (2005), Effects of cargo molecules on the cellular uptake of arginine-rich cell-penetrating peptides, *Biochimica et Biophysica Acta*, *1712*: 161 – 172.

Mancin A. C., Soares A. M., Andriao-Escarso S. H., Faca V.M., Greene L. J., Zuccolotto S. , Pela I. R. and Giglio J. R. (1998*), The analgesic activity of crotamine, a neurotoxin from Crotalus durissus terrificus (South American Rattle snake) venom: A biochemical and pharmacological study, *Toxicon, 36: 1927-1937.*

Martins L.M., Iaccarino I., Tenev T., Gschmeissner S., Totty N.F., Lemoine N.R., Savopoulos J., Gray C.W., Creasy C.L., Dingwall C., Downward J. (2002), The serine protease Omi/HtrA2 regulates apoptosis by binding XIAP through a reaper-like motif, *J Biol Chem., 277*: 439-44.

Meade B. R, and Dowdy S. F. (2008). Enhancing the cellular uptake of siRNA duplexes following noncovalent packaging with protein transduction domain peptides, *Advanced Drug Delivery Review, 60*: 530–536.

Melikov K. and Chernomordik L. V. (2005). Arginine-rich cell penetrating peptides: from endosomal uptake to nuclear delivery, *Cell. Mo. Life Sci.*, *62*: 2739–2749.

Mier W., Graham K.A.N., Wang Q., Krämer S. (2004). Synthesis of peptide conjugated chelator oligomers for endoradiotherapy and MRT imaging, *Tetrahedron Letters, 45:* 5453–5455.

Mitchell D.J., Kim D.T., Steinman L., Fathman C.G., Rothbard, J.B. (2000). Polyarginine enters cells more efficiently than other polycationic homopolymers, *J. Peptide Res., 56*: 318-325.

Mizukami S., Takikawa R., Sugihara F., Hori Y., Tochio H., Wlchli M., Shirakawa M., Kikuchi K. *(*2008). Paramagnetic Relaxation-Based 19F MRI Probe To Detect Protease Activity, *J. Am. Chem. Soc.*, *130*: 794-795.

Moroder L., (2005). Isosteric replacement of sulfur with other chalcogens in peptides and proteins, *J. Peptide Sci.*, *11*: 187–214.

Morris M. C., Depollier J. , Méry J , Heitz F. and Divita G. (2001). A peptide carrier for the delivery of biologically active proteins into mammalian cells, *Nat. Biotechnol.,* 19: 1173-1176.

Muratovska A. and Eccles M. R. (2004). Conjugate for efficient delivery of short interfering RNA (siRNA) into mammalian cells, *FEBS Letters, 558*: 63-68.

Nicastro G., Franzoni L., de Chiara C., Mancin A. C., Giglio J. R.and Spisni A. (2003). Solution structure of crotamine, a Na$^+$ channel affecting toxin from *Crotalus durissus terrificus* venom, *Eur. J. Biochem.,* 270: 1969-1979.

Nielsen P. E. (1995). Peptide nucleic acid (PNA): A lead for gene therapeutic drugs, *Perspectives in Drug Discovery and Design, 4*: 76-84.

Nielsen P. E. (2005). Addressing the challenges of cellular delivery and bioavailability of peptidenucleic acids (PNA), *Quarterly Reviews of Biophysics, 38*: 345–350.

Oguiura N., Boni-Mitake M., and Rádis-Baptista G. (2005). New view on crotamine, a small basic polypeptide myotoxin from South American rattlesnake venom, *Toxicon., 46*: 363–370.

Ohmori N., Niidome T., Kiyota T., Lee S., Sugihara G., Wada A., Hirayama T., Aoyagi H. (1998). Importance of Hydrophobic Region in Amphiphilic Structures of a-Helical Peptides for Their Gene Transfer-Ability into *Cells Biochemical and Biophysical Research Communications, 245*: 259–265.

Parton R. G. and Richards A.A., (2003), Lipid Rafts and Caveolae as Portals for Endocytosis: New Insights and Common Mechanisms, *Traffic,* 4: 724–738.

Patel L. N. Zaro J. L., and Shen W.-C., (2007), Cell Penetrating Peptides: Intracellular Pathways and Pharmaceutical Perspectives, *Pharmaceutical Research*, *24*.

Plank C., Oberhauser B., Mechtler K., Koch C., Wagner E. (1994).The Influence of Endosome-disruptive Peptides on Gene Transfer Using Synthetic Virus-like Gene Transfer Systems , *The Journal of Biological Chemistry, 269*: 12918–12924.

Pooga M., Hällbrink M., Zorko M., Langel Ü. (1998). Cell penetration by transportan, *The FASEB Journal, 12*, 67-77.

Pooga M., Kut C., Kihlmark M., Hallbrink M., Fernaeus S., Raid R., Land T., Hallberg E, Bartfai T, and Langel Ü., (2001). Cellular translocation of proteins by transportan, *The FASEB Journal,*1451-1453.

Prantner A. M., Sharma V., Garbow J. R., and Piwnica-Worms D., (2003). Synthesis and Characterization of a Gd-DOTA-D-Permeation Peptide for Magnetic Resonance Relaxation Enhancement of Intracellular Targets, *Molecular Imaging*. *2*: 333 – 341.

Prochiantz A. (1996), Getting Hydrophilic Compounds into Cells - Lessons from Homeopeptides – Commentary, *Current Opinion in Neurobiology, 6*: 629-634.

Rádis-Baptista G., Kerkis A., Prieto-Silva Á. R., Hayashi M. A. F., Kerkis I., and Yamane T. (2008)**.** Membrane-translocating Peptides and Toxins: from Nature to Bedside, *J. Braz. Chem. Soc.**, 19*: 211-225.

Rádis-Baptista G., Kubo T., Oguiura N., Svartman M., Almeida T.M.B., Batistic R. F., Oliveira E. B., Vianna-Morgante A . M., Yamane T. *(2003)* Structure and chromosomal localization of the gene for crotamine, a toxin from the South American rattlesnake, Crotalus durissus terrificus, *Toxicon, 42: 747– 752.*

Ranganathan R. S., Fernandez M. E., Kang S. I., Nunn A. D., Ratsep P.C., Pillai K. M. R., Zhang X., Tweedle M. F. (1998). New Multimeric Magnetic Resonance Imaging Agents, *Investigative Radiology, 33*: 779-797.

Rennert R., Wespe C., Beck-Sickinger A. G., and Neundorf I., (2006). Developing novel hCT derived cell-penetrating peptides with improved metabolic stability, *Biochimica et Biophysica Acta*., *1758*: 347-354.

Richard J. P., Melikov K, Vives E, Ramos C., Verbeure B., Gait M. J., Chernomordik L.V., Lebleu B. (2003). Cell-penetrating Peptides: a Reevaluation of the mechanism of cellular uptake, *J Biol Chem., 278*: 585–590.

Richard J. P., Melikov K., Brooks H., Prevot P., Lebleu B., and Chernomordik L. V. (2005), Cellular Uptake of Unconjugated TAT Peptide Involves Clathrin dependent Endocytosis and Heparan Sulfate Receptors, *The Journal of Biological chemistry*, 280: 15300–15306,

Rothbard J. B., Jessop T. C., Lewis R. S., Murray B. A., and Wender P. A. (2004). Role of Membrane Potential and Hydrogen Bonding in the Mechanism of Translocation of Guanidinium-Rich Peptides into Cells, *J. Am. Chem. Soc., 126*: 9506-9507.

Rothbard J. B., Kreider E., VanDeusen C. L., Wright L., Wylie B. L., and. Wender P.A*, (2002), Arginine-Rich Molecular Transporters for Drug Delivery: Role of Backbone Spacing in Cellular Uptake, *J. Med. Chem., 45:* 3612-3618.

Ruben S., Perkins A., Purcell R., Joung K., Sia R., Burghoff R., Haseltine W. A., Rosen C. A. (1989). Structural and Functional Characterization of Human Immunodeficiency Virus *tat* Protein, *Journal of Virology*, 1-8.

Rueping M., Mahajan Y., Sauer M., and Seebach D., (2002). Cellular Uptake Studies with β-Peptides, *ChemBioChem., 02-03*: 257-259.

Saab-Ismail N. H., Simor T., Gaszner B., Lóránd T., Szo¨llo¨sy M., and Elgavish G. A., (1999). Synthesis and in Vivo Evaluation of New Contrast Agents for Cardiac MRI, *J. Med. Chem., 42:* 2852-2861.

Sarin V. K., Kent S.B.H., Tam J. P., and Merrifield R.B. (1981). Quantitative monitoring of solid-phase peptide synthesis by the ninhydrin reaction. *Anal.Biochem., 117*: 147-157.

Schwarze S.R., Dowdy S.F. (2000), In vivo protein transduction: intracellular delivery of biologically active proteins, compounds and DNA. *Trends in Pharmacological Sciences, 21*: 45-48.

Sebbage V., (2009). Cell-penetrating peptides and their therapeutic applications *Bioscience Horizons*, *2*: 64-72.

Siedler F., Weyher E., and Moroder L. (1996). Cysteine Racemization in Peptide Synthesis: A New and Easy Detection Method, *J. Pept. Sci., 2*: 271-275.

Siegmund D., Hadwiger P. , Pfizenmaier K., Vornlocher H.-P., Wajant H., (2002). Selective Inhibition of FLICE-like Inhibitory Protein (FLIP) Expression With Small Interfering RNA Oligonucleotides (siRNAs) Is Sufficient to Sensitize Tumor Cells for TRAIL-Induced Apoptosis *Molecular Medicine,8*: 725–732.

Singh D., Bisland S. K., Kawamura K., Gariépy J. (1999). Peptide-Based Intracellular Shuttle Able To Facilitate Gene Transfer in Mammalian Cells *Bioconjugate Chem.*, *10:* 745-754.

Snyder E. L. and Dowdy S. F. (2004). Cell Penetrating Peptides in Drug Delivery, *Pharmaceutical Research., 21*: 3.

Stewart K. M., Horton *K*. L. and Kelley S. O., (2008), Cell-penetrating peptides as delivery vehicles for biology and medicine, *Org. Biomol. Chem.*, 6: 2242–2255.

Strijkers G. J., Hak S., Kok M. B., Springer C. S. and Nicolay K., (2009),Three Compartment *T*1 Relaxation Model for Intracellular Paramagnetic Contrast Agents, *Magnetic Resonance in Medicine, 61*: 1049–1058.

Sturzu A., Klose U., Echner H., Beck A., Gharabaghi A., Kalbacher H., Heckl S. (2009). Cellular uptake of cationic gadolinium-DOTA peptide conjugates with and without N-terminal myristoylation, *Amino Acids, 37*: 249–255.

Su W., (2007), Design and synthesis of Antisense Peptide Nucleic Acid Conjugated MR Contrast Agents, *PhD thesis*, Fakultät für Chemie and Pharmazie, Eberhard-Karls-Universität, Tübingen.

Sun H., Nikolovska-Coleska Z., Yang C.-Y., Qian D., Lu J., Qiu S., Bai L., Peng Y., Cai Q., Wang S. (2008). Design of Small-Molecule Peptidic and Nonpeptidic Smac Mimetics, *Acc. Chem. Res.*, *41*: 1264-1277.

Terreno E., Geninatti Crich S., Belfiore S., Biancone L., Cabella C., Esposito G., Manazza A. D., Aime S. (2006). Effect of the Intracellular Localization of a Gd-Based Imaging Probe on the Relaxation Enhancement of Water Protons, *Magnetic Resonance in Medicine, 55*: 491–497.

Toyama M. H., Carneiro E. M., Marangoni S., Barbosa R. L., Corso G., Boschero A. C. *(*2000*)* Biochemical characterization of two crotamine isoforms isolated by a single step RP-HPLC from Crotalus durissus terrifcus (South American rattlesnake) venom and their action on insulin secretion by pancreatic islets, *Biochimica et Biophysica Acta, 1474: 56-60.*

Tréhin R. and Merkle H. P. (2004). Chances and pitfalls of cell penetrating peptides for cellular drug delivery, *Eur J Pharm Biopharm.*, *58*: 209–223.

Turner J. J., Arzumanov A. A. and Gait M. J. (2005). Synthesis, cellular uptake and HIV-1 Tat-dependent trans-activation inhibition activity of oligonucleotide analogues disulphide-conjugated to cell-penetrating peptides, *Nucleic Acids Research, 33*: 27–42.

Turner J. J., Ivanova G. D., Verbeure B., Williams D., Arzumanov A.A., Abes S., Lebleu B., and Gait M. J. (2005). Cell-penetrating peptide conjugates of peptide nucleic acids (PNA) as inhibitors of HIV-1 Tat-dependent trans-activation in cells, *Nucleic Acids Research, 33*:6837–6849.

Usui I., Imamura T., Huang J., Satoh H., Olefsky J.M. (2003). Cdc42 is a Rho GTPase family member that can mediate insulin signaling to glucose transport in 3T3-L1 adipocytes, *J Biol Chem*, *278*: 13765-74.

Vives E., Brodin P., Lebleu B., (1997), A truncated HIV-1 Tat protein basic domain rapidly translocates through the plasma membrane and accumulates in the cell nucleus, *J Biol Chem., 272*: 16010-7.

Wacker B. K., Alford S. K., Scott E. A., Thakur M. D., Longmore G. D., Elbert D. L. (2008). Endothelial Cell Migration on RGD-Peptide-Containing PEG Hydrogels in the Presence of Sphingosine 1-Phosphate, *Biophysical Journal, 94*: 273–285.

Wadia J.S. and Dowdy S.F. (2005). Transmembrane delivery of protein and peptide drugs by TAT-mediated transduction in the treatment of cancer, *Adv. Drug Deliv. Rev.*, *57: 579*–596.

Wadia J.S., Stan R.V., and Dowdy S.F. (2004). Transducible TAT-HA fusogenic peptide enhances escape of TAT-fusion proteins after lipid raft macropinocytosis, *Nat. Med., 10*: 310–315.

Weeks K. M., Ampe C., Schultz S.C., Steitz T. A., Crothers D. M. (1991). Fragments of the HIV-1 Tat Protein Specifically Bind TAR RNA, *Science*, *249:* 1281-1285.

Wender P. A., Mitchell D. J., Pattabiraman K., Pelkey E. T., Steinman L., and Rothbard J. B. (2000). The design, synthesis, and evaluation of molecules that enable or enhance cellular uptake: peptoid molecular transporters, *Proc. Natl. Acad. Sci.*, *97*: 13003–13008.

Wieland T. and Bodanszky M. The World of Peptides. A Brief History of Peptide Chemistry. Springer-Verlag: Heidelberg, FRG, 1991.

Wolf M., Hull W. E., Mier W., Heiland S., Bauder-Wst U., Kinscherf R., Haberkorn U., Eisenhut M., (2007). Polyamine-Substituted Gadolinium Chelates: A New Class of Intracellular Contrast Agents for Magnetic Resonance Imaging of Tumors, *J. Med. Chem.*, 50, 139-148.

Wünsch E., Jaeger E., Kisfaludy L., and Löw M., (1977). Side Reactions in Peptide Synthesis: tert-Butylation of Tryptophan, *Angew. Chem. Int. Ed., 16*: 317-318.

Yamane T., Kerkis I., Kerkis A., Baptista G.-R., Hayashi M.A.F., Akemi F., Konno K., Da Silva A.R.B.P., Pereira L.V., De Oliveira E.B. (2006). USE OF CROTAMINE, KIT AND COMPOSITION, PCT/BR2006/000052.

You-min G., Min L., Jun-le Y., Xiao-juan G., Si-cen W., Xiao-yi D. and Peng W. (2007). Intercellular imaging by a polyarginine derived cell penetrating peptide labeled magnetic resonance contrast agent, diethylenetriamine pentaacetic acid gadolinium, *Chin Med J., 120: 50-55*.

Zhang Z., Greenfield M. T., Spiller M., McMurry T. J., Lauffer R. B., and Caravan P., (2005). Multilocus Binding Increases the Relaxivity of Protein-Bound MRI Contrast Agents *Angew. Chem. Int. Ed.*, *44*: 2–5.

Zorko M., and Langel U. (2005). Cell-penetrating peptides: mechanism and kinetics of cargo delivery, *Adv Drug Delivery Rev., 57*: 529– 545.